Biotechnological removal of H_2S and thiols from sour gas streams under haloalkaline conditions

Paweł Roman

Biotechnological removal of H$_2$S and thiols

from sour gas streams

under haloalkaline conditions

Paweł Roman

Thesis committee

Promotor
Prof. Dr A.J.H. Janssen
Professor of Biological Gas Treating Processes
Wageningen University

Co-promotor
Dr M.F.M. Bijmans
Manager Europe, Wetsus, European Centre of Excellence for Sustainable Water
Technology, Leeuwarden

Other members
Prof. Dr M.W.F. Nielen, Wageningen University
Prof. Dr G. Eggink, Wageningen University
Dr N.W. van den Brink, Wageningen University
Dr P. van den Bosch, Nederlandse Aardolie Maatschappij B.V., Assen, the
Netherlands

This research was conducted under the auspices of the Graduate School for Socio-
Economic and Natural Sciences of the Environment (SENSE)

Biotechnological removal of H$_2$S and thiols from sour gas streams under haloalkaline conditions

Paweł Roman

Thesis

submitted in fulfillment of the requirements for the degree of doctor
at Wageningen University
by the authority of the Rector Magnificus
Prof. Dr A.P.J. Mol,
in the presence of the
Thesis Committee appointed by the Academic Board
to be defended in public
on Thursday 12 May 2016
at 11 a.m. in the Aula.

Table of contents

Chapter 1

Introduction

1

1.1. The need for gas desulfurization

Sulfur is a key element to sustain life on Earth as it plays a significant role in biological and geochemical sulfur cycles. Sulfur has a wide range of oxidation states [1]. In its most reduced form, S(-II), it is a constituent of many biologically active compounds and therefore involved in many biochemical reactions. In its most oxidized form, S(VI), sulfur is present in sulfate (SO_4^{2-}) ions, which after HCO_3^- and Cl^- is the third most abundant anion in rivers and seawater [2].

The biological and geological sulfur cycles have been significantly perturbed by human activities leading to the emission of sulfur dioxide (SO_2) into the atmosphere. SO_2 contributes to the increase of the rainwater acidity and dry acid deposition (as sulfates) leading to environmental problems. In Europe, SO_2 emissions are the most dominant ones after carbon dioxide (CO_2), carbon monoxide (CO) and nitrogen oxides (NO_x) (Fig. 1) [3].
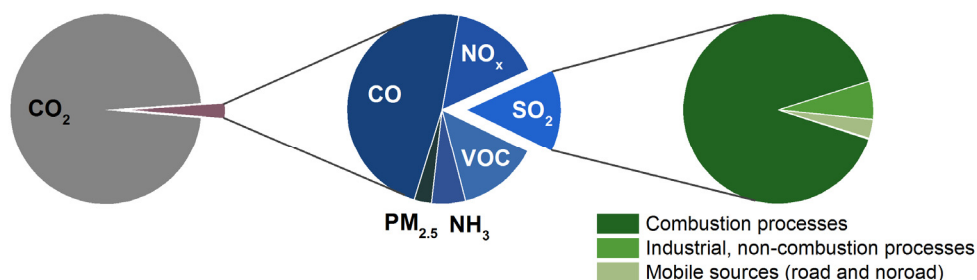
Figure 1. Annual emission estimates for different pollutants (left) and for sulfur dioxide by source (right) for Europe in 2006 [3,4]. VOC - volatile organic compounds.

Around 90 vol.% of the total SO_2 emissions originating from land-based anthropogenic sources can be contributed to the combustion of fossil fuels (Fig. 1) [3]. The sulfur atom is entrapped in organosulfur compounds like thiophenes, thiols (RSH) or thioethers (R_2S) [5]. Without treatment, burning these sulfur compounds leads to SO_2 formation. The adverse effects of sulfur pollution are well known, such as acid rain, health effects, odor irritation and corrosion of steel [6–9]. An example of SO_2 pollution is the Great Smog of London in 1952 during which almost 5000 people died due to increased concentrations of air pollutants in combination with bad weather conditions [10]. Taking into account these negative

effects and rapid growth of SO_2 emissions in the 1960's (Fig. 2), governments of industrialized nations set up emission control strategies to protect the public health and the environment [11].
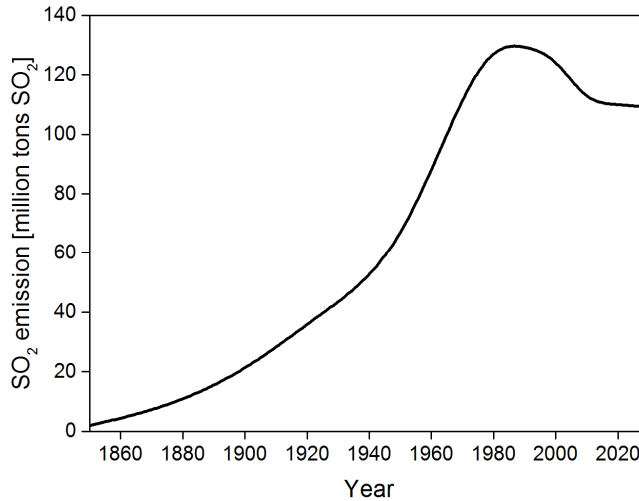
Figure 2. Global sulfur dioxide emission levels due to fuel combustion and process emissions. Predicted values are given for the period 2015 - 2030 [12,13].

Although a set of emission control strategies stopped the further increase in SO_2 emissions in 1980 (Fig. 2), actual values will remain high i.e. 110 million tons SO_2 per year in 2015. It is expected that SO_2 emissions will remain at this level up to 2030 (Fig. 2) [13]. The total world petroleum consumption increased from 49.4 in 1971 to 91.2 million barrels per day in 2013 [4,14], representing a 84% increase. Steadily increasing demand for transportation fuels and increasingly stringent legislation to mitigate against high SO_2 emissions encourage the development of innovative and cost-effective technologies that can be applied for the removal of sulfur pollutants from crude oil and gas streams. The Thiopaq O&G process is an example of such an innovative method for gas desulfurization, in which specialized microorganisms are applied to convert dissociated hydrogen sulfide (HS^-) to elemental sulfur (S_8) under ambient pressures and temperatures. This process was developed in the early 90's and after 25 years more than 200 commercial installations have been built worldwide thereby reflecting the demand for such processes (Fig. 3).

1

Nowadays, biodesulfurization processes mainly focus on the removal of H_2S but not on organosulfur compounds (VOSC), which can also be present in sour gas streams (Section 1.2). VOSCs contribute to air pollution and are much more toxic to humans than hydrogen sulfide. They are also notoriously difficult to biodegrade. The knowledge about the effects of organosulfur compounds on biodesulfurization processes is relatively scarce. In the long term, cost-effective technologies are required to remove both H_2S and organosulfur compounds to prevent air pollution and to meet the required product specifications, e.g. in case of natural gas treatment.
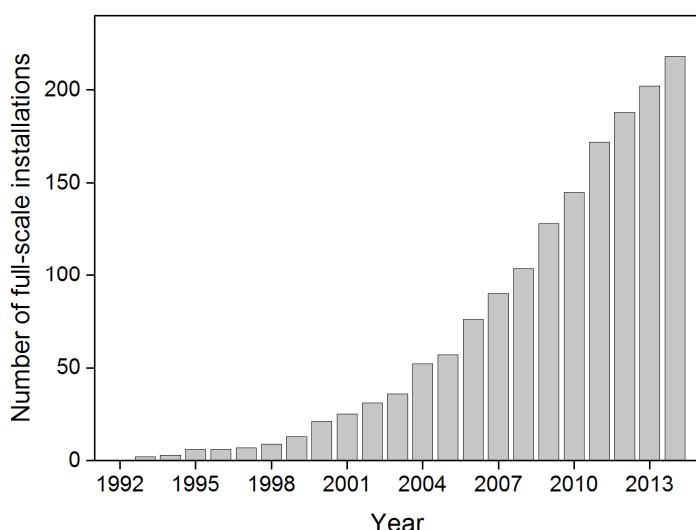
Figure 3. Cumulative number of full-scale Thiopaq installations for biogas, refinery gas and natural gas biodesulfurization.

1.2. Sulfur compounds polluting gas streams

Emissions of sulfur oxides are governed by the crude oil sulfur content [15], which can range from 0.025 to more than 5 wt% [16]. Thus, the total sulfur content is a key parameter in most of petrochemical quality control processes [17]. The new US EPA 2010-2015 regulations for highway and non-road fuels reduced the maximum allowable sulfur content from 500 ppm(w) down to 15 ppm(w) per gallon average [18,19].

In sour gas, the main sulfur impurities in sour gas streams are H_2S, thiols (RSH), diorgano polysulfanes (R_2S_x), carbonyl sulfide (COS) and carbon disulfide (CS_2) as presented in Table 1. Too high concentrations of polluting compounds in gases will lead to problems during processing and transportation. Typically, H_2S has to be below 3 ppm(v) to meet the sales specifications of natural gas and synthesis gas [20]. Based on the information in Table 1, it can be seen that H_2S and methanethiol are the major sulfur impurities in various gas streams. The physicochemical properties of H_2S and thiols are described in the following sections.

1.2.1. Hydrogen sulfide

Hydrogen sulfide is a colorless gas having a characteristic rotten eggs odor (Table 2). Wet H_2S is very corrosive to carbon steel which corrosion rates can exceed 2.5 mm per year [21]. This rate is dependent on pH, temperature and H_2S concentration. Hydrogen sulfide is soluble in polar solvents, especially in alkanolamines, which are used as scrubbing liquids for H_2S removal from gas streams [22,23]. Hydrogen sulfide can be oxidized by a number of oxidizing agents, from which O_2 and SO_2 are the most relevant in respectively the production of SO_2 in sulfuric acid plants and for the recovery of elemental sulfur in the Claus process [24]. Moreover, H_2S causes the precipitation of many heavy metal containing salts, which enables the recovery of these compounds from diluted aqueous waste streams [25]. Important reactions of H_2S with respect to biodesulfurization are described in section 1.4.1.

Inhalation of H_2S can lead to serious health problems. Exposure to 0.002 - 8 ppm(v) of H_2S for 4 - 7 hours causes shortness of breath, nausea, headache, throat and eye irritation, while exposure to 1000 ppm(v) for 1 min leads to sudden death [26]. Above 100 ppm(v) the sense of smell is deadened, preventing that its odor can warn against its presence in the air. An exposed person to H_2S may become unconscious, with no chance to escape from the contaminated area [27]. Because of the above reasons, the American Conference of Governmental Industrial Hygienists (ACGIH) established in 2015 the time-weighted average (TWA) concentration for H_2S at 1 ppm(v) for a conventional 8-hour workday to which workers may be exposed without adverse effect (Table 2).

1

Table 1. Examples of gas streams contaminated with sulfur compounds.

Type of gas stream / source	Unit	Typical concentration									Ref.
		H_2S	MT	ET	PT	BT	DMS	DMDS	CS_2	COS	
Landfill gas	ppb(v)	540000	4000					10	3300		[28]
Landfill gas	ppb(v)	280000	1500					210	240		[29]
Landfill gas	ppb(v)	190	164000		2800				60	710	[30]
Landfill gas	ppb(v)	110	4					20	2		[31]
Landfill gas	ppb(v)	2200	14					4	125		[32]
Synthetic natural gas	ppb(v)	150	130	400			220	230			[33]
Liquefied petroleum gas	ppm(v)	2000	250					<10		50	[34]
Liquefied petroleum gas	ppm(v)	60	430	220							[35]
Liquefied petroleum gas	ppm(v)		1500	5000							[34]
Liquefied petroleum gas	ppm(v)	2000	1000	500							[36]
Propane	ppm(v)	1000	600	10						500	[34]
n-butane	ppm(v)	1000	1900	10000							[34]
Gas samples of sewage management plants	ppb(v)						610	860	520		[37]
Low pressure fuel gas	ppm(v)	12000	140	50							[38]
Condensate from chiller separator	ppm(v)	90	151	139	159	10					[38]
Anaerobic brewery waste water treatment plant	ppm(v)	4	30								[39]
Rendering cookers	ppm(v)	<800	<200								[40]
Kraft paper production process	ppm(v)	100					20	20			[41]

MT - methanethiol; ET - propanethiol; PT - propanethiol; BT - butanethiol; DMS - dimethyl sulfide; DMDS - dimethyl disulfide

1.2.2. Thiols

Thiols are sulfur analogues of alcohols with a general formula of RSH, where R represents an aliphatic chain. The property that distinguishes thiols most from other compounds is their unbearable odor (Table 2). For example, thiols are used as malodorants in combustible gases to warn for a gas leakage. ACGIH set the TWA concentration at 0.5 ppm(v), which is 2 times lower than for H_2S (Table 2). Thiols react with many rubber-containing materials, e.g. gaskets used in flanges [42]. Thus, alternative materials should be considered when working with thiols in the laboratory, e.g. Teflon or Viton. Short-chain thiols are weak acids with pK_a values around 10.4 [43,44]. This enables their removal in gas absorbers by strong alkaline solvents under the formation of reactive nucleophiles [45]:

$$RSH + OH^- \rightarrow RS^- + H_2O \tag{1}$$

In contrast to alcohols, which can be oxidized to their corresponding carbonyl compounds (e.g. aldehydes or ketones), thiols are not oxidized to thiocarbonyls [46]. This is because of the larger size of the sulfur atom compared to the oxygen atom. Consequently, oxidation of the thiol group can lead to disulfides, sulfenic, sulfinic or sulfonic acids [47]. Symmetric disulfides are formed in exothermic reaction of thiols with variety of oxidants, like hydrogen peroxide, oxygen or sulfur [45,48]:

$$2\ RSH + 0.5\ O_2 \rightarrow RS_2R + H_2O \tag{2}$$

$$RSH + S_8 \rightarrow RS_9^- + H^+ \tag{3}$$

$$RSH + RS_9^- \rightarrow RS_nR + S_x^{2-} + H^+, \text{ with } n+x = 10 \tag{4}$$
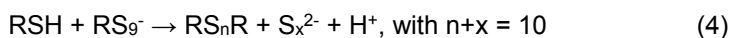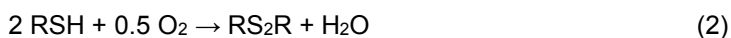
The chemical oxidation rate of thiols decreases with increasing chain length because of steric hindrance [49]. The main product from the reaction between elemental sulfur and thiols is diorgano pentasulfide, which immediately undergoes interconversion reactions to form a complex mixture of organosulfur compounds:

$$2\ RS_nR \leftrightarrow RS_{n-1}R + RS_{n+1}R, \text{ with } n>3 \tag{5}$$

Asymmetric sulfides can be formed by exchanging the organic groups or by reaction with thiols [45]:

$$R_1S_nR_1 + R_2S_nR_2 \leftrightarrow 2\ R_1S_nR_2 \tag{6}$$

$$R_1SH + R_2S_nR_2 \leftrightarrow R_1S_nR_2 + R_2SH \tag{7}$$
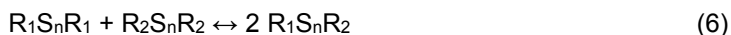
Thiols also readily react with alkenes to form diorgano sulfides [50]:

$$R_1SH + R_2CH=CH_2 \rightarrow R_1SCH_2CH_2R_2 \tag{8}$$

1
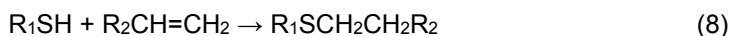
Table 2. Physicochemical properties of volatile sulfur compounds.

IUPAC name	Structure	Odor description [51]	Henry's constant at 25 °C [52,53]	Odor threshold [ppb(v)] [51,54–56]	TLV-TWA [ppm(v)] [57]	LD$_{50}$ [mg kg^{-1}] [58–61]
Hydrogen sulfide	H$_2$S	rotten eggs	0.41	95	1	110
Methanethiol	CH$_3$SH	rotten cabbage	0.1	12	0.5	682
Ethanethiol	CH$_3$CH$_2$SH	rotten cabbage	0.15	0.35	0.5	1790
1-Propanethiol	CH$_3$CH$_2$CH$_2$SH	unpleasant	0.17	3.1		3300
Dimethyl sulfide	CH$_3$SCH$_3$	rotten cabbage	0.073	24	10	190
Dimethyl disulfide	(CH$_3$)$_2$S$_2$	rotten cabbage	0.045	9.2	0.5	2030
Diethyl disulfide	(CH$_3$CH$_2$)$_2$S$_2$	onion, garlic		0.02		2000
Dipropyl disulfide	(CH$_3$CH$_2$CH$_2$)$_2$S$_2$	onion		21.2		

TLV-TWA - Threshold limit value - time-weighted average; LD$_{50}$ - dose that is lethal to 50% of the animals tested

Reaction 7 and 8 show that the sulfhydryl can disrupt the intermolecular disulfide bonds and double bound in alkenes. These bonds are essential for stability of the biological structures, therefore, thiols can result in alteration of enzyme structures and its inactivity [62]. Besides thiols, dissociated sulfide anions can disrupt the disulfide that generates persulfides:

$$RS_2R + HS^- \leftrightarrow RS_2H + RS^- \tag{9}$$

Persulfides exhibits ambiphilic properties, i.e. can behave as an electrophile or a nucleophile, which makes these compounds important in redox biology [63,64].

1.3. Physicochemical removal of volatile sulfur compounds from gas streams.

Atmospheric pollution is a result of anthropogenic activities, among which combustion of fossil fuels is a major source (Section 1.1). Emissions of H_2S and volatile organic sulfur compounds (VOSC) represents a worldwide environmental problem. Therefore, a priority nowadays is to minimize emissions of these sulfur compounds by desulfurization of sour gas streams, which are defined as streams exceeding 4 ppm of H_2S [65].

Removal of H_2S from industrial gas streams is performed on a large scale (> 50 tons of sulfur per day) in the natural gas and refining industries. Most processes for H_2S removal are based on a closed recirculation systems that consists of H_2S absorption and regeneration of the treating solution, e.g. amine solvent [66]. At large scale, H_2S is usually removed in a combined process including amine treatment and the Claus process (Fig. 4). In the amine treatment, H_2S is removed from the gas stream in a gas-liquid countercurrent flow contactor (Fig. 4) by a fast reaction with the amine to form hydrosulfide species. Key parameters of the amine treatment step are the circulation rate and the strength of the washing solution [67]. The extracted H_2S is stripped from the amine solvent to form a concentrated H_2S stream, commonly called "acid gas" (Fig. 4). Further, acid gas is sent to the Claus sulfur recovery plant (Fig. 4), which is a complex and highly integrated system consisting of a high temperature furnace stage and a series of catalytic stages. In the Claus process H_2S is oxidized to elemental sulfur according the following reaction:

$$H_2S + 0.5\ O_2 \rightarrow 1/8\ S_8 + H_2O \tag{10}$$

1
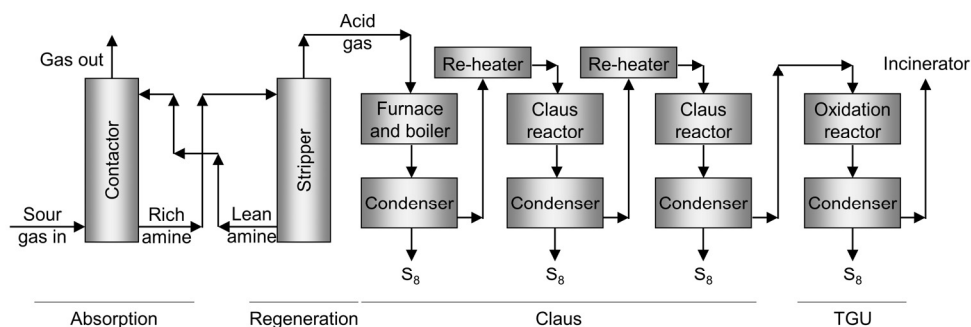
Figure 4. Simplified process scheme for the amine sweetening process in combination with Claus sulfur recovery process and tail gas unit (TGU).

Around 65 - 70 % of sulfur is recovered in the furnace stage, in which besides sulfur also SO_2 is formed [68]. Before a sulfur condenser, hot gas from the furnace is cooled in a waste heat boiler which generates high pressure steam [68]. Produced SO_2 is later used to react with H_2S in the catalytic stages over an alumina- or titanium dioxide-based catalyst. The simplified equation for production of sulfur in the catalytic converters is as follows:

$$2 H_2S + SO_2 \leftrightarrow 3/8 S_8 + 2 H_2O \qquad\qquad (11)$$

The above reaction is an equilibrium reaction and therefore it is not possible to convert all incoming H_2S into elemental sulfur. For this reason, two or more stages are applied to achieve >99% conversion of the inlet H_2S to elemental sulfur [66]. For improved sulfur recovery (>99.8%), the tail gas unit (TGU) can be applied, such as SCOT or Superclaus [69,70]. In TGU, the remaining H_2S is selectively oxidized to elemental sulfur by applying specific catalysts.

Besides the Claus process, H_2S can also be removed in other physicochemical processes, such as Lo-Cat and SulFerox process [71]. In these processes, chelate complexes of iron(III) are used as catalysts to oxidize sulfide to elemental sulfur. Afterwards, iron(III) is regenerated by oxidation of the formed iron(II), by blowing air into the process solution. Systems in which sulfide is oxidized in redox processes are characterized by high maintenance costs, frequent process disruptions and large volumes of toxic waste products [71].

Next to the air pollution caused by H_2S, the emission of VOSCs is a major environmental problem. Therefore, several chemical processes to remove VOSCs from sour gas streams were developed as well, such as Merox, Sulfex, Mericat

and Thiolex in combination with a regeneration technology [72]. These processes are mainly based on the application of a fiber-film contactor [72], which consist of a cylinder packed with metal fibers. This contactor is characterized by a high interfacial surface area between gas and liquid phase, which allows VOSCs to easily diffuse from the gas to the liquid phase. Technologies applying fiber-film contactors require smaller processing vessels. Moreover, they are characterized by lower waste generation and up to six times shorter separation times than conventional contactor systems [73].

Merox and Thiolex are the most commonly applied processes for chemical removal of VOSCs. More than 200 references of Thiolex systems worldwide are built to desulfurize sour gas streams in fields such as gas production, crude distillation and fluid catalytic cracking. In the Thiolex process, thiols are removed by caustic extraction in a fiber-film contactor (Fig. 5). Typically, the Thiolex process is coupled with a technology in which rich caustic streams are regenerated (Fig. 5).
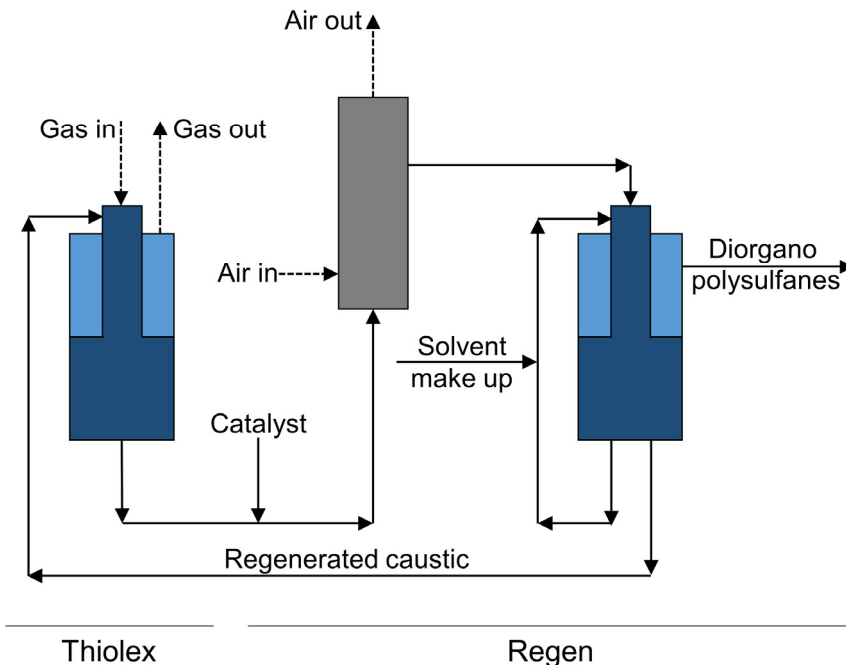
Figure 5. Schematic representation of the Thiolex process coupled with a solvent regeneration step (Regen) [74].

Extracted thiols in the Thiolex process are converted in the solvent regeneration step (Regen process) to diorgano polysulfanes with air (Eq. 2) in the presence of a catalyst, such as iron containing chelates [75]. Hereafter, the formed diorgano polysulfanes are separated and removed in a second fiber-film contactor. The Merox process is similar to the Thiolex process, except a multistage extraction contactor is used instead of a fiber-film contactor to enable the contact between untreated gas stream and the caustic solvent stream.

1.4. Biological gas desulfurization

A variety of physicochemical processes can be applied to treat sour gas streams. However, these are characterized by high installation and operating cost due to high temperatures, pressure and chemical use and, often, relatively high residual concentrations. Alternatively, biological processes have been developed, which operate under ambient temperature and atmospheric pressure, and the chemical consumption is minimal [76]. Next to lower power consumption, biological processes are characterized by high rates of pollutants removal, much lower residual (tails) concentrations and small footprint [77]. Because of very low sulfide concentrations in the off-gas, a TGU is not needed resulting in lower investment cost. Moreover, in biological processes emission of CO_2 is strongly reduced while emission of SO_2 is eliminated.

The use of biological gas desulfurization processes become increasingly popular and cover relatively wide range of techniques, e.g. biofilters, biotrickling filters gas lift reactors, continuous stirred-tank reactors (CSTR) or membrane reactors. Most of these processes consist of two-steps [78], in which the first step is meant to transfer pollutants from the gas phase into a liquid phase. In the second step, the transferred pollutants are degraded by microorganisms. The individual techniques differ in bioreactor configuration and biomass location. Reactors with immobilized biomass, like biofilters, are exposed to many factors affecting their performance. For example, biomass build-up can result in high back pressures, anaerobic zones and decreased reactor performance [79]. Inefficient mixing can lead to pH-gradients, which in turn, can affect biological activity and the overall process performance [80]. Although in biotrickling filters some of these problems were solved, product accumulation can occur, which then can lead to clogging problems, unwanted

pressure drops, and therefore, a decreased process performance [81]. Methods for solving these problems were described [81–84] but they are not necessarily practical. Two-stage reactor systems are proposed to avoid aforementioned problems. An example of such a system is a process for biogas desulfurization known as Thiopaq O&G [85]. The objective of this thesis is to increase the operating window of the Thiopaq O&G process.

1.4.1. Technology and the sulfur cycle

The Thiopaq O&G process consists of a gas absorber, a bioreactor and a sulfur removal unit (Fig. 6). In the gas absorber, H_2S is absorbed in an alkaline solvent according to [86]:

$$H_2S_{(G)} \leftrightarrow H_2S_{(L)} \tag{12}$$
$$H_2S_{(L)} + OH^- \leftrightarrow HS^- + H_2O \tag{13}$$
$$H_2S_{(L)} + HCO_3^- \leftrightarrow HS^- + CO_2 + H_2O \tag{14}$$
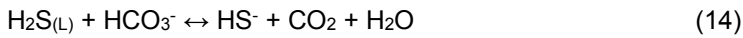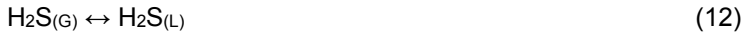
Dissolved H_2S will react with hydroxyl ions (Eq. 13). The operating pressure ranges from atmospheric pressure up to 75 bar [87]. Next, the loaded solvent is fed to the gas-lift-loop bioreactor (Fig. 6). In the bioreactor, sulfide is biologically oxidized to elemental sulfur, referred to as biosulfur according to:

$$HS^- + 0.5\ O_2 \rightarrow 1/8\ S_8 + OH^-\ (biotic) \tag{15}$$
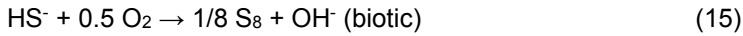
It can be seen that the acidity produced during the absorption of H_2S (Eq. 13) is compensated by the formation of hydroxyl ions (Eq. 15). Next to biosulfur particles, also small amounts of sulfate are produced [86,88]:

$$HS^- + 2\ O_2 \rightarrow SO_4^{2-} + H^+\ (biotic) \tag{16}$$
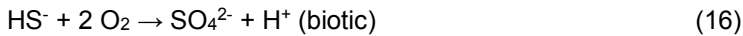
It shall be noted that the above equations are simplified versions of the underlying biochemical pathways [89]. Formation of sulfur and sulfate in the bioreactor is related to the O_2/H_2S supply ratio resulting in a certain equilibrium sulfide concentration, which, in turn, results in a particular value of oxidation-reduction potential (ORP) of the process liquid [90]. In the final section, elemental sulfur is separated from the solvent in the sulfur settler (Fig. 6). The recovered biosulfur is hydrophilic and dispersible in water [91], and can be used for sulfuric acid production, as a soil fertilizer and as fungicide [92]. It could also be a source of elemental sulfur for large-scale biosynthetic applications such as the synthesis of methionine.
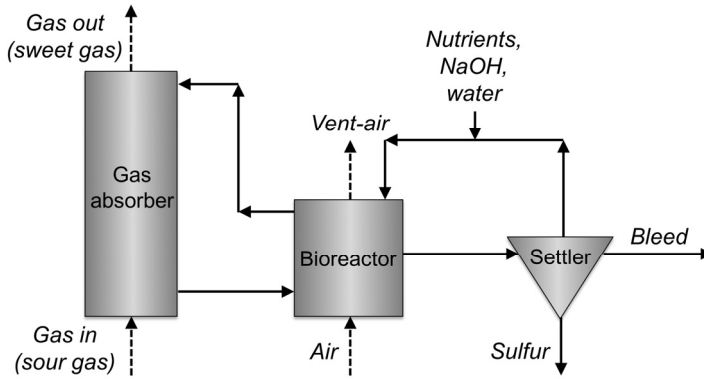
Figure 6. Block process diagram of Thiopaq O&G process for sour gas desulfurization.

Besides aforementioned biological sulfide oxidation (Eq. 15 and 16) the chemical, i.e. non-biological, oxidation of sulfide proceeds through a chain reaction mechanism [93]. In the first step, sulfide is transformed in the presence of oxygen to elemental sulfur:

$$2\ HS^- + O_2 + 2\ H^+ \rightarrow 1/4\ S_8 + 2\ H_2O \tag{17}$$
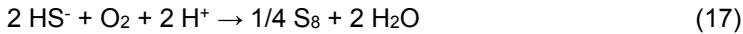
In the second step, sulfide reacts with sulfur to form pentasulfide anions in a two-step reaction:

$$HS^- + S_8 \leftrightarrow S_9^{2-} + H^+ \tag{18}$$

$$S_9^{2-} + HS^- \rightarrow 2\ S_5^{2-} + H^+ \tag{19}$$

The formed pentasulfide anions (Eq. 19) undergo an interconversion reaction and a chemical equilibrium will be established [94] according to:

$$2\ S_x^{2-} \leftrightarrow S_{x-1}^{2-} + S_{x+1}^{2-},\ x \geq 2 \tag{20}$$

It should be noted that reactions 18 - 20 can take place in the gas absorber as well as the bioreactor (Fig. 6) and contribute to dissolution of elemental sulfur, which has an autocatalytic effect:

$$S_x^{2-} + 1/8\ S_8 \rightarrow S_{x+1}^{2-} \tag{21}$$

Finally, the formed polysulfide anions follow an auto-oxidation reaction in the presence of molecular oxygen [95]:

$$S_x^{2-} + 1.5\ O_2 \rightarrow S_2O_3^{2-} + (x-2)/8\ S_8 \tag{22}$$
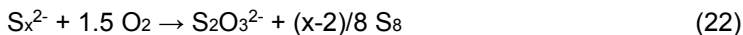
Reactions 17 to 22 give an overview of chemical sulfide oxidation, which in the current thesis will be written in a simplified form:

$$HS^- + O_2 \rightarrow 0.5\ S_2O_3^{2-} + 0.5\ H_2O \tag{23}$$
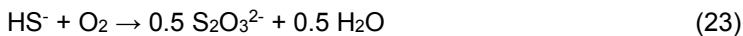
Polysulfide anions play a significant role in biodesulfurization systems as they enhance the physical dissolution of sulfide due to equilibrium reactions [96] and can be biologically oxidized to elemental sulfur [97–99]. Speciation of polysulfide anions is not affected by pH within the range of polysulfides chemical stability (i.e. pH = ~7 - 12) [100]. At lower pH values polysulfide anions react with hydrogen ions [101] to form elemental sulfur:

$$S_x^{2-} + H^+ \leftrightarrow HS^- + (x-1)/8\ S_8 \tag{24}$$

Moreover, it is known that the total concentration of polysulfide anions increases with increasing pH (Fig. 7). This, has a significant effect on the product selectivity of the overall biodesulfurization process. For example, with increasing pH, formation of thiosulfate (Eq. 22) increases, while formation of biosulfur decreases [102]. It was found that the most optimal pH for the process is around 8.5, at which complete H_2S absorption occur and formation of thiosulfate is minimal [102].
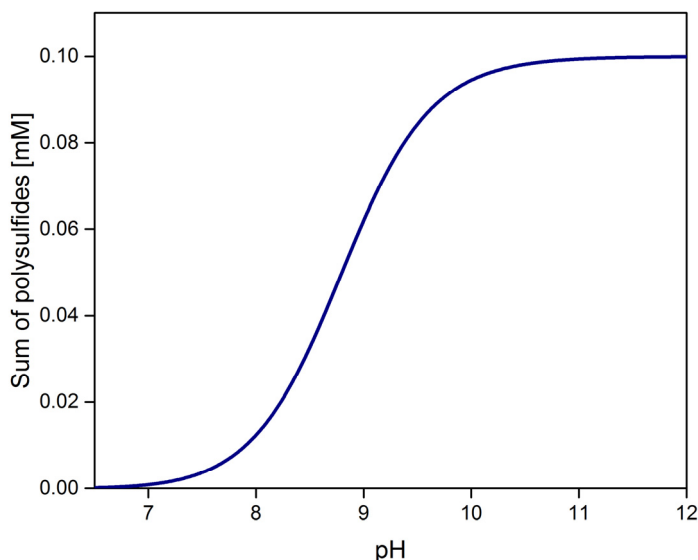
Figure 7. Total concentration of polysulfide anions at different pH values with initial sulfide and sulfur concentration of 0.1 and 1 mM, respectively. Calculations were made by using OLI Analyzer Studio software (Version 3.1, OLI Systems Inc., NJ).

1.4.2. Microorganisms and sulfide oxidation pathway

The Thiopaq O&G process operates under haloalkaline conditions, i.e. at elevated pH values (>8.5) and sodium carbonate concentrations above 1 M to ensure high H_2S absorption efficiencies and to minimize freshwater requirements. Previous studies have shown that certain groups of gammaproteobacterial chemolithotrophic sulfur-oxidizing bacteria (SOB) are suitable biocatalysts for sulfide oxidation because of their high salt and pH tolerance [97,99]. In particular, *Thioalkalivibrio sulfidophilus* was identified as the dominant SOB species in Industriewater Eerbeek B.V., the Netherlands [103,104], which has been used as an inoculum for most of the Thiopaq O&G plants. The genus *Thioalkalivibrio* is characterized by a high-salt tolerance between 0.5 - 2 M Na^+ and an optimum pH for growth and activity of sulfide oxidation between 9 and 10 [97]. The salt concentration is the most important driving force influencing the microbial composition and survival of haloalkaliphilic SOB [105]. *Thioalkalivibrio* utilizes reduced sulfur compounds, such as sulfide, polysulfide anions, thiosulfate, elemental sulfur (all species), tetrathionate and thiocyanate (some species) as electron donor [97–99,106]. Its capability for the simultaneous oxidation of both sulfide and polysulfide anions, produced in reaction between dissolved H_2S and biosulfur (Eq. 18 - 21), makes *Thioalkalivibrio* spp. A highly suitable biocatalyst to be applied in the Thiopaq process.

Thioalkalivibrio spp. can use a range of reduced sulfur compounds as *e*-donor. Based on the genome analysis of *Thioalkalivibrio sulfidophilus*, a hypothetical pathway was proposed for sulfide and thiosulfate oxidation (Fig. 8) [107]. From this pathway, it can be seen that sulfide is first transformed to zero-valent sulfur (S°) using flavocytochrome *c* sulfide dehydrogenase (FCC), which contains a flavin-binding catalytic subunit and a diheme cytochrome *c* subunit [108]. The active site of the former consists of a disulfide bridge that is responsible for binding the sulfide. During the dehydrogenation of sulfide electrons are transferred to the respiratory *c*-type cytochromes (cyt). As ubiquinone-depended sulfide oxidation activity have also been observed in *Thioalkalivibrio* [107], it was also suggested that FCC additionally may use ubiquinones as electron acceptors [99,109], similar to its more ancient sister enzyme, sulfide-quionone oxido-reductase (SQR). Produced proton gradients enable SOB to gain energy for growth and maintenance. Depending

on the reduction degree of cytochrome *c* oxidase (CcO), the formed S° can be further transformed to sulfite [110], using a reversed dissimulatory sulfide reductase [107]. Finally, sulfite can be oxidized to sulfate by the two alternative routes (Fig. 8). First is a direct route, which uses sulfite dehydrogenase. Secondly, in an indirect route, sulfite is phosphorilated and then oxidized to sulfate in a two stage process by action of adenosine phosphosulfate reductase (Apr) and ATP-sulfurilase (Sat). In summary, sulfide oxidation to sulfur or sulfate in *Thioalkalivibrio sulfidophilus* can be considered as a single pathway that is redox dependent, i.e. at low redox values (high sulfide concentrations) the pathway is mainly limited to sulfur production. At higher redox values, zero-valent sulfur is further oxidized to sulfate [110]. In the literature these pathways can also be found as limited oxygen route (LOR) and full oxygen route (FOR) [111]. Oxidation of sulfide via LOR occurs under limited oxygen conditions (low redox conditions) and leads to the sulfur formation, whereas oxidation via FOR leads to the sulfate formation.
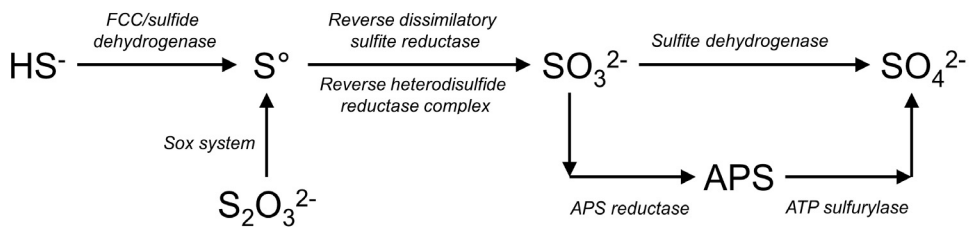
Figure 8. Hypothetical pathway of biological sulfide oxidation in *Thioalkalivibrio sulfidophilus* proposed based on genome analysis [107].

1.4.3. Control of oxygen supply to bioreactor

In most industrial processes the choice of a proper process control strategy is of crucial importance to ensure an efficient process performance. In our sulfur-producing biodesulfurization process, the oxygen supply has to be accurately controlled to minimize the formation of sulfate ions and maximize the sulfur production. In addition, the pH and specific conductivity should be controlled to ensure optimal conditions for the microbial population. Modern model-based control systems can be able to predict a deviation of actual state variables from

1

desired values which can be counteracted by taking appropriate measures to avoid loss of process performance [112]. However, when microbial metabolisms are involved, this is not a straightforward task due to the complexity of the underlying biochemical reactions and non-linear behavior of the system. The likelihood that the system changes over time as a result of natural adaptation to changing process conditions and lack of understanding of the biochemical mechanisms may result in poor mathematical models. In recent years, various publications addressing several of these challenges were published [89,113].

In case of gas biodesulfurization processes, it is known that the production of biosulfur is strongly correlated with the sulfide concentration and the availability of oxygen [86,90]. Therefore, the application of a sulfide sensor in control systems could be beneficial. However, commercially available sensors for sulfide measurements are not robust at pH ≥ 8.5. For example, selective ion electrodes and amperometric sensors are characterized by temperature and ionic strength sensitivity, and have a short lifetime [114–116]. Because in the absence of other strong reductants the ORP is mainly determined by the sulfide concentration [90], ORP sensors are commonly applied instead of sulfide sensors. The ORP sensor is often used in combination with a proportional-integral-derivative (PID) controller to control the oxygen supply (Fig. 9) [117]. The advantage of this control strategy is its simplicity while no mathematical models are needed (black box). However, the effect of thiols and diorgano polysulfanes on this system is unknown. A spin off from this PhD project, is a patent submission for a new type sulfide sensor. This sensor overcomes aforementioned drawbacks of conventionally applied sulfide sensors [118].
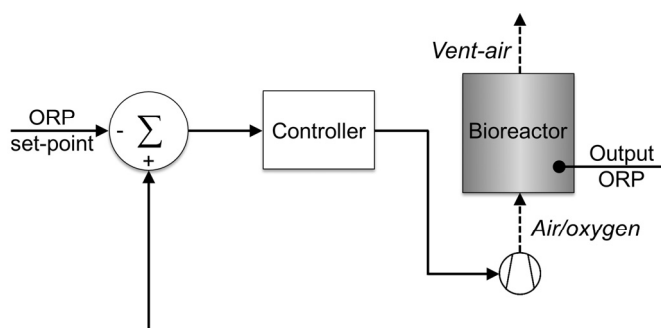
Figure 9. Schematic representation of a simple feedback control system used to control the ORP in a bioreactor suspension.

1.5. Scope and outline of the thesis

Without treatment the combustion of fossil fuels will contribute considerably to air pollution. New bio-based processes have been developed to treat polluted gas streams [119,120]. Biological processes used to remove H_2S from sour gas stream are currently most cost-effective at small and medium scales (less than 50 tons H_2S per day). Broadening the application window of these processes will have a positive impact on air pollution and will allow for further reduction of costs related to gas desulfurization. However, the effect of thiols on aerobic bioprocesses is not understood while so far only preliminary studies were performed [121,122]. Hence, the research described in this thesis focuses on the effect of thiols on bioprocesses for H_2S removal. The main research tasks are defined as follows:

• Development of an analytical tool set to measure (in)organic sulfur compounds at low levels;

• Investigation of the thiols chemistry and fate of thiols in biodesulfurization systems;

• Assessment of the effect of elemental sulfur particles on the absorption rate of thiols;

• Investigation of the thiols presence on overall performance of biodesulfurization systems;

• Development of a strategy to mitigate the adverse effects of thiols on the performance of biodesulfurization systems;

• Proposition of a new system for combined H_2S and thiols removal.

In **Chapter 2** analytical tools are described to quantify individual polysulfide anions in high saline matrixes. On the basis of our analysis, the average sulfur chain was calculated under different ORP conditions in both laboratory and full-scale biodesulfurization systems. The obtained results showed that laboratory systems mimics full-scale conditions and can be used for further experiments, and furthermore, can be applied in mathematical models describing gas biodesulfurization processes.

Although thiols exhibit inhibitory effects on SOB, their effect on biodesulfurization systems operated under haloalkaline conditions is yet unknown. To increase our understanding, the effect of methanethiol on biodesulfurization systems was studied under multiple redox conditions (**Chapter 3**). Our findings

suggest different susceptibilities of sulfur and sulfate production due to the presence of MT. This observation can be explained by the inhibition of a specific enzyme for the sulfate production.

1

Chapter 4 focuses on the inhibition of sulfur production by methanethiol. From two most dominant organosulfur compounds present in the bioreactor (methanethiol and its derivative dimethyl disulfide), methanethiol is the one responsible for the biomass inhibition. Moreover, a mathematical model was proposed to predict the bioreactor performance. Finally, a novel approach to measure the enzyme kinetic is proposed.

The results presented in the previous two chapters show a need to know the kinetic parameters describing inhibition of sulfide oxidation by SOB. In **Chapter 5**, the inhibition mode of sulfur and sulfate production is studied for three most common thiols and their diorgano polysulfanes. On this basis, the inhibition constants for sulfide oxidation were estimated for each inhibitor. The obtained parameters were used for validation of developed mathematical model describing sulfide oxidation pathway in SOB in independent experiments.

To expand the operational window of existing biodesulfurization systems for gas streams containing high concentrations of thiols, it is necessary to find microorganisms that are tolerant to withstand or convert these toxic compounds. In **Chapter 6**, the haloalkaliphilic SOB biomass originating from a full-scale gas desulfurization system fed with thiol-containing gas was adapted to methanethiol and used for experiments with higher thiols (ethanethiol and propanethiol). From our results it can be concluded that it is possible to remove H_2S together with high thiol concentration. However, the results also show that new bioreactor controlling methods are necessary if feed gas streams contain other than sulfide redox-reducing compounds. Moreover, it is shown that the absorption capacity for thiols can be effectively enhanced by having biologically produced hydrophilic sulfur particles in the recirculating wash liquid.

Finally, **Chapter 7** provides the summary of the most significant results and conclusions from the research chapters in perspective of development of the biodesulfurization technology for thiols removal. In this chapter discussion with respect to remaining research questions is provided.

References

1. Charlson R, Anderson T, McDuff R. The sulfur cycle. *Earth system science: from biogeochemical cycles to global change*. Academic Press, New York; 2000. p. 343–359.
2. Lee CC-W, Savarino J, Thiemens MH. Mass independent oxygen isotopic composition of atmospheric sulfate: Origin and implications for the present and past atmosphere of Earth and Mars. *Geophys. Res. Lett.* Wiley Online Library; 2001;28:1783–1786.
3. Pouliot G, Pierce T, van der Gon HD, Schaap M, Moran M, Nopmongcol U. Comparing emission inventories and model-ready emission datasets between Europe and North America for the AQMEII project. *Atmos. Environ.* Elsevier; 2012;53:4–14.
4. International Energy Statistics [Internet]. Available from: www.eia.gov/cfapps/ipdbproject/.
5. Sohrabi M, Kamyab H, Janalizadeh N, Huyop FZ. Bacterial desulfurization of organic sulfur compounds exist in fossil fuels. *Journal of pure and applied microbiology*. 2012;6.
6. Chen W, Hao L, Dong J, Ke W. Effect of sulphur dioxide on the corrosion of a low alloy steel in simulated coastal industrial atmosphere. *Corros. Sci.* Elsevier; 2014;83:155–163.
7. Reis S, Grennfelt P, Klimont Z, Amann M, ApSimon H, Hettelingh J-P, Holland M, LeGall A-C, Maas R, Posch M, others. From acid rain to climate change. *Science*. American Association for the Advancement of Science; 2012;338:1153–1154.
8. Kim K-H. Emissions of reduced sulfur compounds (RSC) as a landfill gas (LFG): A comparative study of young and old landfill facilities. *Atmos. Environ.* Elsevier; 2006;40:6567–6578.
9. Bernstein JA, Alexis N, Barnes C, Bernstein IL, Nel A, Peden D, Diaz-Sanchez D, Tarlo SM, Williams PB. Health effects of air pollution. *J. Allergy. Clin. Immun.* Elsevier; 2004;114:1116–1123.
10. The London Smog Disaster of 1952 [Internet]. Available from: www.portfolio.mvm.ed.ac.uk/studentwebs/session4/27/greatsmog52.htm.
11. Belden RS. Clean Air Act. 2001.
12. Smith SJ, Aardenne J van, Klimont Z, Andres RJ, Volke A, Delgado Arias S. Anthropogenic sulfur dioxide emissions: 1850-2005. *Atmos. Chem. Phys.* Copernicus GmbH; 2011;11:1101–1116.
13. Cofala J, Amann M, Mechler R. Scenarios of world anthropogenic emissions of air pollutants and methane up to 2030. 2005.
14. EIA/IEA, International Energy Annual 2001, Energy Information Administration. Washington, DC; 2002.
15. Levy A, Miller S, Barnett R, Schulz E, Melvin R, Axtman W, Locklin D. A field investigation of emissions from fuel oil combustion for space heating. *API Bulletin*. 1971;4099.
16. Monticello D, Finnerty W. Microbial desulfurization of fossil fuels. *Annual Reviews in Microbiology*. Annual Reviews 4139 El Camino Way, PO Box 10139, Palo Alto, CA 94303-0139, USA; 1985;39:371–389.
17. Chambers L, Duffy ML. Determination of total and speciated sulfur content in petrochemical samples using a pulsed flame photometric detector. *J. Chromatogr. Sci.* Oxford University Press; 2003;41:528–534.

1

1

18. Song C. An overview of new approaches to deep desulfurization for ultra-clean gasoline, diesel fuel and jet fuel. *Catal. Today*. Elsevier; 2003;86:211–263.

19. Federal Emission Standards [Internet]. Available from: http://www3.epa.gov/otaq/standards/allstandards.htm.

20. Lagas J. Survey of H_2S and SO_2 removal processes. *Environmental technologies to treat sulfur pollutions; principles and engineering, PNL Lens and LW Hulshoff Pol Eds. IWA Publishing, London*. 2000;237–264.

21. Javaherdashti R, Nwaoha C, Tan H. Corrosion and materials in the oil and gas industries. CRC Press; 2013.

22. Kohl AL, Nielsen R. Gas purification. Gulf Professional Publishing; 1997.

23. Crynes BL, others. Chemical reactions as a means of separation. M. Dekker; 1977.

24. Piéplu, A., Saur, O., Lavalley, J.C., Legendre, O., and Nédez, C. Claus catalysis and H_2S selective oxidation. *Catal. Rev.* Taylor & Francis; 1998;40:409–450.

25. Fu F, Wang Q. Removal of heavy metal ions from wastewaters: a review. *J. Environ. Manage.* Elsevier; 2011;92:407–418.

26. Finklea J. Criteria for a recommended standard occupational exposure to hydrogen sulfide. *National Institute for Occupational Safety and Health DHEW,(NIOSH) publication*. 1977;185.

27. Weil ED, Sandler SR, Gernon M. Sulfur compounds. *Kirk-Othmer Encyclopedia of Chemical Technology*. Wiley Online Library; 1997.

28. Kim K-H, Choi Y, Jeon E, Sunwoo Y. Characterization of malodorous sulfur compounds in landfill gas. *Atmos. Environ.* Elsevier; 2005;39:1103–1112.

29. Kim K-H. Emissions of reduced sulfur compounds (RSC) as a landfill gas (LFG): A comparative study of young and old landfill facilities. *Atmos. Environ.* Elsevier; 2006;40:6567–6578.

30. Lee S, Xu Q, Booth M, Townsend TG, Chadik P, Bitton G. Reduced sulfur compounds in gas from construction and demolition debris landfills. *Waste Manage.* Elsevier; 2006;26:526–533.

31. Fang J-J, Yang N, Cen D-Y, Shao L-M, He P-J. Odor compounds from different sources of landfill: characterization and source identification. *Waste Manage.* Elsevier; 2012;32:1401–1410.

32. Song S-K, Shon Z-H, Kim K-H, Kim SC, Kim Y-K, Kim J-K. Monitoring of atmospheric reduced sulfur compounds and their oxidation in two coastal landfill areas. *Atmos. Environ.* Elsevier; 2007;41:974–988.

33. Cui H, Turn SQ, Reese MA. Removal of sulfur compounds from utility pipelined synthetic natural gas using modified activated carbons. *Catal. Today*. Elsevier; 2009;139:274–279.

34. Leerdam van R. Anaerobic degradation of methanethiol in a process for liquefied petroleum gas (LPG) biodesulfurization. 2007.

35. Manieh A, Ghorayeb N. How to design a caustic wash. *Hydrocarbon processing*. Gulf Publ CO BOX 2608, Houston, TX 77252-2608; 1981;60:143–144.

36. Beychok MR. Aqueous wastes from petroleum and petrochemical plants. Wiley; 1967.

37. Ras MR, Borrull F, Marcé RM. Determination of volatile organic sulfur compounds in the air at sewage management areas by thermal desorption and gas chromatography-mass spectrometry. *Talanta*. Elsevier; 2008;74:562–569.

38. Fredericks E, Harlow G. Determination of mercaptans in sour natural gases by gas liquid chromatography and microcoulometric titration. *Anal. Chem.* ACS Publications; 1964;36:263–266.

39. Gerards R, Gevaert D, Vriens L. Biotreatment of waste gases with full-scale seghobioclean systems. *Odours & VOC's*. 1994;1.

40. Chélu G, Nominé M. Characterization and control of odoriferous pollutants in process. In: Vigneron, S., Hermia, J. and Chaouki, J., editor. Elsevier Science B.V.; 1984. p. 397–405.

41. Sivelä S. Dimethyl sulphide as a growth substrate for an obligately chemolithotrophic Thiobacillus. Societas Scientiarum Fennica; 1980.

42. Ignatz-Hoover F, To B, Rodgers B. Rubber Compounding: Chemistry and Applications. *Rubber Compounding: Chemistry and Applications*. Marcel Dekker New York; 2004.

43. Weast RC. CRC handbook of chemistry and physics. CRC Press, Boca Raton; 1986.

44. Crampton M. The Chemistry of the Thiol Group: Part 1. Patai, S., editor. Acidity and Hydrogen Bonding. New York, NY: John Wiley & Sons; 1974. p. 379–415.

45. Steudel R. The chemistry of organic polysulfanes RS (n)-R (n> 2). *Chem. Rev.* 2002;102:3905.

46. Mitchell SC. Biological interactions of sulfur compounds. CRC Press; 2003.

47. Koval' I. Reactions of thiols. *Russ. J. Org. Chem.* Springer; 2007;43:319–346.

48. Van Leerdam RC, Bosch PLF, Lens PNL, Janssen AJH. Reactions between methanethiol and biologically produced sulfur. *Environ. Sci. Technol.* 2011;45:1320–1326.

49. Jocelyn PC. Biochemistry of the SH Group. Academic Press London; 1972.

50. Nedolya NA, Trofimov BA. Sulfur-Containing Vinyl Ethers. *Sulfur reports*. Taylor & Francis; 1994;15:237–310.

51. Tangerman A, Winkel EG. Volatile sulfur compounds as the cause of bad breath: a review. *Phosphorus, Sulfur, and Silicon and the Related Elements*. Taylor & Francis; 2013;188:396–402.

52. Przyjazny A, Janicki W, Chrzanowski W, Staszewski R. Headspace gas chromatographic determination of distribution coefficients of selected organosulphur compounds and their dependence on some parameters. *J. Chromatogr. A*. Elsevier; 1983;280:249–260.

53. Green DW, others. Perry's chemical engineers' handbook. McGraw-hill New York; 2008.

54. Taylor K, Wick C, Castada H, Kent K, Harper WJ. Discrimination of Swiss cheese from 5 different factories by high impact volatile organic compound profiles determined by odor activity value using selected ion flow tube mass spectrometry and odor threshold. *Journal of food science*. Wiley Online Library; 2013;78:C1509–C1515.

55. Ruth JH. Odor thresholds and irritation levels of several chemical substances: a review. *Am. Ind. Hyg. Assoc. J.* Taylor & Francis; 1986;47:A–142.

56. Løkke MM, Edelenbos M, Larsen E, Feilberg A. Investigation of volatiles emitted from freshly cut onions (Allium cepa L.) by real time proton-transfer reaction-mass spectrometry (PTR-MS). *Sensors*. Molecular Diversity Preservation International; 2012;12:16060–16076.

57. TLVs® and BEIs®Threshold Limit Valuesfor Chemical Substancesand Biological Exposure Indices [Internet]. Available from: http://www.acgih.org/.
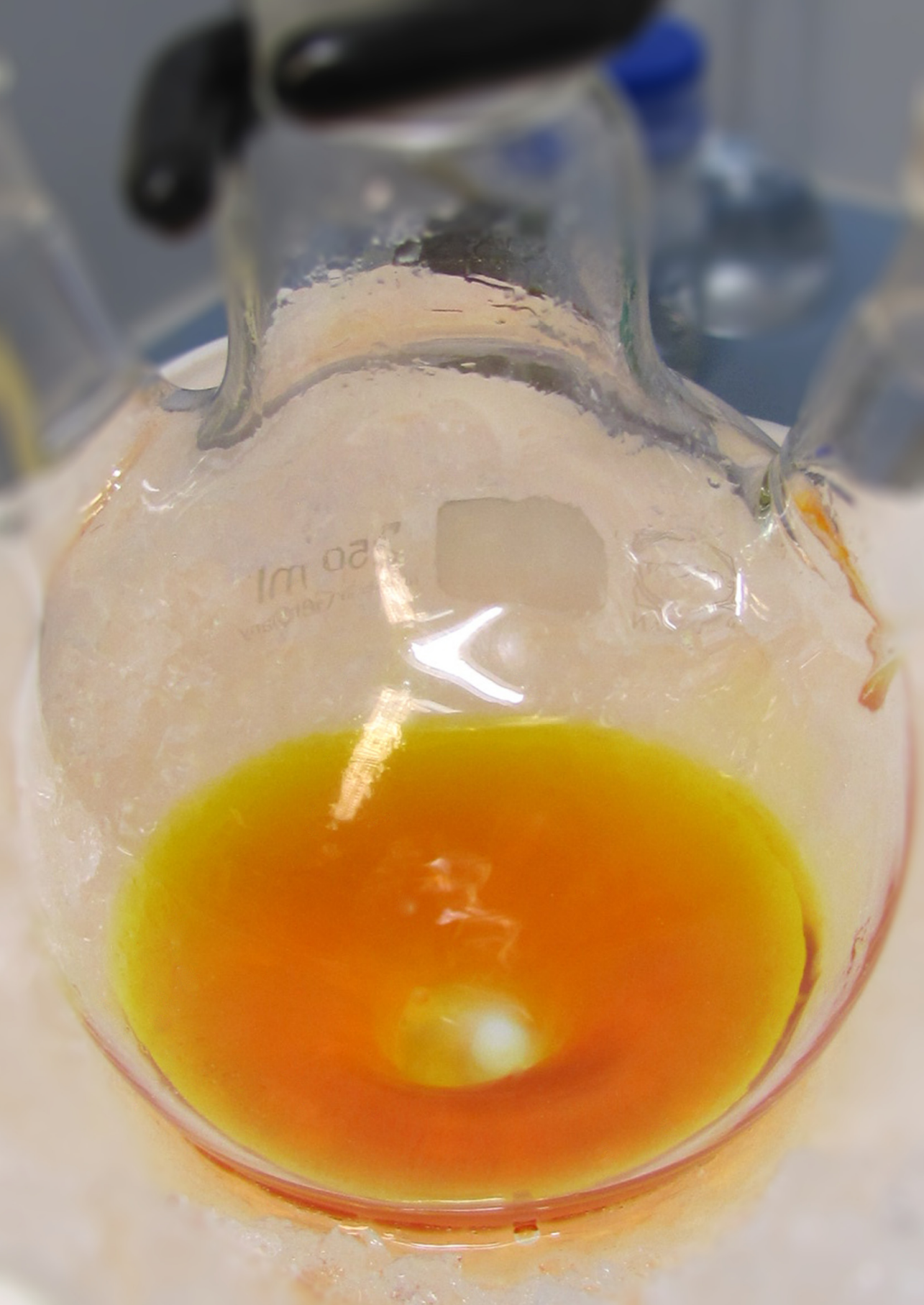
1

58. GPS Safety Summary: Methanethiol [Internet]. Available from: http://corporate.evonik.de/_layouts/Websites/Internet/DownloadCenterFileHandler.ashx?fileid=1155.

59. Fairchild E, Stokinger H. Toxicologic studies on organic sulfur compounds. I. Acute toxicity of some aliphatic and aromatic thiols (mercaptans). *American Industrial Hygiene Association Journal*. 1958;19:171.

60. National Technical Information Service. Vol. OTS0540990.

61. The Good Scents Company Information System [Internet]. Available from: http://www.thegoodscentscompany.com/.

62. Finkelstein A, Benevenga NJ. The effect of methanethiol and methionine toxicity on the activities of cytochrome c oxidase and enzymes involved in protection from peroxidative damage. *J. Nutr.* 1986;116:204–215.

63. Park C-M, Weerasinghe L, Day JJ, Fukuto JM, Xian M. Persulfides: current knowledge and challenges in chemistry and chemical biology. *Molecular BioSystems*. Royal Society of Chemistry; 2015.

64. Conte ML, Carroll KS. The chemistry of thiol oxidation and detection. *Oxidative Stress and Redox Regulation*. Springer; 2013. p. 1–42.

65. Adib H, Sharifi F, Mehranbod N, Kazerooni NM, Koolivand M. Support Vector Machine based modeling of an industrial natural gas sweetening plant. *J. Nat. Gas Sci. Eng.* Elsevier; 2013;14:121–131.

66. Eow JS. Recovery of sulfur from sour acid gas: a review of the technology. *Environ. Prog.* 2002;21:143–162.

67. Blauwhoff P, Kamphuis B, Swaaij W van, Westerterp K. Absorber design in sour natural gas treatment plants: Impact of process variables on operation and economics; Absorberentwurf für Anlagen zur Behandlung von sauren Erdgasen: Einfluss Prozessparameter auf Betriebsführung und Prozesswirtschaftlichkeit. *Chem. Eng. Process.* Elsevier Sequoia; 1985;19:1–25.

68. Abedini R, Salooki MK, Ghasemian S. Modeling and simulation of condensed sulfur in catalytic beds of CLAUS process: rapid estimation. *Chemical Engineering Research Bulletin*. 2010;14:110–114.

69. Superclaus Process: [Internet]. Available from: http://www.jacobs.com/uploadedFiles/wwwjacobscom/20_Learn_About_Us/25_Products/253_Comprimo_Sulfur_Solutions/Technologies/Handout%20Jacobs%20CSS%20-%20SUPERCLAUS%20Process.pdf.

70. Scot process: [Internet]. Available from: http://s02.static-shell.com/content/dam/shell/static/globalsolutions/downloads/products-services/licensed-technologies/factsheet-scot-screen.pdf.

71. Steudel R. Mechanism for the formation of elemental sulfur from aqueous sulfide in chemical and microbiological desulfurization processes. *Ind. Eng. Chem. Res.* ACS Publications; 1996;35:1417–1423.

72. Merichem Liquid hydrocarbon-treating Technologies [Internet]. Available from: https://s04.static-shell.com/content/dam/shell/static/globalsolutions/downloads/products-services/licensed-technologies/fact-sheet-merichem.pdf.

73. Merichem [Internet]. Available from: http://www.merichem.com.

74. Bloch HP. Segment 1: Gas Processing. *Compressors and Modern Process Applications*. Wiley Online Library; 157–208.

75. Greaney MA, Wang K, Wang FC. Electrochemical treatment of heavy oil streams followed by caustic extraction. Google Patents; 2013.

76. Jensen AB, Webb C. Treatment of H$_2$S-containing gases: A review of microbiological alternatives. *Enzyme and Microbial Technology*. Elsevier; 1995;17:2–10.

77. Kennes C, Rene ER, Veiga MC. Bioprocesses for air pollution control. *J. Chem. Technol. Biotechnol.* Wiley Online Library; 2009;84:1419–1436.

78. Kennes C, Montes M, López ME, Veiga MC. Waste gas treatment in bioreactors: environmental engineering aspects This article is one of a selection of papers published in this Special Issue on Biological Air Treatment. *Can. J. Civ. Eng.* NRC Research Press; 2009;36:1887–1894.

79. Iliuta I, Iliuta M, Larachi F. Hydrodynamics modeling of bioclogging in waste gas treating trickle-bed bioreactors. *Ind. Eng. Chem. Res.* . ACS Publications; 2005;44:5044–5052.

80. Oh Y-S, Bartha R. Design and performance of a trickling air biofilter for chlorobenzene and o-dichlorobenzene vapors. *Appl. Environ. Microbiol.* Am Soc Microbiol; 1994;60:2717–2722.

81. Fortuny M, Guisasola A, Casas C, Gamisans X, Lafuente J, Gabriel D. Oxidation of biologically produced elemental sulfur under neutrophilic conditions. *J. Chem. Technol. Biotechnol.* Wiley Online Library; 2010;85:378–386.

82. Van Groenestijn J, Van Heiningen W, Kraakman N. Biofilters based on the action of fungi. *Water Sci. Technol.* 2001;44:227–232.

83. Kennes C, Veiga MC. Inert filter media for the biofiltration of waste gases-characteristics and biomass control. *Rev. Environ. Sci. Biotechnol.* Springer; 2002;1:201–214.

84. Mendoza J, Prado O, Veiga M, Kennes C. Hydrodynamic behaviour and comparison of technologies for the removal of excess biomass in gas-phase biofilters. *Water Res.* Elsevier; 2004;38:404–413.

85. Cline C, Hoksberg A, Abry R, Janssen AJH. Biological Process for H$_2$S Removal from Gas Streams: The Shell-Paques/THIOPAQ^{TM} Gas Desulfurization Process. *Proceedings of the Laurance Reid Gas Conditioning Conference*. 2003. p. 1–18.

86. Van den Bosch PLF, van Beusekom OC, Buisman CJN, Janssen AJH. Sulfide oxidation at halo-alkaline conditions in a fed-batch bioreactor. *Biotechnol. Bioeng.* Wiley Online Library; 2007;97:1053–1063.

87. Janssen AJH, UOP BA, Plaines D, Kijlstra S. New Developments of The Thiopaq process for The Removal of H$_2$S from Gaseous Streams. *Preprints of Sulphur 2000 Conference*. 2000;29:179–187.

88. Alcántara S, Velasco A, Muñoz A, Cid J, Revah S, Razo-Flores E. Hydrogen sulfide oxidation by a microbial consortium in a recirculation reactor system: sulfur formation under oxygen limitation and removal of phenols. *Environ. Sci. Technol.* ACS Publications; 2004;38:918–923.

89. Klok J, de Graaff M, van den Bosch PLF, Boelee NC, Keesman KJ, Janssen AJH. A physiologically based kinetic model for bacterial sulfide oxidation. *Water Res.* Elsevier; 2013;47(2):483–492.

90. Janssen AJH, Meijer S, Bontsema J, Lettinga G. Application of the redox potential for controling a sulfide oxidizing bioreactor. *Biotechnol. Bioeng.* Wiley Online Library; 1998;60:147–155.

91. Janssen A, De Keizer A, Lettinga G. Colloidal properties of a microbiologically produced sulphur suspension in comparison to a LaMer sulphur sol. *Colloids and Surfaces B: Biointerfaces*. Elsevier; 1994;3:111–117.

92. Jam BJ, Shekari F, Zangani E, others. Application of bio-sulfur fertilizer and seed pretreatment with salicylic acid improved photosynthetic parameters of safflower. *International Journal of Agronomy and Plant Production*. Victor Quest Publications; 2013;4:3068–3075.

93. Chen KY, Morris JC. Kinetics of oxidation of aqueous sulfide by oxygen. *Environ. Sci. Technol.* ACS Publications; 1972;6:529–537.

94. Giggenbach W. Optical spectra and equilibrium distribution of polysulfide ions in aqueous solution at 20. deg. *Inorg. Chem.* ACS Publications; 1972;11:1201–1207.

95. Steudel R, Holdt G, Nagorka R. On the Autoxidation of Aqueous Sodium Polysulfide. *Zeitschrift für Naturforschung B*. 1986;41:1519–1522.

96. Kleinjan WE, Lammers JNJJ, de Keizer A, Janssen AJH. Effect of biologically produced sulfur on gas absorption in a biotechnological hydrogen sulfide removal process. *Biotechnology and bioengineering*. Wiley Online Library; 2006;94:633–644.

97. Sorokin DY, Kuenen JG. Haloalkaliphilic sulfur-oxidizing bacteria in soda lakes. *FEMS Microbiol. Rev.* Wiley Online Library; 2005;29:685–702.

98. Sorokin DY, Foti M, Tindall B, Muyzer G. Desulfurispirillum alkaliphilum gen. nov. sp. nov., a novel obligately anaerobic sulfur-and dissimilatory nitrate-reducing bacterium from a full-scale sulfide-removing bioreactor. *Extremophiles*. Springer; 2007;11:363–370.

99. Sorokin D, van den Bosch PLF, Abbas B, Janssen AJH, Muyzer G. Microbiological analysis of the population of extremely haloalkaliphilic sulfur-oxidizing bacteria dominating in lab-scale sulfide-removing bioreactors. *Appl. Microbiol. Biotechnol.* Springer; 2008;80:965–975.

100. Kamyshny A, Goifman A, Gun J, Rizkov D, Lev O. Equilibrium distribution of polysulfide ions in aqueous solutions at 25 C: a new approach for the study of polysulfides' equilibria. *Environ. Sci. Technol.* ACS Publications; 2004;38:6633–6644.

101. Giggenbach W. Blue solutions of sulfur in water at elevated temperatures. *Inorg. Chem.* ACS Publications; 1971;10:1306–1308.

102. Van den Bosch PLF, Sorokin DY, Buisman CJ, Janssen AJH. The effect of pH on thiosulfate formation in a biotechnological process for the removal of hydrogen sulfide from gas streams. *Environ. Sci. Technol.* ACS Publications; 2008;42:2637–2642.

103. Sorokin DY, Muntyan MS, Panteleeva AN, Muyzer G. *Thioalkalivibrio sulfidiphilus* sp. nov., a haloalkaliphilic, sulfur-oxidizing gammaproteobacterium from alkaline habitats. *Int. J. Syst. Evol. Microbiol.* Soc General Microbiol; 2012;62:1884–1889.

104. Janssen AJH, Lens PNL, Stams AJM, Plugge CM, Sorokin DY, Muyzer G, Dijkman H, Van Zessen E, Luimes P, Buisman CJN. Application of bacteria involved in the biological sulfur cycle for paper mill effluent purification. *Sci. Total Environ.* Elsevier; 2009;407:1333–1343.

105. Sorokin DY, Banciu H, Robertson LA, Kuenen JG, Muntyan MS, Muyzer G. Halophilic and haloalkaliphilic sulfur-oxidizing bacteria. In: Rosenberg E. et al., editor. *The Prokaryotes*. Springer-Verlag: Berlin-Heidelberg; 2013. p. 529–554.

106. Banciu H, Sorokin DY, Kleerebezem R, Muyzer G, Galinski EA, Kuenen JG. Growth kinetics of haloalkaliphilic, sulfur-oxidizing bacterium *Thioalkalivibrio versutus* strain ALJ 15 in continuous culture. *Extremophiles*. Springer; 2004;8:185–192.

107. Muyzer G, Sorokin DY, Mavromatis K, Lapidus A, Clum A, Ivanova N, Pati A, d' Haeseleer P, Woyke T, Kyrpides NC. Complete genome sequence of "*Thioalkalivibrio sulfidophilus*" HL-EbGr7. *Stand. Genomic. Sci.* Genomic Standards Consortium; 2011;4:23.

108. Chen Z-W, Koh M, Van Driessche G, Van Beeumen JJ, Bartsch RG, Meyer TE, Cusanovich MA, Mathews FS. The structure of flavocytochrome c sulfide dehydrogenase from a purple phototrophic bacterium. *Science*. American Association for the Advancement of Science; 1994;266:430–432.

109. Sorokin DY, Lysenko AM, Mityushina LL, Tourova TP, Jones BE, Rainey FA, Robertson LA, Kuenen GJ. *Thioalkalimicrobium aerophilum* gen. nov., sp. nov. and *Thioalkalimicrobium sibericum* sp. nov., and *Thioalkalivibrio versutus* gen. nov., sp. nov., *Thioalkalivibrio nitratis* sp. nov. and *Thioalkalivibrio denitrificans* sp. nov., novel obligately alkaliphilic and obligately chemolithoautotrophic sulfur-oxidizing bacteria from soda lakes. *International journal of systematic and evolutionary microbiology*. Soc General Microbiol; 2001;51:565–580.

110. Visser JM, Robertson LA, Van Verseveld HW, Kuenen JG. Sulfur production by obligately chemolithoautotrophic thiobacillus species. *Appl. Environ. Microbiol.* Am Soc Microbiol; 1997;63:2300–2305.

111. Klok JBM, van den Bosch PLF, Buisman CJN, Stams AJM, Keesman KJ, Janssen AJH. Pathways of sulfide oxidation by haloalkaliphilic bacteria in limited-oxygen gas lift bioreactors. *Environ. Sci. Technol.* ACS Publications; 2012;46:7581–7586.

112. Prechel S, Sabo F. Intelligent biofilters: new control and monitoring techniques to optimise the efficiency of biological systems. *Biotechniques for air pollution control: proceedings of the international congress Biotechniques for Air Pollution Control: A Coruña, Spain, October 5-7, 2005*. 2005. p. 217–223.

113. Roosta A, Jahanmiri A, Mowla D, Niazi A. Mathematical modeling of biological sulfide removal in a fed batch bioreactor. *Biochem. Eng. J.* Elsevier; 2011;58:50–56.

114. Pandey SK, Kim K-H, Tang K-T. A review of sensor-based methods for monitoring hydrogen sulfide. *TrAC Trends Anal. Chem.* Elsevier; 2012;32:87–99

115. Tse Y-H, Janda P, Lam H, Lever A. Electrode with electropolymerized tetraaminophthalocyanatocobalt (II) for detection of sulfide ion. *Anal. Chem.* ACS Publications; 1995;67:981–985.

116. Jeroschewski P, Steuckart C, Kühl M. An amperometric microsensor for the determination of H2S in aquatic environments. *Anal. Chem.* ACS Publications; 1996;68:4351–4357.

117. Van den Bosch PL. Biological sulfide oxidation by natron-alkaliphilic bacteria: application in gas desulfurization. 2008.

118. Roman P, Yntema D, Bijmans MFM, Janssen AJH. Sensor system for spectrophotometric measurement of components and method therefore. NL Patent 2015580, Filed October 7, 2015.

119. Kennes C, Veiga MC. Air pollution prevention and control: bioreactors and bioenergy. Wiley Chichester; 2013.

120. Syed M, Soreanu G, Falletta P, Béland M, others. Removal of hydrogen sulfide from gas streams using biological processes - A review. *Can. Biosyst. Eng.* 2006;48:2.

121. Van den Bosch PLF, de Graaff M, Fortuny-Picornell M, van Leerdam RC, Janssen AJH. Inhibition of microbiological sulfide oxidation by methanethiol

and dimethyl polysulfides at natron-alkaline conditions. *Appl. Microbiol. Biotechnol.* Springer; 2009;83:579–587.

122. Van den Bosch PLF, Fortuny-Picornell M, Janssen AJ. Effects of methanethiol on the biological oxidation of sulfide at natron-alkaline conditions. *Environ. Sci. Technol.* ACS Publications; 2009;43:453–459.

1

1

Quantification of individual polysulfides in lab-scale and full-scale desulfurization bioreactors

2

Abstract

Environmental pollution caused by the combustion of fuel sources containing inorganic and organic sulfur compounds such as hydrogen sulfide (H_2S) and thiols, is a global issue as it leads to SO_2 emissions. To remove H_2S from gas streams such as liquefied petroleum gas (LPG), biological processes can be applied. In these processes, polysulfide anions (S_x^{2-}) play a significant role as they enhance the dissolution of H_2S and act as intermediates in the biological oxidation of hydrogen sulfide ion to elemental sulfur. Despite their important role, the distribution of the various polysulfide species in full-scale biodesulfurization systems has not yet been reported. With conventionally applied spectrophotometric analysis it is only possible to determine the total concentration of S_x^{2-}. Moreover, this method is very sensitive to matrix effects. In this paper, we apply a method that relies on the derivatization of S_x^{2-} to dimethyl polysulfanes. Owing to the instability of higher dimethyl polysulfanes (Me_2S_4 to Me_2S_8), standards are not commercially available and had to be prepared by us. We present a simplified quantification method for higher dimethyl polysulfanes by calculating HPLC-UV response factors based on the addition of internal standards. The method was subsequently used to assess the distribution of polysulfide anions in both a lab-scale and a full-scale biodesulfurization unit. We found that the average chain length of polysulfides strongly depends on the process conditions and a maximum of 5.33 sulfur atoms per polysulfide molecule was found. Results of this study are required by mechanistic and kinetic models that attempt to describe product selectivity of sulfide oxidizing bioreactors.

2.1. Introduction

Inorganic polysulfides (S_x^{2-}) and their methylated forms (R_2S_x) play a significant role in biological and geological sulfur cycles [1]. Polysulfides are constituents of many biologically active compounds and are therefore involved in many biomechanisms [2,3]. Their biological significance in enzyme chemistry has been extensively reviewed [4]. Moreover, polysulfides play a crucial role in lithium-sulfur batteries as they increase the capability rate and the range of operating temperatures [5], they are key reactants in industrial processes, e.g. in bioleaching of metal sulfides [6]. Polysulfides also are important in gas biodesulfurization processes that are used to remove toxic hydrogen sulfide (H_2S) and organic sulfur compounds from a variety of gas streams (e.g. biogas, natural gas and synthesis gas from coal gasification processes). They enhance the dissolution of H_2S by increasing the physical dissolution of sulfide due to equilibrium reactions [7] and can be biologically oxidized to elemental sulfur [8–10]. A two-step biological treatment process is often used to remove hydrogen sulfide from sour gas streams [11]. In the first step, H_2S is absorbed in a mildly alkaline solution; in the second step, sulfur-oxidizing bacteria oxidize under oxygen-limiting conditions the hydrogen sulfide ions (HS^-), hereafter referred to as "sulfide", to elemental biosulfur. The exact mechanism of the underlying biochemical reactions is not yet fully understood but the overall reaction can be written in the following simplified form:

$$HS^- + 0.5\ O_2 \rightarrow 1/8\ S_8 + OH^- \qquad\qquad (1)$$
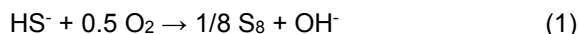
It has been shown that the biologically produced sulfur particles have different properties than standard yellow sulfur flower (S_8). The formation of biosulfur in the periplasm of the organism relies on the transformation of amorfous sulfur compounds into biosulfur crystals that exhibit a hydrophilic character whereas standard orthorhombic, hydrophobic S_8 crystals are hydrophobic [12,13]. At these conditions, polysulfide anions (S_x^{2-}) are easily produced from the abiotic reaction between sulfide and the formed biosulfur particles as was described by Kleinjan et al. (2005) [14] (Eq. 2). In a biotechnological process for H_2S removal this reactions takes place in the bottom section of the gas absorber before the sulfide loaded liquid enters the bioreactor [15].

$$HS^- + (x\text{-}1)/8\ S_8 \leftrightarrow S_x^{2-} + H^+ \qquad\qquad (2)$$
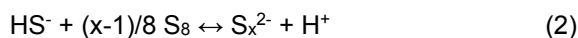
The product selectivity of the biological oxidation of sulfide is governed by the oxidation-reduction potential (ORP) [15,16]. Any change in the sulfide-to-oxygen supply ratio influences the sulfide and polysulfide concentrations, and consequently affects the selectivity for S_8, $S_2O_3^{2-}$ and SO_4^{2-} formation [15].

In aqueous solutions, polysulfide anions are present as complex mixtures of S_x^{2-} with $x \geq 2$. Since the various polysulfide species rapidly establish chemical equilibrium (Eq. 3) [17], they cannot be separated by ion exchange chromatography [18]. Their spectrophotometric determination at a wavelength of 285 nm is possible, as described earlier by Teder (1967) [19], but this indirect method still only determines the total polysulfide concentration. Another disadvantage of this method is the significant influence of the aqueous matrix. For example, in the presence of thiols (R-SH), diorgano polysulfanes (R-S_x-R) are formed, which will also absorb light at a wavelength of 285 nm.

$$2 \, S_x^{2-} \leftrightarrow S_{x-1}^{2-} + S_{x+1}^{2-}, \, x \geq 2 \qquad\qquad (3)$$
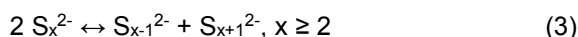
Van Leerdam et al. (2011) [20] studied the combined formation of S_x^{2-} and dimethyl polysulfanes from reaction between methanethiol and biosulfur. However, this study concerned only a qualitative analysis as no quantification of the polysulfide species was possible.

The aim of current study is to test whether a known method for the measurement of polysulfide species in surface water and seawater [21] is also suitable for high saline matrices (up to 1.5 M). And then, to describe the speciation of the individual polysulfide anions in samples obtained from lab-scale as well as full-scale biodesulfurization systems. In contrast to small lab-scale reactors with spatially homogeneous reactor conditions, spatial and temporal heterogeneity can occur in full-scale reactors which will lead to changing ORP values which in turn will have an impact on the overall product selectivity.

2.2. Materials and methods

2.2.1. Experimental setup

The experiments were performed in a glass falling film absorber that is integrated with a bioreactor (Fig. 1). Hydrogen sulfide (99.8 vol.%, 0-17 mL min^{-1}) and nitrogen gas (99.995 vol.%, 0-350 mL min^{-1}) were supplied to the gas absorber

using mass flow controllers (type EL-FLOW, model F-201DV-AGD-33-K/E, Bronkhorst, the Netherlands). The same type of mass flow controller was used to feed oxygen gas (99.995 vol.%, 0-30 mL min^{-1}) to the reactor. Carbon dioxide (99.99 vol.%) was fed to the inlet of the gas absorber using solenoid valve (125318, Burkert, Germany). The oxygen and carbon dioxide supply were controlled with a multiparameter transmitter (Liquiline CM442; Endress+Hauser, Germany) based on the signals from the ORP sensor with an integrated Ag/AgCl reference electrode (Orbisint CPS12D; Endress+Hauser, Germany) and the pH sensor (Orbisint CPS11D; Endress+Hauser, Germany). Liquid recirculation (0.166 L min^{-1}) between the reactor and the gas absorber was assured by a gear pump (EW-74014-40, Cole-Parmer, USA). A gas compressor (N-840, KNF Laboport, USA) continuously recycled the gas phase (34 L min^{-1}). The reactor and the gas absorber were kept at 35 °C with a thermostat bath (DC10-P5/U, Haake, Germany). Liquid samples were taken for analysis from two sampling points, located at the outlet of the gas absorber and in the bioreactor (Fig. 1).
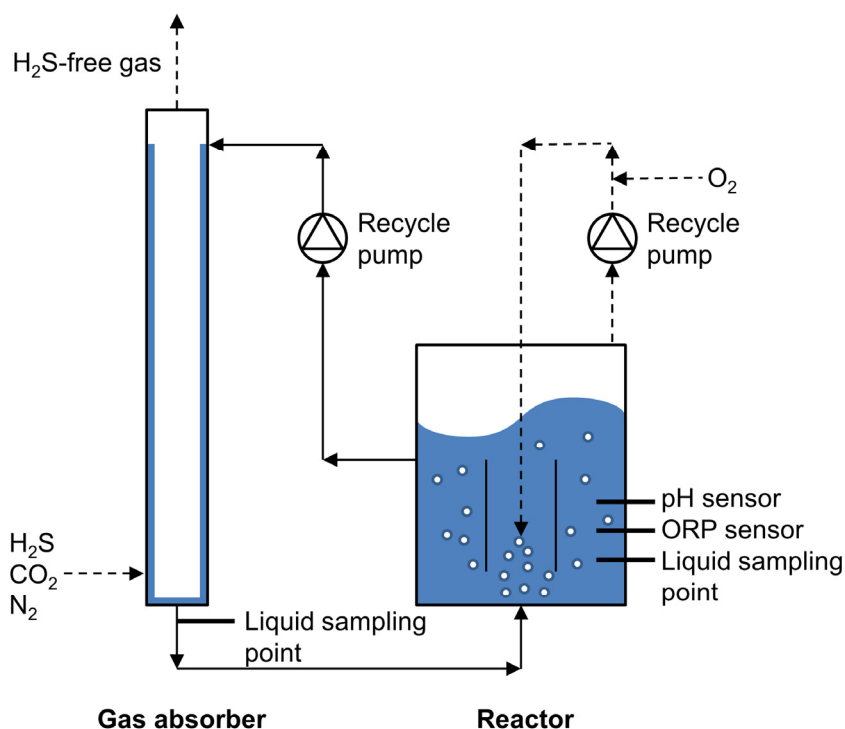
Figure 1. Flow scheme of the experimental setup used for lab-scale experiments.

2.2.2. Medium composition

The carbonate/bicarbonate medium was buffered with 0.051 M Na_2CO_3, 0.698 M $NaHCO_3$ and 0.700 M $KHCO_3$. The medium contained 1.0 g K_2HPO_4, 6.0 g NaCl, 0.20 g $MgCl_2 \times 6\ H_2O$, and 0.60 g urea, each per 1 L of demineralized water, and trace elements as described elsewhere [22]. The pH of the medium was 8.50 ± 0.01 at 35 °C.

2.2.3. Inoculum

The reactor was inoculated with centrifuged biomass (1L before centrifugation) from a laboratory bioreactor. The original biomass came from a full-scale system for gas biodesulfurization located at Industriewater Eerbeek B.V. in the Netherlands [11]. Bacteria isolated from this reactor were recently identified as belonging to the genus *Thioalkalivibrio* [23].

2.2.4. Experimental design

The experiments were performed in duplicate and at four different ORP values (-250, -350, -410 and -450 mV). Each experiment lasted for 24 hours during which sampling was done in triplicate at regular time intervals. To maintain the desired ORP value, pure oxygen gas was supplied to the gas recirculation loop in the bioreactor. The ORP value was the key control variable parameter during each experiment. Despite the fact that the medium was highly buffered, pH control was necessary because of the continuous stripping of carbon dioxide from the gas absorber. To maintain the desired pH, carbon dioxide was supplied to the inlet of the gas absorber. Table 1 shows an overview of the process properties and experimental conditions.

2.2.5. Sampling from a full-scale unit

Sampling also took place at the full-scale installation for biogas desulfurization at Industriewater Eerbeek, the Netherlands, where the wastewater from three paper mills is treated in an anaerobic sludge blanket (UASB) reactor [11]. Liquid samples were taken from the loaded wash water after the gas absorber and from

the bioreactor. They were collected in glass bottles that were filled without leaving a headspace. Time of transport of the samples to the laboratory was about two hours. Analyses of samples from full-scale unit were carried out immediately after arrival in the lab.

Table 1. Overview of the process conditions and properties of the lab-scale system.

Properties and process conditions				
Reactor			*Falling Film Absorber*	
Total reactor volume [L]	2.3	Temperature [°C]	35
pH:	8.5	Column diameter [m]	0.011
Salinity [M]:		Column height [m]	0.8
Na^+	0.8	Total gas flow [$Nm^3 s^{-1}$]	2.8×10^{-6}
K^+	0.7	H_2S loading [$Nm^3 s^{-1}$]	2.5×10^{-8}
Temperature [°C]	35	Liquid flow [$Nm^3 s^{-1}$]	2.8×10^{-6}
H_2S loading [$mM\,d^{-1}$]	38.4	Gas velocity [$m\,s^{-1}$]	0.035
ORP set points [mV]	(O_2/H_2S)	Liquid velocity [$m\,s^{-1}$]	0.186
Run 1 -250	(2.18)		
Run 2 -350	(1.51)		
Run 3 -410	(0.63)		
Run 4 -450	(0.53)		

2.2.6. Analytical techniques

All reagents were of analytical grade unless stated otherwise.

Sulfide was measured as total sulfide (S^{2-}_{tot}) using a methylene blue method with a cuvette test (LCK653, Hach Lange, USA). Sulfide analysis was carried out immediately after sampling (or arrival in the lab), filtration over a 0.22 µm syringe filter (Millex G5 filter unit; Merck, Amsterdam, the Netherlands) and dilution with oxygen-free Milli-Q water at least two times.

Dimethyl disulfide (DMDS), dimethyl trisulfide (DMTS) and higher dimethyl polysulfanes (Me_2S_4 to Me_2S_8) were determined with an HPLC equipped with a UV detector (Dionex UltiMate 3000RS, USA). The separation of these fractions was performed with an Agilent column (Zorbax Extend-C18 1.8 µm, 2.1 x 50 mm) at 20 °C; the UV detector was set to 210 nm. The mobile phase initially consisted of a mixture of methanol (15 vol.%) and water (85 vol.%). At 0.72 min, a convex gradient developed that led to the methanol concentration of 85% at 10 min. During the next 10 min, the conditions were isocratic; in the following 5 min, the methanol concentration decreased to 15%. In the final 5 min, the conditions were isocratic. The flow rate was maintained at 0.371 mL min^{-1} and the injection volume was 1.25 µL.

The analysis method for polysulfide anions requires a derivatization of S_x^{2-} using methyl triflate (≥98% pure, Sigma-Aldrich, the Netherlands) to form more stable dimethyl polysulfanes (Eq. 4) [21].

$$S_x^{2-} + 2\, CF_3SO_3Me \rightarrow Me_2S_x + 2\, CF_3SO_3^- \qquad (4)$$

Samples for polysulfide anions analyses were taken with glass syringes only (1010 TLL SYR, Hamilton, USA) to avoid significant losses of any compounds due to adsorption onto plastic pipette tips etc. Sample filtration over a 0.7 µm glass fiber filter (AP40, 25 mm, Millipore, USA) enclosed in a metal housing (Microsyringe Filter Holder 25 mm, Merck) and subsequent derivatization was carried out immediately after sampling (or arrival in the lab) in a glove box to prevent the ingress of oxygen (oxygen was less than 0.1 vol.%). Separate S_x^{2-} analyses before and after filtration, carried out in triplicate, indicated that the filtration step has no impact on the total sum and the average chain length of the polysulfides (x_{av}) with the relative standard deviation (RSD) below 3% and 2%, respectively. After filtration step, sample was mixed with 60 µL methyl triflate in methanol-water medium as described elsewhere [21]. Depending on the type of reactor sample, salt precipitates sometimes occurred after addition of methanol. This, however, had no influence on the total sum and the average chain length of polysulfides as confirmed in tests performed in 0.37, 0.75 and 1.5 M salt medium. For each of these salinities, samples were prepared in triplicate and then analyzed. The RSD for x_{av} and the total sum of polysulfides was below 2% and 3%, respectively. After derivatization step, the internal standard (dibenzo-a,h-anthracene, Supelco

46

Analytical, USA) in benzene (Sigma-Aldrich, the Netherlands) was added to a final concentration of 8 mg L^{-1}. To remove the salt precipitates, we centrifuged the samples under anaerobic conditions in glass vials at 3300 x *g* for 10 min. Supernatant was analyzed immediately after centrifugation.

2.2.7. Polysulfide standards preparation

Only DMDS and DMTS are commercially available, as higher dimethyl polysulfanes are unstable. We prepared solutions containing higher dimethyl polysulfanes according to the following steps.

1) A mixture of dimethyl polysulfanes ranging from Me_2S_2 to Me_2S_{11} was synthesized according to a description given by Rizkov et al. (2004) [24] with the exceptions that hydrazine hydrate was used instead of hydrazine sulfate and that no elemental sulfur precipitation occurred in the final step.

2) The dimethyl polysulfanes Me_2S_4 to Me_2S_8 were separated using high-performance liquid chromatography (Dionex UltiMate 3000RS, USA) with an Alltima C18 column (Fisher Scientific; 10 μm, 10 x 250 mm) at 20 °C; the UV detector was set to 210 nm. Elution was accomplished with an isocratic mixture consisting of 95:5 (v/v) methanol:water at a flow rate of 2 mL min^{-1} and an injection volume of 25 μL. The separated fractions were stable for 24 hours in the case of Me_2S_{4-6} and 6 hours in the case of Me_2S_{7-8} (data not shown). Acetonitrile and water were tested as alternative mobile phases for the separation of dimethyl polysulfanes; however, all fractions were unstable at these conditions.

3) Determination of the dimethyl polysulfane concentration in each fraction was carried out after oxidation with nitric acid in a high-pressure vessel for 3 hours at 180 °C. The samples were analyzed for their total sulfur content with an inductively coupled plasma optical emission spectrometer (ICP-OES) (Perkin Elmer, Optima 5300 DV, USA). Commercially available DMTS (Sigma-Aldrich, the Netherlands) was used to validate the method for determination of the dimethyl polysulfane concentration. The difference between the DMTS concentration of prepared solutions and the obtained results from ICP-OES analysis was below 1.5% in each of five replicates. Knowing the concentration of dimethyl polysulfanes, a three-point calibration curves were constructed from dilutions of the separated fractions.

2.2.8. Calculation of response factors

UV response factors (RF) to quantify higher dimethyl polysulfanes for which no standards are available were determined through calibration with an internal standard (dibenzo-a,h-anthracene), according to Equation 5.

$$\frac{A_{Sx}}{c_{Sx}} = \mathrm{RF}\,\frac{A_{IST}}{c_{IST}} \tag{5}$$

A_{Sx} and A_{IST} are the peak areas of dimethyl polysulfane and the internal standard, respectively. C_{Sx} and C_{IST} are the dimethyl polysulfane and the internal standard concentration in the sample. Table 2 lists the derived RFs for the quantification of Me_2S_4 to Me_2S_8. Detection limits were calculated including residual standard deviations and standard deviations of the estimated slopes (Table 2) [25].

Table 2. Response factors (RF) with corresponding standard deviation (σ) and measuring ranges for various dimethyl polysulfanes relative to internal standard dibenzo-a,h-anthracene.

Compound	RF (σ)	Measuring range [mg L^{-1}]
Me_2S_4	1.0 (0.1)	1.8 - 12.0
Me_2S_5	0.97 (0.07)	1.2 - 18.2
Me_2S_6	0.59 (0.04)	0.7 - 6.1
Me_2S_7	0.38 (0.02)	0.7 - 11.0
Me_2S_8	0.178 (0.007)	1.2 - 7.1

2.3. Results and discussion

In our laboratory-scale experiments, polysulfide anions were present in the liquid outlet of the gas absorber at all molar O_2/H_2S supply ratios (0.53 - 2.18 mol mol^{-1}), whereas they could only be detected in the reactor at the lowest ratio (0.53 mol mol^{-1}). As a result of chemical and biological oxidation processes, the total sum of polysulfides in the reactor was 15% lower than in the outlet of the gas absorber (i.e. 3.43 ± 0.05 mM S *v.* 2.93 ± 0.05 mM S).

At an O_2/H_2S supply ratio of 0.53 mol mol^{-1}, too little dissolved oxygen was available to oxidize all the sulfide; therefore, the sulfide concentration in the reactor was substantially higher under these conditions than at higher O_2/H_2S supply ratios, leading to the formation of more polysulfides (Eq. 2). For the same reason, the concentration of sulfide and polysulfide anions in the outlet of the gas absorber decrease at increasing O_2/H_2S supply ratios (Fig. 2).
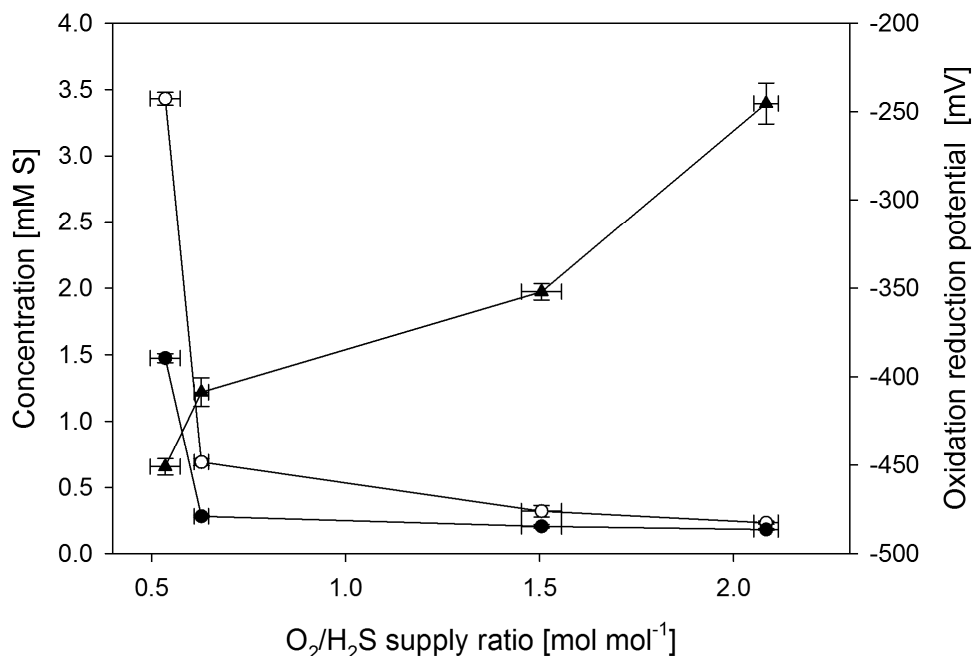
Figure 2. Polysulfide (○) and sulfide (●) concentration in the outlet of the gas absorber at different oxidation reduction potentials (▲) and different molar O_2/H_2S supply ratios to the reactor. The H_2S supply was 38.4 mM d^{-1} for all experiments. The pH for these measurements was 8.5.

Pentasulfide was the most predominant polysulfide compound at all measured ORP values (Fig. 3), which formed according to Eq. 6 and 7:

$$HS^- + S_8 \leftrightarrow S_9^{2-} + H^+ \tag{6}$$

$$S_9^{2-} + HS^- \rightarrow 2\,S_5^{2-} + H^+ \tag{7}$$
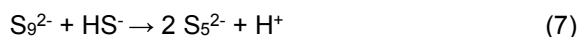
These pentasulfide ions form complex mixtures of S_x^{2-} with $x \geq 2$ (Eq. 3). As pentasulfide was in equilibrium with other polysulfide species, the second most dominant anions were tetrasulfide and hexasulfide (followed by trisulfide and heptasulfide). The percentage of tetrasulfide ions constantly increased with increasing ORP values, whereas the higher polysulfide anions became less dominant at high O_2/H_2S supply ratios (Fig. 3). An explanation for this observation cannot be provided.

2
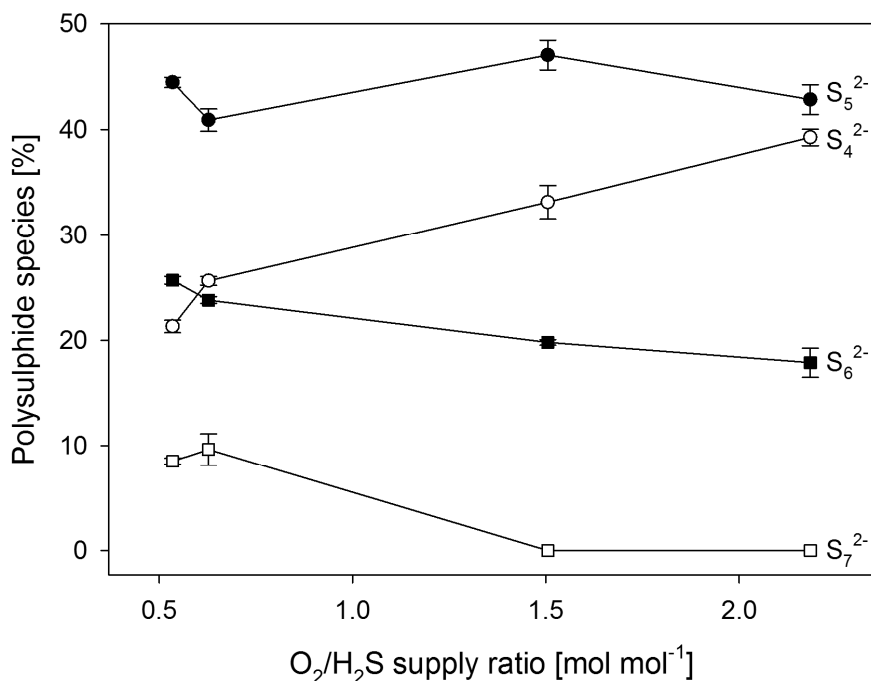
Figure 3. Percentage of polysulfide species as a function of molar O_2/H_2S supply ratio. The applied sulfide load was 38.4 mM d^{-1}, pH=8.5, T=35 °C.

The average chain length can be calculated based on polysulfide speciation. In the liquid outlet of the gas absorber, the average polysulfide chain length decreased with increasing O_2/H_2S supply ratios (Fig. 4) what is related to increasing ORP values. At an ORP value of -450 mV, x_{av} in the reactor was determined to be 5.28 ± 0.02. This is in good agreement with the calculated value of x_{av} based on

50

a kinetic model by Kamyshny et al. (2004) [26], which is 5.33 at fully anaerobic conditions ($O_2/H_2S = 0$). Moreover, there was a good correlation ($R^2=0.987$) between x_{av} in the liquid outlet of the gas absorber and the molar O_2/H_2S supply ratios (Eq. 8).

$$x_{av} = -0.262 \cdot \frac{[O_2]}{[H_2S]} + 5.334 \qquad (8)$$
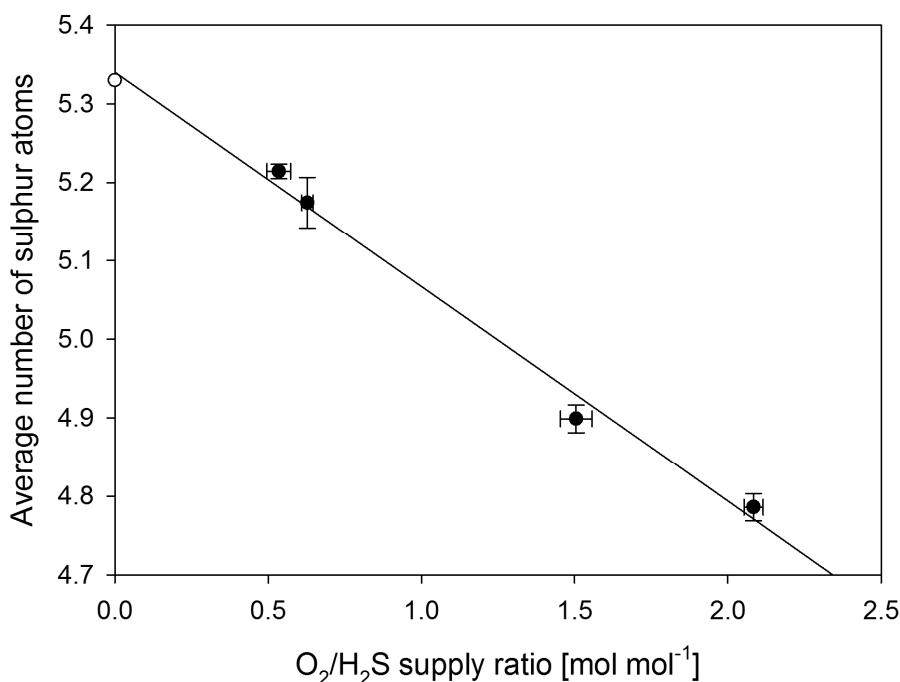
Figure 4. The average chain length at different molar O_2/H_2S supply ratios calculated based on speciation of polysulfide anions (●) and calculated based on kinetic model presented by Kamyshny et al. (2004) [26] for O_2-free conditions (○) with fitted regression line (solid). The H_2S load for all points was constant at 38.4 mM d^{-1}. The pH for these measurements was 8.5.

Several authors studied x_{av} under similar experimental conditions with respect to sulfide and oxygen loading rates, pH, salinity, temperature but with different analytical methods [12,24]. Kleinjan et al. (2005) [14] found the polysulfide average chain length to be 4.59 ± 0.31, which is lower compared with the results presented in this study. However, the large standard deviation in the results of Kleinjan

51

and coworkers indicate that their method is less accurate than the one presented here. In addition, their measurements were not carried out in anaerobic conditions which likely lowered the average chain length of the polysulfides, owing to oxidation. Van den Bosch et al. (2007) [15] reported a value of 5.9 for x_{av}, which is significantly higher than the values found by us. However, van den Bosch and colleagues used an indirect method to determine the average chain length, which may explain the different result.

Several parameters influence the speciation of polysulfides in desulfurization reactors. First, our results show that oxygen has an important effect. Above 180 °C, temperature also has a significant effect [27], but this is not a factor in biological gas desulfurization processes. No significant effect of salinity on S_x^{2-} speciation was found [15,21]. The method presented in this paper is not affected by high dissolved salt concentrations (up to 1.5 M), as confirmed by polysulfides analysis in different salinity samples (see Materials and methods). Moreover, pH does not affect the polysulfide speciation in the range in which polysulfides are stable (i.e. pH = 7 - 12) [26]. In situations in which pentasulfide is obtained from the reaction between sulfide and elemental sulfur (Eq. 2), the quantities of these substrates can be considered important factors as well. When elemental sulfur is not available in excess, a secondary reaction takes place, leading to a lower value of x_{av} (Eq. 9).

$$S_5^{2-} + HS^- \rightarrow 2\ S_3^{2-} + H^+ \tag{9}$$
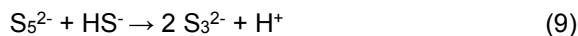
The nucleophilic attack of the disulfide and trisulfide anions on elemental sulfur particles promotes their dissolution, which leads to hexasulfide formation (Eq. 10).

$$S_2^{2-} + 0.5\ S_8 \leftrightarrow S_6^{2-} \tag{10}$$
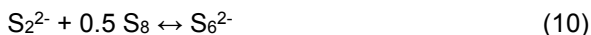
Then, the hexasulfide anion immediately disproportionates according to Eq. 3 resulting in an increase of the value of x_{av}.

In addition to samples from the lab-scale reactor, also samples from a full-scale biodesulfurization system were analyzed. To allow a like-for-like comparison only laboratory results for an O_2/H_2S supply ratio of 0.63 mol mol^{-1} were used because at these conditions both systems have the same overall redox value. The distribution of polysulfides after the gas absorber was similar for both systems (Fig. 5). The average polysulfide chain length in both systems was also similar, i.e. 5.18 ± 0.09 for the full-scale unit and 5.17 ± 0.03 for the lab setup. The trisulfide anion concentration was above the quantification limit (0.1 mg L^{-1})

in the full-scale unit. This can be explained by the higher volumetric H_2S loading in the full-scale unit which leads to higher pentasulfide concentrations that serves as the precursor for other polysulfides (Eq. 6 and 7). The total sum of polysulfides in the outlet of the gas absorber in the full-scale unit was almost eight times higher than in the laboratory version (0.69 ± 0.03 mM S *v.* 5.41 ± 0.39 mM S); this is also because of higher H_2S loading rates in the full-scale system. In both, full-scale and lab-scale bioreactor the O_2/H_2S supply ratio was above 0.63 mol mol^{-1} and the polysulfide concentrations were below the detection limit (Table 2).
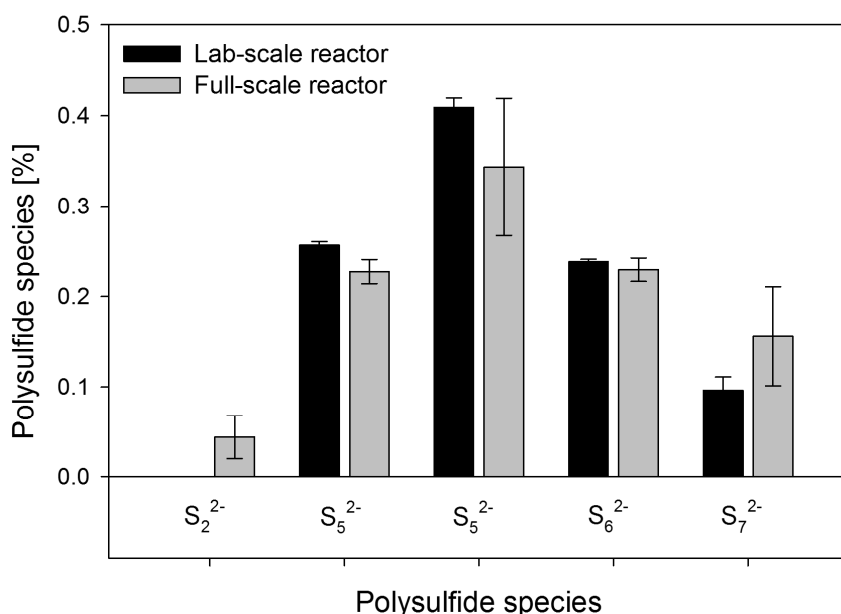
Figure 5. The distribution of polysulfide species in samples taken from the outlet of the gas absorber in the lab-scale setup at an oxidation reduction potential of -410 mV and taken from the full-scale unit for biological H_2S removal in Eerbeek (the Netherlands).

2.4. Conclusions

In summary, this paper describes the application of a known analytical method for dimethyl polysulfanes and polysulfides analysis at elevated salt levels. We present simplified quantification of higher dimethyl polysulfanes and S_x^{2-} after methylation by calculating response factors based on the regression of the calibration

2

curves with internal standard addition. The method can be used to monitor upset situations in gas biodesulfurization systems that contain thiols which are characterized by a steep increase in the polysulfide concentration. In such situations, conventionally applied spectrophotometric method is biased because of matrix effects. Moreover, the method may also be used to measure polysulfides in many other fields of science where S_x^{2-} can be present in high saline samples, e.g. bioelectrochemical or anaerobic sulfate reduction systems.

This investigation of polysulfide speciation shows that there is an increase in the average chain length with decreasing redox conditions in desulfurization bioreactors. In the absorber outlet, the polysulfide average chain length was 5.17 ± 0.03 at the commonly used ORP value of -410 mV [15]. This is the first study presenting the average chain length of polysulfides in biodesulfurization systems with such high accuracy. A comparison between the results for the laboratory and full-scale units shows that the distribution of polysulfide anions is highly comparable; this allows performance improvements of full-scale systems to be explored in bench-scale experiments. Based on the results described here and those presented elsewhere [26], it can be concluded that in the described systems, the maximum average number of sulfur atoms in polysulfide anions is 5.33. Presented values of average number of sulfur atoms in polysulfide species at different ORP values are required by mechanistic and kinetic models that attempt to describe product selectivity of sulfide oxidizing bioreactors [28,29].

Acknowledgements

References

1. Eckert B, Okazaki R, Steudel R, Takeda N, Tokitoh N, Wong M. Elemental sulfur and sulfur-rich compounds II. *Top. Curr. Chem.* Springer; 2003;231:32–98.
2. Griesbeck C, Schütz M, Schödl T, Bathe S, Nausch L, Mederer N, Vielreicher M, Hauska G. Mechanism of sulfide-quinone reductase investigated using site-directed mutagenesis and sulfur analysis. *Biochemistry.* ACS Publications; 2002;41:11552–11565.
3. Schippers A, Sand W. Bacterial leaching of metal sulfides proceeds by two indirect mechanisms via thiosulfate or via polysulfides and sulfur. *Appl. Environ. Microbiol*; 1999;65:319–321.
4. Mitchell SC. Biological interactions of sulfur compounds. CRC Press; 2003.
5. Mikhaylik YV, Akridge JR. Polysulfide shuttle study in the Li/S battery system. *J. Electrochem. Soc.* The Electrochemical Society; 2004;151:A1969–A1976.
6. Rohwerder T, Gehrke T, Kinzler K, Sand W. Bioleaching review part A. *Appl. Microbiol. Biotechnol.* Springer; 2003;63:239–248.
7. Kleinjan WE, Lammers JNJJ, de Keizer A, Janssen AJH. Effect of biologically produced sulfur on gas absorption in a biotechnological hydrogen sulfide removal process. *Biotechnol. Bioeng.* Wiley Online Library; 2006;94:633–644.
8. Sorokin DY, Kuenen JG. Haloalkaliphilic sulfur-oxidizing bacteria in soda lakes. *FEMS Microbiol. Rev.* Wiley Online Library; 2005;29:685–702.
9. Sorokin DY, Foti M, Tindall B, Muyzer G. *Desulfurispirillum alkaliphilum* gen. nov. sp. nov., a novel obligately anaerobic sulfur-and dissimilatory nitrate-reducing bacterium from a full-scale sulfide-removing bioreactor. *Extremophiles*. Springer; 2007;11:363–370.
10. Sorokin D, van den Bosch PLF, Abbas B, Janssen AJH, Muyzer G. Microbiological analysis of the population of extremely haloalkaliphilic sulfur-oxidizing bacteria dominating in lab-scale sulfide-removing bioreactors. *Appl. Microbiol. Biotechnol.* Springer; 2008;80:965–975.
11. Janssen AJH, Lens PNL, Stams AJM, Plugge CM, Sorokin DY, Muyzer G, Dijkman H, Van Zessen E, Luimes P, Buisman CJN. Application of bacteria involved in the biological sulfur cycle for paper mill effluent purification. *Sci. Total Environ.* Elsevier; 2009;407:1333–1343.
12. Kleinjan WE, de Keizer A, Janssen AJ. Biologically produced sulfur. Elemental Sulfur and Sulfur-Rich Compounds I. Springer; 2003. p. 167–188.
13. R. S. Biology of Autotrophic Bacteria. In: Schlegel H, Bowien B, editor. Madison, WI, USA: Science Technology Publications, ; 1989. p. 289–303.
14. Kleinjan WE, Keizer A, Janssen AJH. Equilibrium of the reaction between dissolved sodium sulfide and biologically produced sulfur. *Colloids and Surfaces B: Biointerfaces.* Elsevier; 2005;43:228–237.
15. Van den Bosch PLF, van Beusekom OC, Buisman CJN, Janssen AJH. Sulfide oxidation at halo-alkaline conditions in a fed-batch bioreactor. *Biotechnol. Bioeng.* Wiley Online Library; 2007;97:1053–1063.
16. Janssen AJH, Meijer S, Bontsema J, Lettinga G. Application of the redox potential for controling a sulfide oxidizing bioreactor. *Biotechnol. Bioeng.* Wiley Online Library; 1998;60:147–155.
17. Giggenbach W. Optical spectra and equilibrium distribution of polysulfide ions in aqueous solution at 20. deg. *Inorganic Chemistry.* ACS Publications; 1972;11:1201–1207.

2

18. Steudel R, Holdt G, Göbel T. Ion-pair chromatographic separation of inorganic sulphur anions including polysulphide. *J. Chromatogr*. Elsevier; 1989;475:442–446.
19. Teder A. Spectrophotometric determination of polysulfide excess sulfur in aqueous solutions. Sven. Papperstidn. 1967;70:197–200.
20. Van Leerdam RC, Bosch PLF, Lens PNL, Janssen AJH. Reactions between methanethiol and biologically produced sulfur. *Environ. Sci. Technol.* 2011;45:1320–1326.
21. Kamyshny A, Ekeltchik I, Gun J, Lev O. Method for the determination of inorganic polysulfide distribution in aquatic systems. *Anal. Chem.* ACS Publications; 2006;78:2631–2639.
22. Pfennig N, Lippert KD. Über das vitamin B_{12}-bedürfnis phototropher Schwefelbakterien. *Arch. Microbiol.* Springer; 1966;55:245–256.
23. Sorokin DY, Muntyan MS, Panteleeva AN, Muyzer G. *Thioalkalivibrio sulfidiphilus* sp. nov., a haloalkaliphilic, sulfur-oxidizing gammaproteobacterium from alkaline habitats. *Int. J. Syst. Evol. Microbiol. Soc*. General Microbiol; 2012;62:1884–1889.
24. Rizkov D, Lev O, Gun J, Anisimov B, Kuselman I. Development of in-house reference materials for determination of inorganic polysulfides in water. Accreditation and Quality Assurance: Journal for Quality, Comparability and Reliability in Chemical Measurement. Springer; 2004;9:399–403.
25. Danzer K, Currie L. Guidelines for calibration in analytical chemistry. *Pure Appl. Chem.* 1998;70:993–1014.
26. Kamyshny A, Goifman A, Gun J, Rizkov D, Lev O. Equilibrium distribution of polysulfide ions in aqueous solutions at 25 °C: a new approach for the study of polysulfides' equilibria. *Environ. Sci. Technol.* ACS Publications; 2004;38:6633–6644.
27. Giggenbach WF. Equilibriums involving polysulfide ions in aqueous sulfide solutions up to 240. deg. *Inorg. Chem.* ACS Publications; 1974;13:1724–1730.
28. Roosta A, Jahanmiri A, Mowla D, Niazi A. Mathematical modeling of biological sulfide removal in a fed batch bioreactor. *Biochem. Eng. J.* Elsevier; 2011;58:50–56.
29. Van den Bosch PLF, Sorokin DY, Buisman CJ, Janssen AJH. The effect of pH on thiosulfate formation in a biotechnological process for the removal of hydrogen sulfide from gas streams. *Environ. Sci. Technol.* ACS Publications; 2008;42:2637–2642.

2

Chapter 3

Influence of methanethiol on biological sulfide oxidation in gas treatment system

Abstract

3

Inorganic and organic sulfur compounds such as hydrogen sulfide (H_2S) and thiols (RSH) are unwanted component in sour gas streams (e.g. biogas and refinery gases) because of their toxicity, corrosivity and bad smell. Biological treatment processes are often used to remove H_2S at small and medium scales (<50 tons per day of H_2S). Preliminarily research by our group focused on achieving maximum sulfur production from biological H_2S oxidation in the presence of methanethiol. In this paper the underlying principles have been further studied by assessing the effect of methanethiol on the biological conversion of H_2S under a wide range of redox conditions covering not only sulfur but also sulfate producing conditions. Furthermore, our experiments were performed in an integrated system consisting of a gas absorber and a bioreactor in order to assess the effect of methanethiol on the overall gas treatment efficiency. This study shows that methanethiol inhibits the biological oxidation of H_2S to sulfate by way of direct suppression of the cytochrome c oxidase activity in biomass, whereas the oxidation of H_2S to sulfur was hardly affected. We estimated the kinetic parameters of biological H_2S oxidation that can be used to develop a mathematical model to quantitatively describe the biodesulfurization process. Finally, it was found that methanethiol acts as a competitive inhibitor, therefore, its negative effect can be minimized by increasing the enzyme (biomass) concentration and the substrate (sulfide) concentration, which in practice means operation the biodesulfurization systems under low redox conditions.

3.1. Introduction

Inorganic and organic sulfur compounds such as hydrogen sulfide (H_2S) and thiols (RSH) are abundant in sour gases such as landfill gas, biogas, natural gas and refinery gas [1]. These compounds can be removed either by conventional physicochemical processes or by employing (haloalkaliphilic) sulfur-oxidizing bacteria (SOB) [2–4]. A commonly applied process for the biological removal of H_2S consists of a gas absorber, a sulfide-oxidizing bioreactor and a gravity settler for the removal of the formed sulfur particles (Fig. 1) [5]. The absorbed H_2S, hereafter referred to as "sulfide", is biologically oxidized to elemental sulfur (Eq. 1) and to sulfate (Eq. 2) but it can also be chemically oxidized to thiosulfate through intermediate polysulfide anions [6]; Eq. 3 is a simplified equation for this abiotic oxidation of sulfide.

$$HS^- + 0.5\ O_2 \rightarrow S_8 + OH^- \tag{1}$$

$$HS^- + 2\ O_2 \rightarrow SO_4^{2-} + H^+ \tag{2}$$

$$HS^- + O_2 \rightarrow 0.5\ S_2O_3^{2-} + 0.5\ H_2O \tag{3}$$
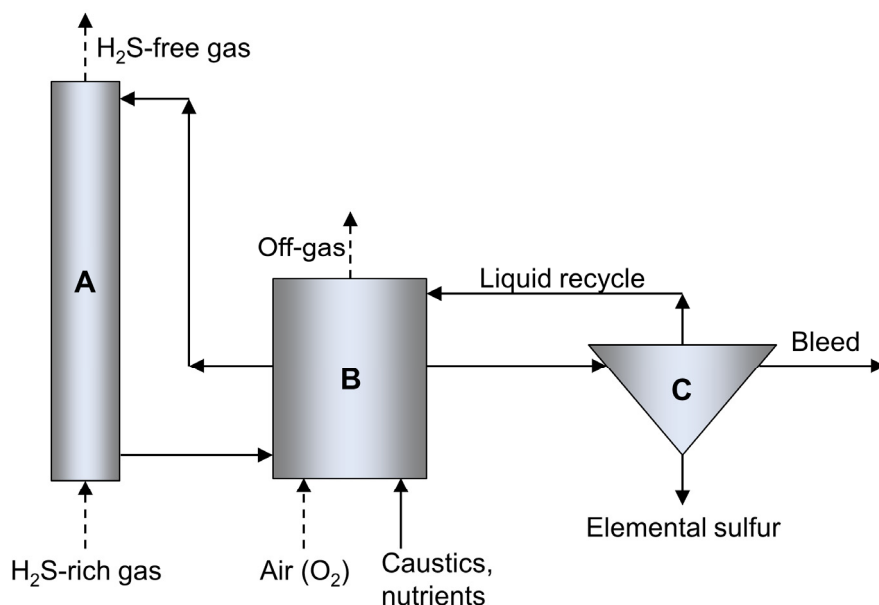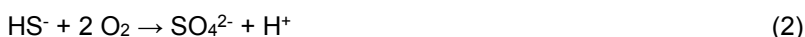
Figure 1. Simplified scheme of the process for biotechnological removal of H_2S from gas streams. **A**. Gas absorber; **B**. Bioreactor; **C**. Sulfur settler.

The selectivity for the biological reactions (Eq. 1 and 2) depends on the oxidation-reduction potential (ORP) of cytochromes in SOB [7], which can be controlled by the ORP of the reactor medium. The latter is primarily governed by the sulfide concentration [8], which can be regulated via the oxygen-to-sulfide (O_2/H_2S) supply ratio to the bioreactor. A previous study of biological sulfide removal under natron-alkaline conditions shows that, under optimal process conditions ($O_2/H_2S = 0.6$), about 83 mol% of the absorbed sulfide is biologically oxidized to sulfur [9]. Less than 2 mol% is oxidized to sulfate and the remainder, about 15 mol%, is chemically converted to thiosulfate [9]. Furthermore, it should be noted that at an O_2/H_2S supply ratio of 0.5 mol mol^{-1} no oxygen is available for sulfate production, while at a ratio of 2 mol mol^{-1} sulfate is the sole end-product [10].

Sour gas streams also often contain organic sulfur compounds or thiols, which inhibit the SOB [11], leading to lower sulfide oxidation rates. Consequently, toxic sulfide will accumulate which, in turn, will lead to the inhibition of reaction (1) thereby preventing the formation of hydroxyl ions that are needed to absorb H_2S from the sour gas. Finally, the system will collapse. The predominant thiol in natural gas is methanethiol (CH_3SH) [12]. Depending on the design of the absorber column, a fraction of the methanethiol is absorbed in the gas washer, and then fed to the bioreactor where it is chemically oxidized to dimethyl disulfide (DMDS), according to the following reaction:

$$2 CH_3SH + 0.5 O_2 \rightarrow CH_3S_2CH_3 + H_2O \qquad (4)$$
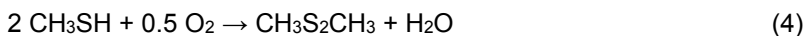
Methanethiol can also chemically react with elemental biosulfur particles [13]. The main reaction products are polysulfide anions (S_x^{-2}) and their associated methylated species, namely dimethyl polysulfanes (Eq. 5 and 6).

$$CH_3SH + S_8 \leftrightarrow CH_3S_9^- + H^+ \qquad (5)$$

$$CH_3SH + CH_3S_9^- \leftrightarrow CH_3S_nCH_3 + S_x^{2-} + H^+ \qquad \text{with } n+x = 10 \qquad (6)$$
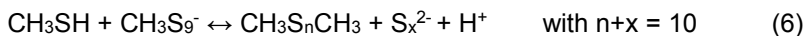
Promoted by nucleophilic catalysts like HS^- or CH_3S^-, the products of reaction 6 undergo inter-conversion reactions according to Eq. 7 and 8 [14].
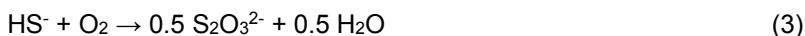
$$2 S_x^{2-} \leftrightarrow S_{x-1}^{2-} + S_{x+1}^{2-} \qquad (7)$$

$$2 CH_3S_nCH_3 \leftrightarrow CH_3S_{n-1}CH_3 + CH_3S_{n+1}CH_3 \qquad (8)$$

Subsequently, the formed polysulfide anions are chemically oxidized to thiosulfate and sulfur according to Eq. 9 [15] or biologically oxidized to sulfur in a reaction analogous to Eq. 1 [16,17].

$$S_x^{2-} + 1.5\ O_2 \rightarrow S_2O_3^{2-} + (x-2)/8\ S_8 \qquad\qquad (9)$$
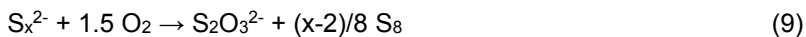
Unfortunately, the number of publications describing the effect of thiols on biological desulfurization processes is limited. A preliminary study by our group focused on achieving maximum sulfur production from biological H_2S oxidation in the presence of methanethiol [11]. This was assured by maintaining a constant ORP value by allowing the system to decrease in O_2/H_2S supply ratio after methanethiol addition to the bioreactor [11]. It was observed that a decrease in O_2/H_2S supply ratio resulted in O_2-limiting conditions and hence in a significantly reduced sulfate formation rate. In order to be able to gain a better fundamental understanding of the effect of methanethiol on sulfur and sulfate formation rates, it is essential to perform experiments at wide range of redox conditions as different enzyme systems are being used for sulfur and sulfate formation [18]. Hence, in this study experiments were carried out at constant O_2/H_2S supply ratios within each experiment [10]. Moreover, to explain our experimental results we studied the inhibition of cytochrome c oxidase activity, enzyme responsible for sulfate formation, by methanethiol in cell-free extracts obtained from different experiments. Finally, we also studied the inhibition mode for sulfide oxidation by estimating the unknown kinetic parameters in rate equations.

To mimic the various reactions that occur in large-scale field installations, H_2S and methanethiol were added to an absorber located upstream of the bioreactor. To the best of our knowledge, such a configuration has not yet been used for experimental studies concerning the removal of H_2S and thiols from gas streams.

3

Table 1. Dimensions and process conditions of gas absorber for H_2S removal in our study.

Dimensions and process conditions	
Column diameter [m]	0.011
Column height [m]	0.8
Total gas flow [Nm^3 s^{-1}]	2.8×10^{-6}
Empty bed retention time [s]	27
H_2S loading rate [Nm^3 s^{-1}]	2.5×10^{-8}
CH_3SH loading rate [Nm^3 s^{-1}]	$0 - 1.7 \times 10^{-10}$
Liquid flow [Nm^3 s^{-1}]	2.8×10^{-6}

3

3.2. Materials and methods

3.2.1. Experimental setup

The experimental setup consisted of a falling-film gas absorber and a fed-batch bioreactor (Fig. 2). A falling-film absorber was chosen to avoid any sulfur plugging issues that did occur when we tested a packed column (unpublished results). Obviously the removal of H_2S and methanethiol from the inlet gas can be simply attributed to acid-base reactions. However, the overall purpose of the process is that the consumed hydroxyl ions (OH^-) in the absorber are regenerated in the bioreactor (Eq. 1-2). Table 1 shows the dimensions and process conditions of the gas absorber. The liquid volume of the bioreactor was 2.2 L and the volume of the gas absorber was 0.2 L. The total liquid volume remained constant throughout each experimental run. Oxygen gas (99.995 vol%) was supplied to the bioreactor with the aid of a mass flow controller (type EL-FLOW, model F-201DV-AGD-33-K/E, 0-30 mL min^{-1}, Bronkhorst, the Netherlands) to control the ORP (ORP-stat). The same type of mass flow controller was used to feed H_2S (99.8 vol%, 0 to 17 mL min^{-1}), CH_3SH (1 vol% in N_2, 0 to 8 mL min^{-1}) and N_2 gas (99.995 vol%, 0 to 350 mL min^{-1}) to the gas absorber. The pH was controlled by providing carbon dioxide (99.99 vol%) to the inlet of the gas absorber, with the use of a solenoid valve (125318, Burkert, Germany). The oxygen and carbon dioxide supply were controlled with a multiparameter transmitter (Liquiline CM442; Endress+Hauser, the Nether-

64

lands), based on real-time signals from the redox potential electrode (Ag/AgCl electrode, Orbisint CPS12D; Endress+Hauser) and a pH sensor (Orbisint CPS11D; Endress+Hauser), respectively. A gear pump (EW-74014-40, Metrohm Applikon, the Netherlands) was used to recycle the liquid between the bioreactor and the gas absorber. The gas phase was continuously recycled (34 L min^{-1}) with a small gas compressor (N-840, KNF, Germany). The bioreactor and the gas absorber were kept at 35 °C with a thermostat bath (DC10-P5/U, Haake, Germany). We collected gas samples from sampling points located at the inlet and outlet of the gas absorber and in the bioreactor (Fig. 2). Liquid samples came from a sampling point in the middle section of the bioreactor (Fig. 2).
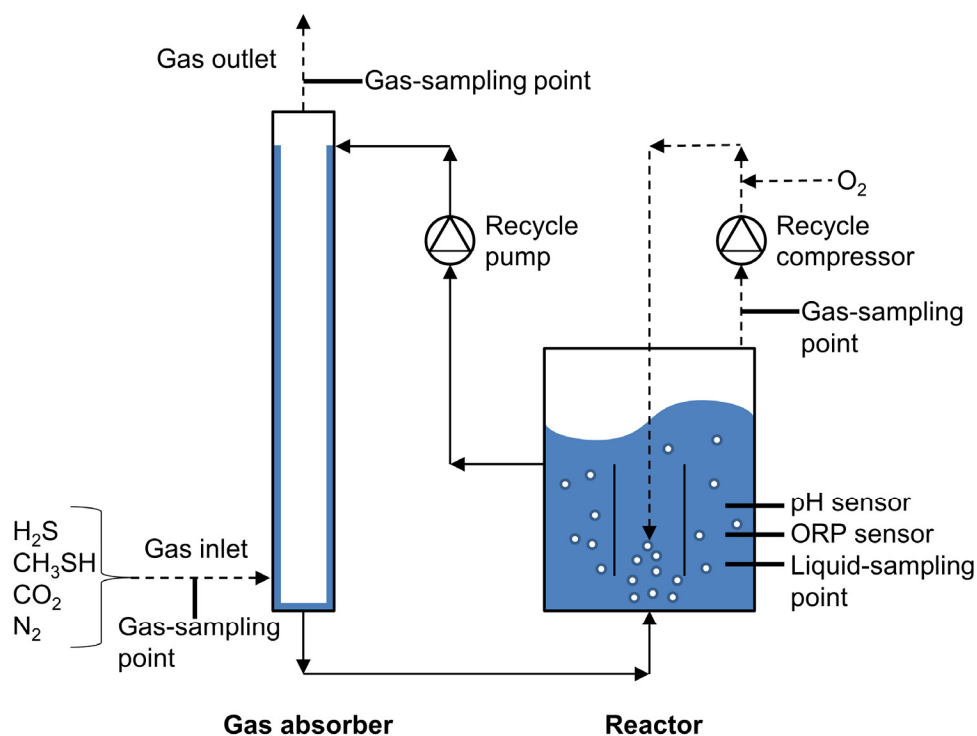
Figure 2. Flow scheme of experimental setup used for fed-batch experiments.

3.2.1.1. Medium composition

The reactor medium included a carbonate/bicarbonate buffer including 0.051 M Na_2CO_3, 0.698 M $NaHCO_3$ and 0.700 M $KHCO_3$, hereafter referred to as "1.5 M [Na^+ + K^+] buffer". Furthermore, the medium contained 1.0 g K_2HPO_4, 6.0 g NaCl, 0.20 g $MgCl_2$ × 6 H_2O, and 0.60 g urea, each per 1 L of Milli-Q water. A trace elements solution (1 mL L^{-1}) was added as described elsewhere [19]. The final pH of the medium was kept constant at a value of 8.50 ± 0.01 at 35 °C.

3.2.1.2. Inoculum

The reactor was inoculated with concentrated biomass obtained by centrifugation (30 min at 16,000 x *g*) of a 1-L culture collected from a full-scale gas biodesulfurization installation at Industriewater Eerbeek B.V., the Netherlands [5]. The dominant SOB species in this bioreactor is *Thioalkalivibrio sulfidophilus* [20].

Table 2. Overview of experimental runs at different operating conditions.

Experiment number	CH₃SH loading rate [mM d⁻¹]	ORP set point [mV]	O₂/H₂S [mol mol⁻¹]
1		-250 ± 14	2.18 ± 0.03
2		-350 ± 5	1.51 ± 0.04
3	0	-410 ± 8	0.63 ± 0.03
4		-450 ± 5	0.53 ± 0.02
5		-250 ± 13	1.89 ± 0.03
6		-270 ± 4	1.65 ± 0.01
7	0.24	-320 ± 4	1.38 ± 0.03
8		-350 ± 5	1.31 ± 0.01
9		-370 ± 4	0.81 ± 0.03
10		-410 ± 5	0.63 ± 0.02
11		-450 ± 3	0.55 ± 0.06

3.2.2. Experimental design

3.2.2.1. Fed-batch experiments

Fed-batch experiments were performed in the setup shown in Figure 2. We conducted eleven experiments in duplicate under various ORP conditions by changing the H_2S and O_2 supply ratio (Table 2). However, during each experiment this ratio remained constant. Experiments 1 to 4 took place in the absence of CH_3SH in the feed gas. In experiments 5 to 11, CH_3SH was supplied at a constant loading rate of 0.24 mM d^{-1} to assess the reactor performance in the presence of methanethiol and any formed methylated sulfur species [13]. We always kept the H_2S loading rate constant at a value of 36.8 mM d^{-1} (Table 2). Each experiment lasted 24 hours during which we took four gas and liquid samples at regular time intervals to confirm that the reactor performance was stable.

3.2.2.2. Cytochrome c oxidase activity measurements

The inhibitory effect of methanethiol on the cytochrome c oxidase activity was assessed by measuring the oxidation rate of N,N,N′,N′-tetramethyl-p-phenylenediamine (TMPD) (Sigma-Aldrich, the Netherlands) spectrophotometrically at 610 nm (UV-1650PC, Shimadzu, Japan) as described by Sorokin et al. [21] To verify the effect of exposed biomass to methanethiol we used non-pre-exposed (3.2.2.2 a) and pre-exposed biomass (3.2.2.2 b) from a laboratory-scale bioreactor to assess the cytochrome c oxidase activity. We also performed batch experiments with biomass exposed to methanethiol in the absence of any sulfide (3.2.2.2 c) to double check the effect of methanethiol on cytochrome c oxidase.

   a) **Biomass collected from a bioreactor; not pre-exposed to methanethiol:** The experimental setup depicted in Figure 2 ran under conditions favorable for expression of cytochrome c oxidase, i.e. sulfate-forming conditions (ORP = -270 mV), and in the absence of methanethiol. Immediately before the start of the activity measurements, 10 µL of a methanethiol solution (sodium thiomethoxide, 95% pure, Sigma Aldrich, the Netherlands), freshly prepared in oxygen-free Milli-Q water, was added to a sample of cell-free extract to obtain a final concentration of 0.05 mM.

b) Biomass collected from a bioreactor; pre-exposed to methanethiol:
The reactor conditions were the same as for (a) except that the reactor was exposed to methanethiol for a period of 3 days (0.37 mM d^{-1}) before collection of the biomass.

c) Biomass collected from a batch bottle; pre-exposed to methanethiol:
Biomass was obtained from the reactor described in (a) and placed into a batch bottle, in which cells were exposed to 0.2 mM methanethiol for 18 hours at 35 °C to double-check the effect of methanethiol on cytochrome c oxidase activity.

For each of these systems, medium with biomass was centrifuged (30 min at 16,000 x *g*) and resuspended in 0.5 M [Na$^+$ + K$^+$] buffer at pH 8.5. This step was repeated two times to remove elemental sulfur particles. After that, cell-free extract was prepared by sonication of the biomass on ice. Unbroken cells and cell debris were removed by centrifugation (20,200 x *g* for 15 min). Total protein content was measured spectrophotometrically with the BCA™ Protein Assay Kit (Thermo Scientific, the Netherlands). We prepared control samples from biomass that was never exposed to methanethiol. All samples were analyzed in triplicate.

3.2.2.3. Determination of the inhibition mode of sulfur oxidizing bacteria

Respiration tests were performed in order to investigate the inhibition mechanism of biological sulfide oxidation in the presence of methanethiol in an air-saturated medium ([Na$^+$ + K$^+$]= 1.5 M, pH = 8.5). We used a similar setup as described elsewhere [22]; it consisted of a glass mini reactor (60 mL) equipped with a magnetic stirrer. The reactor was closed with a Teflon piston to avoid any oxygen ingress. We added stock solutions containing sulfide and methanethiol to the reactor with a syringe passing through the piston. The sulfide oxidation rate was determined by measuring the oxygen consumption rate with a dissolved-oxygen sensor (Oxymax COS22D, Endress+Hauser). We calculated the biological sulfide oxidation rate as the difference between the total oxidation rate (including biological oxidation) and the abiotic oxidation rate (in the absence of biomass). We performed all experiments in triplicate at 35 °C (DC10-P5/U thermostat bath, Haake, Germany).

The biomass used in these respiration tests was grown as described in section 3.2.2.2 a). We centrifuged 700 mL (30 min at 16,000 x g) of biomass-containing solution and carried out a washing step after re-suspension of the pellet in 25 mL 1.5 M [$Na^+ + K^+$] buffer. The biomass concentration used in these respiration tests was always kept at 10 mg N L^{-1}. We prepared separate solutions of sulfide and methanethiol by dissolving sodium sulfide nona-hydrate (98% pure, Sigma Aldrich, the Netherlands) and sodium thiomethoxide (95% pure, Sigma Aldrich, the Netherlands) in 1.5 M [$Na^+ + K^+$] buffer. Sulfide concentrations ranged from 0.05 to 0.4 mM. The biological sulfide oxidation rate was measured in the presence of 0 (absence), 0.02 and 0.05 mM methanethiol.

3.2.2.4. Adsorption of dimethyl polysulfanes onto the surface of biosulfur particles

We investigated the adsorption of dimethyl polysulfanes onto the surface of biosulfur particles by measuring of dimethyl di-, tri- and tetrasulfide present in the headspace of the closed vials. Samples were prepared by adding a mixture of dimethyl polysulfanes (~3 mM S) to a closed glass vial containing purified biosulfur (125 mM), suspended in 5 mL of 1.5 M [$Na^+ + K^+$] buffer. A mixture of dimethyl polysulfanes ranging from dimethyl disulfide to dimethyl octasulfide was prepared as described by Rizkov et al. [23]. We applied the following procedure to purify the biosulfur suspension and remove any cell residue. First, the suspension was cooled to -20 °C to cause cell lysis. Second, a centrifugation step (16,000 x g for 30 min) was applied and the supernatant was replaced with Milli-Q water to obtain a cell-free biosulfur suspension. We repeated this purification procedure four times to ensure a high purity.

Each biosulfur sample was spiked with dimethyl polysulfanes and vigorously shaken for 5 minutes at room temperature, followed by a dimethyl polysulfanes headspace analysis. We verified that the mixing time was sufficient to reach equilibrium between the gas and liquid phase (data not shown). After gas analysis, we concentrated the biosulfur particles by centrifugation (3,300 x g for 10 min) and transferred them to a clean glass vial filled with 5 mL of 1.5 M [$Na^+ + K^+$] buffer. To allow desorption of any adsorbed dimethyl polysulfanes, the sample was vigorously shaken for 5 minutes at room temperature, followed by a second headspace analysis of the vial. We then calculated the percentage of desorbed

3

dimethyl di-, tri- and tetrasulfide by comparing the peak areas of the compounds in the sample, i.e. before and after extraction. Each sample was prepared and analyzed in triplicate.

3.2.3. Analytical techniques

The biomass concentration was measured as the amount of organically bound nitrogen that was oxidized to nitrate by digestion with peroxodisulfate (LCK238, Hach Lange, the Netherlands). Before analysis, we centrifuged the cells twice at 20,200 x *g* for 10 minutes and washed the formed pellet with organic nitrogen-free medium. We did not attempt to remove any biosulfur particles, as their presence does not affect the measurements [9].

We calculated the elemental sulfur concentration by establishing the sulfur species mass balance on the basis of the sulfide, thiosulfate and sulfate analyses, assuming steady-state conditions as confirmed by analysis of four consecutive liquid and gas samples.

We determined the sulfate and thiosulfate concentrations by ion chromatography (Metrohm Compact IC 761, Switzerland) with an anion column (Metrohm Metrosep A Supp 5, 150/4.0 mm, Switzerland) equipped with a pre-column (Metrohm Metrosep A Supp 4/5 Guard, Switzerland). The ion chromatography system included a chemical suppressor (Metrohm, Switzerland), CO_2 suppressor (853, Metrohm, Switzerland) and conductivity detector (Metrohm, Switzerland). In addition, suppressors for eluent conductivity and carbon dioxide were used (Metrohm, Switzerland). The mobile phase flow rate was 0.7 mL min^{-1}. The mobile phase consisted of 3.2 mM sodium carbonate and 1 mM sodium bicarbonate solution and 1% acetone. Before the analyses, we filtered the samples over a 0.22 μm syringe filter (Millex G5 filter unit, Merck, the Netherlands) and mixed them with 0.2 M zinc acetate in a 1:1 ratio to form ZnS, as its presence prevents abiotic sulfide oxidation. We stored the samples at 4 °C.

Dimethyl disulfide (DMDS), dimethyl trisulfide (DMTS) and polysulfides (dimethyl polysulfanes Me_2S_4 to Me_2S_8) were determined with an HPLC equipped with a UV detector (Dionex UltiMate 3000RS, USA) at a wavelength of 210 nm. We separated the organic sulfur compounds with an Agilent column (Zorbax Extend-C18 1.8 μm, 2.1 x 50 mm, the Netherlands) at 20 °C. The mobile phase consisted

of methanol and water. The flow rate was 0.371 mL min^{-1} and the injection volume was 1.25 µL. The purities of the standards were above 98% for DMDS and DMTS (Sigma-Aldrich, the Netherlands).

Polysulfide anions were derivatized to dimethyl polysulfanes with methyl trifluoromethanesulfonate (≥98% pure, Sigma-Aldrich, the Netherlands), as follows:

$$S_x^{2-} + 2CF_3SO_3Me \rightarrow Me_2S_x + 2CF_3SO_3^- \qquad (10)$$
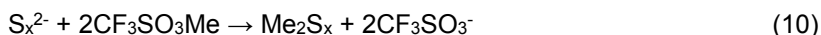
The sample preparation procedure and derivatization protocol are described elsewhere [24].

The gas phase (H_2S, N_2, CO_2 and O_2) was analyzed with a gas chromatograph (Varian CP4900 Micro GC, Agilent, the Netherlands) equipped with two separate column modules, namely a 10-m-long Mol Sieve 5A PLOT (MS5) and a 10-m-long PoraPlot U (PPU). The limit of quantification was 0.1 vol% for all compounds. Both column modules were connected to a thermal conductivity detector for data acquisition. We used argon as a carrier gas with a flow rate of 1.47 ml min^{-1}. The temperature was 80 °C for the MS5, 65 °C for the PPU column, and 105 °C at the injection port.

We measured the gaseous CH_3SH and DMDS concentrations with a gas chromatograph (Varian CP3900 GC, Agilent, the Netherlands) equipped with an Agilent column (VF5-MS, 1 µm x 30 m x 0.25 mm). The limits of quantification were 3.6 ppm(v) and 0.2 ppm(v), respectively. The analysis was carried out with a flame ionization detector at 300 °C. The initial oven temperature was 35 °C. After 5 minutes, we applied a gradient of 4 °C min^{-1} to obtain 45 °C, followed by 100 °C min^{-1} to reach 200 °C, which was held for 1 minute to clean the column. We used helium as carrier gas, with a flow rate of 0.9 mL min^{-1}. The injection volume was 1 mL.

To investigate the adsorption of dimethyl polysulfanes onto the surface of biosulfur particles, we analyzed dimethyl di-, tri- and tetrasulfide concentrations in the headspace by using gas chromatography (6890N, Agilent, the Netherlands) coupled with a triple quadrupole mass spectrometer (5975, Agilent, the Netherlands), equipped with an Agilent column (HP-5MS, 30 m x 0.25 mm x 0.25 µm, Agilent, the Netherlands). Initially, the oven temperature was 50 °C. After 2 minutes, a gradient of 12.5 °C min^{-1} was applied to reach 200 °C. We operated the mass spectrometer in SIM mode with a filament voltage of 70 eV and an electron multiplier

voltage of 1200 to 2800 V. Helium was the carrier gas, with a flow rate of 1.3 mL min^{-1}. The injection volume was 2.5 mL. The syringe temperature was 50 °C. The equilibration time was 10 minutes at 40 °C and the agitation speed was 250 rpm.

3.3. Results and discussion

3.3.1. Methanethiol removal from sour gas

The gas absorber column (Fig. 2) was fed with a mixed-gas stream containing nitrogen gas as a carrier supplemented with H_2S (0.9 vol%) and methanethiol (0.01 vol%). These sulfur compounds were continuously removed by dissolution into the alkaline washing solution. The removal efficiency of H_2S and methanethiol in the gas absorber was around 99.8% and 70%, respectively.

Subsequently, the liquid stream loaded with HS^- and CH_3S^- entered the base of the reactor where HS^- was biologically oxidized to sulfur and sulfate (Eq. 1 and 2); also, some sulfide was chemically oxidized to thiosulfate (Eq. 3). Methanethiol was abiotically oxidized to dimethyl polysulfanes (Eq. 4 - 6). The bioreactor suspension was continuously recycled through the gas absorber where some DMDS was stripped off. The DMDS concentration in the outlet of the gas absorber was almost constant at 7 ± 1 ppm(v) at ORP values between -410 mV and -250 mV. For these ORP conditions, the methanethiol concentration was also almost constant at about 18.5 ± 2.2 ppm(v). However, at ORP values below -450 mV, the concentration of methanethiol at the absorber outlet doubled to 31.3 ± 3.8 ppm(v), whereas no more DMDS was detected in the off-gas. Apparently, under these conditions insufficient oxygen was available in the bioreactor for the chemical oxidation of methanethiol to DMDS (Eq. 4).

When we compared the methanethiol and DMDS concentration in gas samples from the inlet and outlet of the gas absorber, we found a gap of 40 to 60 mol% in the sulfur balance (absorber in - absorber out). There is no evidence that *Thioalkalivibrio sulfidophilus*, the dominant SOB species in the reactor [20], is able to oxidize methanethiol or DMDS. Based on earlier studies, we have strong indications that the dimethyl polysulfanes (resulting from Eq. 5 and 6) were adsorbing onto sulfur particles [11]. To validate our hypothesis, we added dimethyl polysulfanes to a biosulfur suspension in a closed vial. Thereafter, we analyzed the headspace for

72

dimethyl di-, tri- and tetrasulfide. We then removed the biosulfur particles by centrifugation, mixed them with fresh 1.5 M [Na$^+$ + K$^+$] buffer in a new vial, and carried out a second headspace analysis. We found dimethyl di-, tri- and tetrasulfide present at 56, 32 and 5 vol%, respectively. The percentages of dimethyl di-, tri- and tetrasulfide released during the washing process indicate that the strength of the adsorption of the dimethyl polysulfanes onto the biosulfur particles increased with increasing number of sulfur atoms in the dimethyl polysulfide chain. The fact that longer-chain dimethyl polysulfanes are more hydrophobic may explain this higher affinity for the somewhat hydrophobic sulfur particles [25].
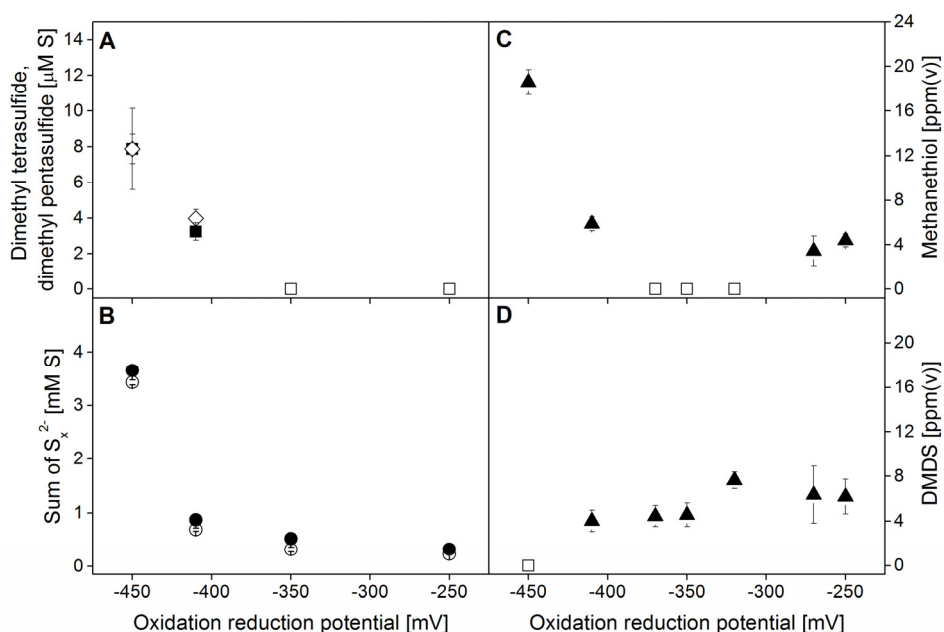
Figure 3. Reactor system operated at H$_2$S = 36.8 mM d^{-1} and methanethiol = 0.24 mM d^{-1}. **A.** Concentration of dimethyl tetrasulfide (■) and dimethyl pentasulfide (◊) in the reactor. **B.** Sum of polysulfides at different oxidation reduction potentials for runs with (●) and without (○) methanethiol. **C.** Concentration of methanethiol (▲) (CH$_3$SH) at different oxidation reduction potentials in headspace of reactor. **D.** Concentration of dimethyl disulfide (DMDS) (▲) at different oxidation reduction potentials in headspace of reactor. The symbol □ indicates that the concentration was below the detection limit.

Dimethyl polysulfanes with more than two sulfur atoms form from the abiotic reaction between methanethiol and biosulfur particles (Eq. 5 and 6) [13]. As these compounds are far less volatile than methanethiol and DMDS, no stripping occurred in the upper section of the gas absorber. Instead, we detected accumulation in the bioreactor suspension up to a total concentration of ~16 μM S at -450 mV (Fig. 3A). Van den Bosch et al. [26] studied the inhibitory effect of DMDS and DMTS on the bacterial oxidation of sulfide and found that DMTS is more toxic to SOB than DMDS. Besides dimethyl polysulfanes, also inorganic polysulfide anions were produced from the reaction between methanethiol and elemental sulfur (Eq. 6), as reflected by the somewhat higher S_x^{2-} concentrations in the experiments with methanethiol (Fig. 3B). In addition, the S_x^{2-} concentrations were higher at lower ORP values because of the increasing sulfide concentrations [9].

At ORP values above -410 mV, methanethiol and DMDS were continuously removed in the gas absorber, and therefore, no accumulation was observed in the headspace of the bioreactor (Fig. 3C and 3D). The DMDS concentration in the headspace of the bioreactor was around 6 ± 2 ppm(v). As this is comparable to the DMDS concentration in the absorber outlet (7 ± 1 ppm(v)) for the same ORP conditions, the gas phase and liquid phase in the gas absorber and bioreactor are in equilibrium.

Furthermore, no methanethiol was detected in the bioreactor when the system transited from sulfur to sulfate formation, i.e. at ORP values between -370 and -320 mV (Fig. 3C; see also Section 3.3.2). Most likely, the formation of sulfur particles allowed methanethiol to react away under the formation of dimethyl polysulfanes (Eq. 5 and 6) as this observed previously by Van Leerdam [13]. At an ORP of -450 mV, the methanethiol concentration in the headspace of the bioreactor suddenly increased to 20 ppm(v), whereas no more DMDS was detected (Fig. 3C and 3D). This is because insufficient oxygen was available to oxidize methanethiol to DMDS under these conditions (Eq. 4). As mentioned, we also saw this reflected in the concentrations in the gas absorber.
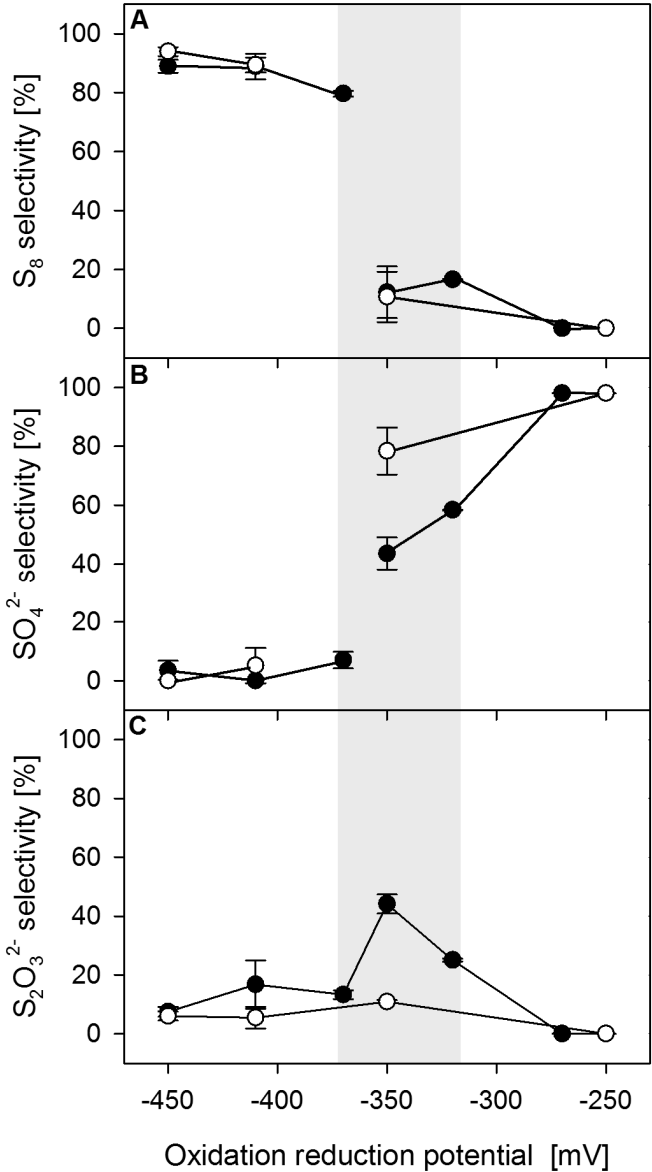
Figure 4. Bioreactor performance during experiment runs with (●) and without (○) methanethiol: **A.** sulfur selectivity. **B.** sulfate selectivity. **C.** thiosulfate selectivity. The area marked in grey is a transition zone between conditions favorable for sulfur (left) or sulfate (right) production.

3.3.2. Effect of methanethiol on biological sulfide oxidation process

Figure 4A and 4B show the two distinct ORP regions we found for sulfur and sulfate formation, respectively. Sulfur mainly formed below -370 mV, whereas sulfate was the main end product at ORP values above -320 mV. These findings are in good agreement with those of Klok et al. [10] and Van den Bosch et al. [9]. In the transition zone between -370 and -320 mV (gray area in Figure 4), the selectivity for sulfur and sulfate formation was lower (Fig. 4A-B) than outside this area; consequently, the rate of abiotic thiosulfate formation was higher in this zone (Fig. 4C). Methanethiol had a clear effect on the selectivity for sulfate formation in the transition zone (Fig. 4B), e.g. at -350 mV; as methanethiol inhibited biological sulfate formation (Fig. 4B), thiosulfate formation increased as a result of abiotic sulfide oxidation (Fig. 4C). The drop in biological sulfate formation (Eq. 2) resulted in lower oxygen requirements (Eq. 2 *v.* Eq. 3) as can be seen in Figure 5. We measured the effect of methanethiol on the oxidation of sulfide to sulfate under two different sulfate-forming conditions, namely -250 mV and -350 mV. At these two ORPs, the O_2/H_2S consumption ratio decreased from 2.18 to 1.89 mol mol^{-1} and from 1.51 to 1.31 mol mol^{-1}, respectively, after the start of methanethiol addition (Fig. 5). For both ORPs, this corresponds to a drop of 13 vol% in the required O_2 supply rate.
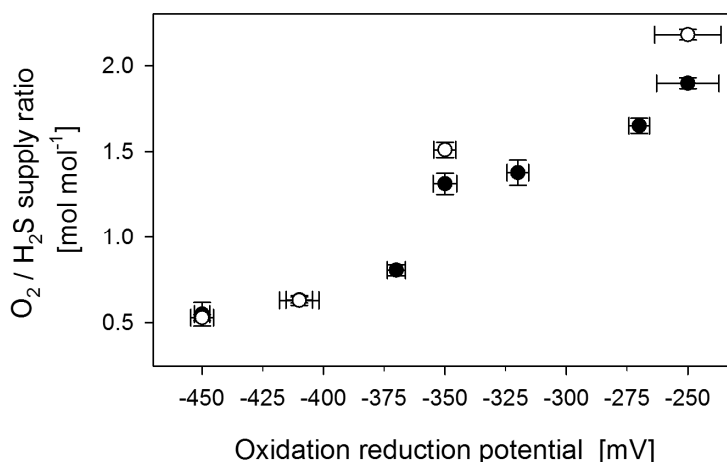

Figure 5. Molar O_2/H_2S supply ratio versus oxidation reduction potential for experimental runs with (●) and without (○) methanethiol. The load of H_2S was 36.8 mM d^{-1} and the load of methanethiol was 0.24 mM d^{-1}.

Although methanethiol clearly inhibited biological sulfate formation, the sulfur production was hardly affected (Fig. 4A and 4B). This is most likely related to the different enzymes that SOB use for the production of sulfur and sulfate, respectively. Sulfide oxidation in SOB involves several enzymes [18]. In the first stage, sulfide is transformed into intracellular polysulfide. In the second stage, depending on redox conditions [7], intracellular polysulfide is either secreted out of the cell as solid biosulfur particles or further oxidized to sulfate. Since the oxidation to sulfate needs to channel six out of the eight electrons of sulfide to oxygen, high activity of the terminal part of respiratory chain, i.e. of cytochrome c oxidase, is critical for sulfate formation [7]. Thiols inhibit cytochrome c oxidase by binding to its heme iron [27–29] and forming a cytochrome-methanethiol complex; this inhibitory effect decreases with increasing steric hindrance of the thiols [29]. As the redox state of the involved cytochromes is lowered by the binding of a thiol to cytochrome c oxidase, intracellular polysulfide oxidation to sulfate is hampered [7,30]. We studied the inhibitory effect of methanethiol on the cytochrome c oxidase activity in more detail by measuring the oxidation rate of TMPD (an artificial electron donor for cytochrome c oxidase). Figure 6 shows that a strong inhibition of cytochrome c oxidase occurred in all samples that were subjected to methanethiol. It was possible to calculate the percentage of inhibition by comparing the cytochrome c oxidase activity of the control samples with samples exposed to methanethiol. The highest inhibition (86%) was observed for cell-free extract spiked with methanethiol (Fig. 6, sample A). In this type of sample, the enzymes were not protected by a cell wall; therefore, methanethiol had easy access to cytochrome c oxidase, resulting in high inhibition. On the other hand, cell-free extract of biomass collected from the sulfide-oxidizing reactor exposed to methanethiol (Fig. 6, sample B) also showed high inhibition (76%). The activity of the enzyme in a sample collected from a batch bottle exposed to methanethiol (Fig. 6, sample C) was least inhibited (53%). These results (samples B and C), indicate a high binding affinity of methanethiol for the active site of cytochrome c oxidase since even after sample preparation (sonication), strong inhibition remained.

3
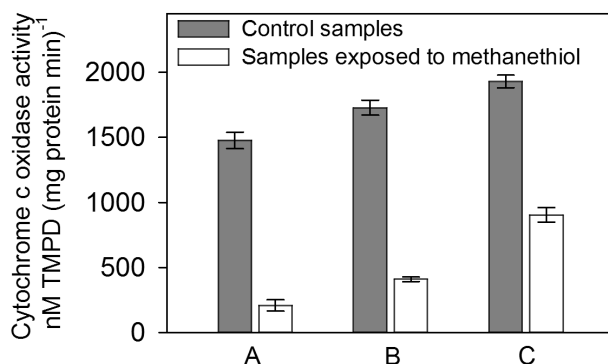
Figure 6. Cytochrome c oxidase activity in cell-free extract of sulfur-oxidizing bacteria obtained from: **A.** a lab-scale sulfide-oxidizing bioreactor that had not yet been exposed to methanethiol but the cell-free extract was spiked with methanethiol to a final concentration of 0.05 mM. **B.** a lab-scale sulfide-oxidizing bioreactor exposed to methanethiol for 3 days (0.37 mM d^{-1}). **C.** batch bottles in which cells were exposed to 0.2 mM of methanethiol for 18 h. For each category, a control sample was analyzed that was not exposed to methanethiol.

In our experiments, methanethiol never suppressed sulfate production by more than 44% (Fig. 4B), compared to ~99% as observed by Van den Bosch et al. [11]. A clear difference with our experiments is that Van den Bosch et al. performed their experiments with low O_2/H_2S supply ratios (0.52 mol mol^{-1}), leading to oxygen-limiting conditions. Even in the absence of methanethiol, hardly any sulfate would have been produced under such conditions [10]. Moreover, the methanethiol loading in our experiments was up to seven times higher than those applied by Van den Bosch et al., i.e. 240 versus 35 - 79 µM d^{-1}.

3.3.3. Effect of methanethiol on biomass growth

In the absence of methanethiol, growth of SOB occurred under all ORP conditions, ranging from -410 mV to -250 mV (Fig. 7). Growth was seriously hampered at -450 mV. According to work by Klok et al. [10], SOB gain most energy for their growth from sulfate production (Eq. 2), and much less from sulfur formation (Eq. 1). As there was insufficient oxygen for sulfate production (Eq. 2), very little growth was possible at -450 mV.

When methanethiol was supplied to the system, it had a significant effect on biomass growth (Fig. 7); growth was arrested at all ORP values, except at the highest ORP (-250 mV). Also at -250 mV, the sulfate production was not affected by methanethiol. Therefore, the arrested growth of the biomass at ORP values between -450 and -350 mV can be explained by lower energy obtained from sulfate formation inhibited by methanethiol (see Section 3.3.2) as follows from Klok's findings [10]. Limited growth can be acceptable for industrial biodesulfurization systems, provided that the biomass minimum growth rate is higher than the wash-out rate.
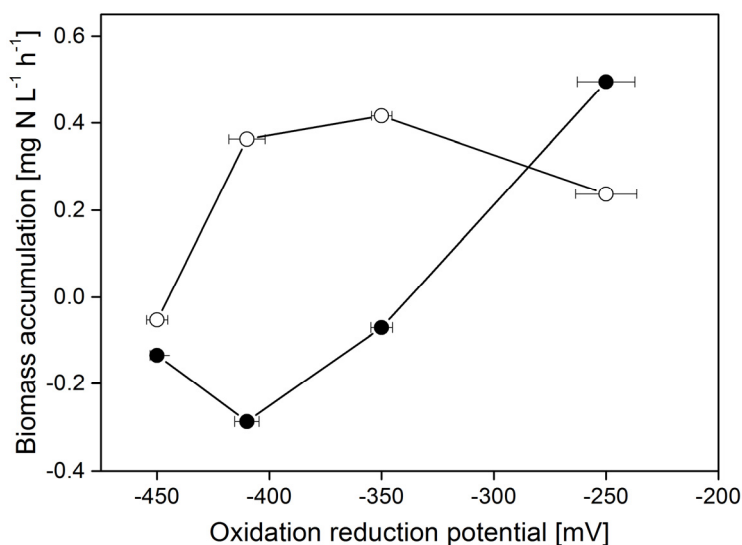
Figure 7. Biomass accumulation at different molar O_2/H_2S supply ratios, with (●) and without (○) methanethiol.

3.3.4. Inhibition type of methanethiol and kinetic parameters of biological sulfide oxidation

To identify the type of inhibition exercised by methanethiol on biological sulfide oxidation, we performed respiration experiments with 20 to 50 µM methanethiol. The resulting Lineweaver-Burk plots (Fig. 8) show that the reaction rate (r) increased with increasing concentrations of sulfide (C_S), indicating that the inhibitory action was

somehow mitigated by the substrate. As all lines intersect at the same point on the Y-axis and the specific maximal reaction rate (r_{max}) does not depend on the concentration of the inhibitor, methanethiol appears to be a competitive inhibitor [31]. With this type of inhibition, the Michaelis-Menten constant (K_M) is greater because the sulfide concentration necessary to reach r_{max} is higher, which could explain the mitigating effect of the substrate. Thus, the reaction rate as given by Eq. 11 changes into Eq. 12, where C_I stands for inhibitor concentration.

$$r = \frac{r_{max}C_S}{K_M + C_S} \tag{11}$$

$$r = \frac{r_{max}C_S}{K_M\left(1 + \frac{C_I}{k_i}\right) + C_S} \tag{12}$$

We estimated the unknown parameters in Eq. 11 and 12 from respiration data, by using a non-linear least-squares method [32]. We took the following stepwise approach to minimize the error. First, we estimated K_M and r_{max} in Eq. 11 to be 36 ± 3 µM and 0.324 ± 0.007 mM (mg N)$^{-1}$ h^{-1}, respectively. Second, these estimated parameters (K_M and r_{max}) were introduced into Eq. 12 to estimate the inhibition constant (k_i) which was found to be 31 ± 5 µM. Appendix A contains the additional uncertainty in the estimate of k_i as a result of the uncertainty in r_{max} and K_M.

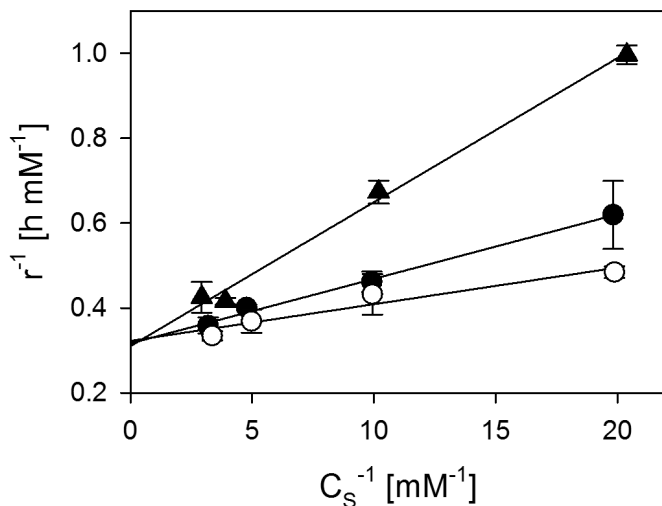**Figure 8.** Lineweaver-Burk plot obtained from a kinetic study of biological sulfide oxidation in the absence (○) and presence of methanethiol at concentrations of 0.02 mM (●) and 0.05 mM (▲). C_S is the concentration of sulfide and r is the reaction rate. Temperature was 35 °C, pH was 8.5, and salinity was 1.5 M.

Very low values of K_M and k_i represent high binding affinities of sulfide and methanethiol for the involved enzymes. This low k_i value also means that methanethiol is a strong inhibitor. An explanation for this could be the structural similarity between CH_3S^- and HS^- [33]. Accordingly, methanethiol would be the most toxic of all thiols.

As methanethiol appears to be a competitive inhibitor of sulfide oxidation by SOB, the stability of the biological H_2S removal process under field conditions can likely be increased by increasing the biomass concentration. Obviously, a greater biomass concentration would lead to a greater total cytochrome oxidase concentration, hence to a lower ratio of methanethiol to cytochrome oxidase and to less biomass inhibition at constant methanethiol loading rates. Also because of that methanethiol is a competitive inhibitor, increasing the substrate (sulfide) concentration will lower the inhibition. In practice this can be achieved by applying lower redox value (e.g. < -390 mV) of the bioreactor suspension, which is correlated with the sulfide concentration [8].

3.4. Conclusions

This study shows that methanethiol inhibits the biological oxidation of sulfide to sulfate whereas oxidation to sulfur is hardly affected. It is likely that this is caused by way of direct suppression of the cytochrome c oxidase activity in SOB.

In addition, we determined that dimethyl polysulfanes, resulting from a reaction between methanethiol and sulfur, reversibly adsorb onto biosulfur particles. This could offer an elegant way for removing those compounds from the bioreactor suspension along with the formed biosulfur particles.

Finally, our findings lead to the conclusion that the inhibitory effect of methanethiol in sour gases can be mitigated by increasing biomass concentrations and keeping redox conditions below -390 mV.

Acknowledgements

3

References

1. Muradov N, Smith F. Thermocatalytic conversion of landfill gas and biogas to alternative transportation fuels. *Energy Fuels*. ACS Publications; 2008;22:2053–2060.

2. Gómez-Ramirez M, Zarco-Tovar K, Aburto J, de León RG, Rojas-Avelizapa NG. Microbial treatment of sulfur-contaminated industrial wastes. *J. Environ. Sci. Health., Part A*. Taylor & Francis; 2014;49:228–232.

3. Li L, Han Y, Yan X, Liu J. H_2S removal and bacterial structure along a full-scale biofilter bed packed with polyurethane foam in a landfill site. *Bioresour. Technol.* Elsevier; 2013;147:52–58.

4. Arellano-Garcia L, González-Sánchez A, Van Langenhove H, Kumar A, Revah S. Removal of odorant dimethyl disulfide under alkaline and neutral conditions in biotrickling filters. *Water Sci. Technol.* IWA Publishing; 2012;66:1641–1646.

5. Janssen AJH, Lens PNL, Stams AJM, Plugge CM, Sorokin DY, Muyzer G, Dijkman H, Van Zessen E, Luimes P, Buisman CJN. Application of bacteria involved in the biological sulfur cycle for paper mill effluent purification. *Sci. Total Environ.* Elsevier; 2009;407:1333–1343.

6. Chen KY, Morris JC. Kinetics of oxidation of aqueous sulfide by oxygen. *Environ. Sci. Technol.* ACS Publications; 1972;6:529–537.

7. Visser JM, Robertson LA, Van Verseveld HW, Kuenen JG. Sulfur production by obligately chemolithoautotrophic thiobacillus species. *Appl. Environ. Microbiol.* Am Soc Microbiol; 1997;63:2300–2305.

8. Janssen AJH, Meijer S, Bontsema J, Lettinga G. Application of the redox potential for controling a sulfide oxidizing bioreactor. *Biotechnol. Bioeng.* Wiley Online Library; 1998;60:147–155.

9. Van den Bosch PLF, van Beusekom OC, Buisman CJN, Janssen AJH. Sulfide oxidation at halo-alkaline conditions in a fed-batch bioreactor. *Biotechnol. Bioeng.* Wiley Online Library; 2007;97:1053–1063.

10. Klok JBM, van den Bosch PLF, Buisman CJN, Stams AJM, Keesman KJ, Janssen AJH. Pathways of sulfide oxidation by haloalkaliphilic bacteria in

limited-oxygen gas lift bioreactors. *Environ. Sci. Technol.* ACS Publications; 2012;46:7581–7586.

11. Van den Bosch PLF, Fortuny-Picornell M, Janssen AJH. Effects of methanethiol on the biological oxidation of sulfide at natron-alkaline conditions. *Environ. Sci. Technol.* ACS Publications; 2009;43:453–459.

12. Fredericks E, Harlow G. Determination of mercaptans in sour natural gases by gas liquid chromatography and microcoulometric titration. *Anal. Chem.* ACS Publications; 1964;36:263–266.

13. Van Leerdam RC, Bosch PLF, Lens PNL, Janssen AJH. Reactions between methanethiol and biologically produced sulfur. *Environ. Sci. Technol.* 2011;45:1320–1326.

14. Steudel R. The chemistry of organic polysulfanes RS (n)-R (n> 2). *Chem. Rev.* 2002;102:3905.

15. Steudel R, Holdt G, Göbel T. Ion-pair chromatographic separation of inorganic sulphur anions including polysulphide. *Journal of chromatography*. Elsevier; 1989;475:442–446.

16. Sorokin DY, Kuenen JG. Haloalkaliphilic sulfur-oxidizing bacteria in soda lakes. *FEMS Microbiol. Rev.* Wiley Online Library; 2005;29:685–702.

17. Sorokin D, van den Bosch PLF, Abbas B, Janssen AJH, Muyzer G. Microbiological analysis of the population of extremely haloalkaliphilic sulfur-oxidizing bacteria dominating in lab-scale sulfide-removing bioreactors. *Appl. Microbiol. Biotechnol.* Springer; 2008;80:965–975.

18. Muyzer G, Sorokin DY, Mavromatis K, Lapidus A, Clum A, Ivanova N, Pati A, d' Haeseleer P, Woyke T, Kyrpides NC. Complete genome sequence of "*Thioalkalivibrio sulfidophilus*" HL-EbGr7. *Stand. Genomic. Sci.* Genomic Standards Consortium; 2011;4:23.

19. Pfennig N, Lippert KD. Über das vitamin B12-bedürfnis phototropher Schwefelbakterien. *Arch. Microbiol.* Springer; 1966;55:245–256.

20. Sorokin DY, Muntyan MS, Panteleeva AN, Muyzer G. Thioalkalivibrio sulfidiphilus sp. nov., a haloalkaliphilic, sulfur-oxidizing gammaproteobacterium from alkaline habitats. *Int. J. Syst. Evol. Microbiol.* Soc General Microbiol; 2012;62:1884–1889.

21. Sorokin DY, Lysenko AM, Mityushina LL, Tourova TP, Jones BE, Rainey FA, Robertson LA, Kuenen GJ. *Thioalkalimicrobium aerophilum* gen. nov., sp. nov. and *Thioalkalimicrobium sibericum* sp. nov., and *Thioalkalivibrio versutus* gen. nov., sp. nov., *Thioalkalivibrio nitratis* sp. nov. and *Thioalkalivibrio denitrificans* sp. nov., novel obligately alkaliphilic and obligately chemolithoautotrophic sulfur-oxidizing bacteria from soda lakes. *International journal of systematic and evolutionary microbiology*. Soc General Microbiol; 2001;51:565–580.

22. Kleinjan WE, Keizer A de, Janssen AJH. Kinetics of the chemical oxidation of polysulfide anions in aqueous solution. *Water Res.* Elsevier; 2005;39:4093–4100.

23. Rizkov D, Lev O, Gun J, Anisimov B, Kuselman I. Development of in-house reference materials for determination of inorganic polysulfides in water. *Accredit. Qual. Assur.* Springer; 2004;9:399–403.

24. Roman P, Bijmans MFM, Janssen AJH. Quantification of individual polysulfides in lab-scale and full-scale desulfurisation bioreactors. *Environ. Chem.* CSIRO; 2014;11:702–708.

25. Kleinjan WE, de Keizer A, Janssen AJ. Biologically produced sulfur. *Elemental Sulfur and Sulfur-Rich Compounds I*. Springer; 2003. p. 167–188.

3

26. Van den Bosch PLF, de Graaff M, Fortuny-Picornell M, van Leerdam RC, Janssen AJH. Inhibition of microbiological sulfide oxidation by methanethiol and dimethyl polysulfides at natron-alkaline conditions. *Appl. Microbiol. Biotechnol.* Springer; 2009;83:579–587.

27. Hu T-M, Ho S-C. Kinetics of Redox Interaction between Cytochrome c and Thiols. *J. Med. Sci*. 2011;31:109–115.

28. Tomkova A, Antalik M, Bágel'ová J, Miskovsky P, Ulicny J. Absorption and Raman spectroscopy study of cyt c-thiol complexes in acidic solutions. *Gen. Physiol. Biophys.* 1992;3:11.

29. Wilms J, Lub J, Wever R. Reactions of mercaptans with cytochrome c oxidase and cytochrome c. *Biochim. Biophys. Acta, Bioenerg.* Elsevier; 1980;589:324–335.

30. Helmann JD. Prokaryotic Redox Switches. *Oxidative Stress and Redox Regulation*. Springer; 2013. p. 233–276.

31. Sharma R. Enzyme Inhibition: Mechanisms and Scope. R. Sharma, editor. InTech; 2012.

32. Keesman KJ. System identification: an Introduction. Springer, Verlag, UK; 2011.

33. Debajyoti D. Biochemistry. Academic Publishers; 2005.

3

APPENDIX A

Table A.1. Estimated inhibition constant ($\widehat{k}_1$) with corresponding standard deviation (σ) for specific maximal reaction rate (r_{max}) and Michaelis-Menten constant (K_M).

r_{max} [mM h^{-1} (mg N)$^{-1}$]	K_M [mM]	$\widehat{k}_1$ [mM]	σ
0.324	0.036	0.031	0.005
0.317	0.033	0.029	0.006
0.331	0.039	0.032	0.004
0.317	0.039	0.039	0.008
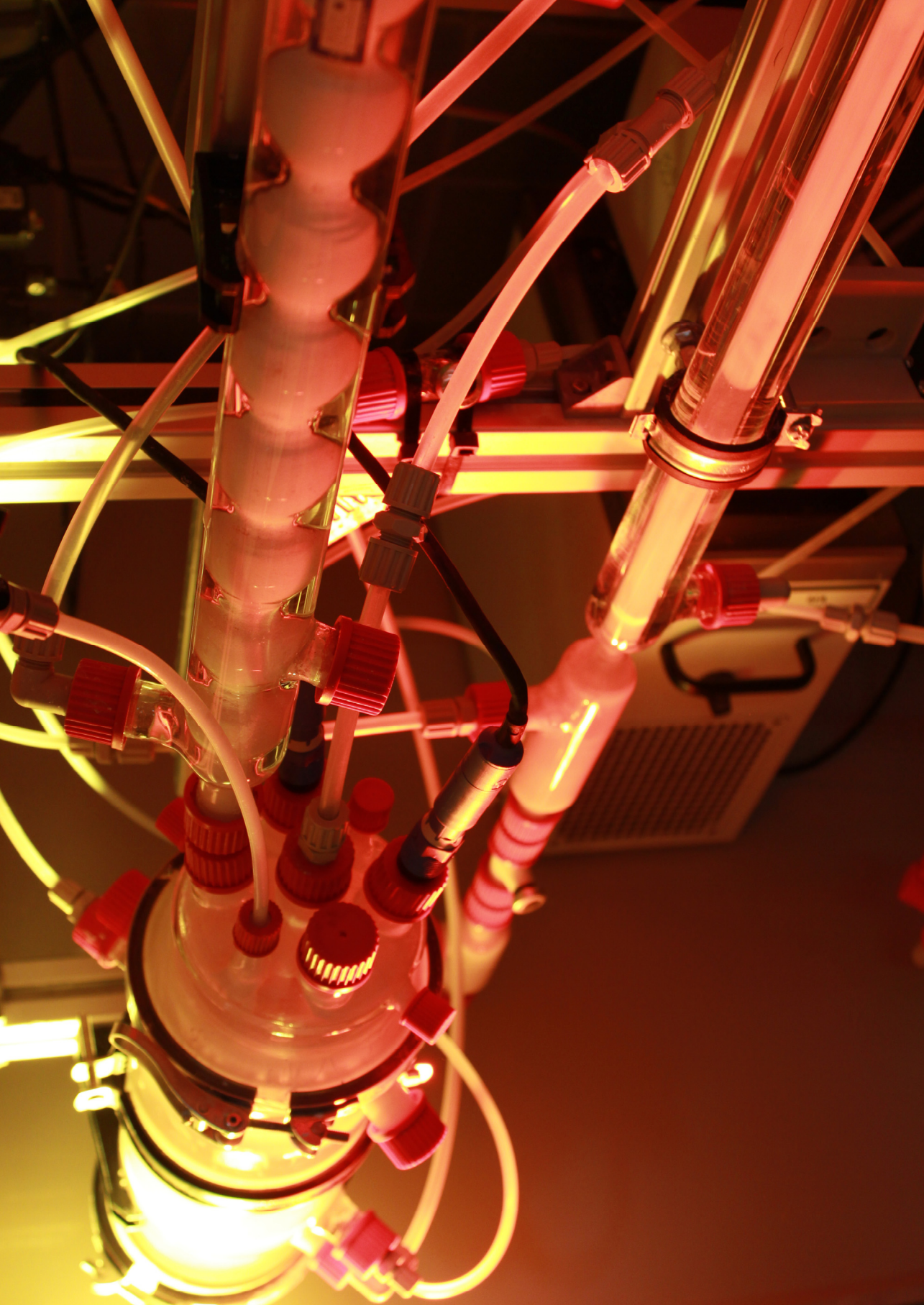
Chapter 4

Effect of methanethiol concentration on sulfur production in biological desulfurization systems under haloalkaline conditions

4

Abstract

Biological removal of H_2S from gas streams became popular in recent years because of high process efficiency and low operational costs. To expand the scope of these processes to gas streams containing volatile organic sulfur compounds, like thiols, it is necessary to provide new insights into their impact on overall biodesulfurization process. Published data on the effect of thiols on biodesulfurization processes are scarce. In this study, we investigated the effect of methanethiol on the selectivity for sulfur production in a bioreactor integrated with a gas absorber. This is the first time that the inhibition of biological sulfur formation by methanethiol is investigated. In our reactor system, inhibition of sulfur production started to occur at a methanethiol loading rate of 0.3 mM d^{-1}. The experimental results were also described by a mathematical model that includes recent findings on the mode of biomass inhibition by methanethiol. We also found that the negative effect of methanethiol can be mitigated by lowering the salinity of the bioreactor medium. Furthermore, we developed a novel approach to measure the biological activity by sulfide measurements using UV-spectrophotometry. Based on this measurement method, it is possible to accurately estimate the unknown kinetic parameters in the mathematical model.

4.1. Introduction

Air pollution and acid deposition, also referred as acid rain, are related to sulfur emissions released during combustion of hydrocarbon fuel sources containing sulfur compounds. Hydrogen sulfide (H_2S) is the main sulfur pollutant in fuel gasses, where gases exceeding 4 ppm of H_2S are considered as sour gas [1]. Besides H_2S, volatile organic sulfur compounds (VOSC) can be present in sour gasses, which next to their negative environmental effects, are also known for their toxic and corrosive effects and obnoxious smell [2].

Treatment of sour gas streams can be achieved by applying biological desulfurization processes [3,4]. In a typical biodesulfurization process, product selectivity of the H_2S oxidation process is controlled by the oxidation-reduction potential (ORP), which is related to oxygen and sulfide supply ratios to the bioreactor [5]. The specific ratios for sulfur and sulfate production follow from the stoichiometry of the simplified biooxidation reactions (Eq. 1-2), which show a theoretical O_2/H_2S molar ratio of 0.5 mol mol^{-1} for sulfur and 2 mol mol^{-1} for sulfate selectivity [6]. An extended description of Eq. 2 is given by Klok et al. [7] and Muyzer et al. [8]. In addition to these biological reactions, thiosulfate can be formed under undesired abiotic oxidation of sulfide through polysulfide anions, as described by Chen and Morris [9], where the overall reaction can be written in the simplified form of Eq. 3.

$$HS^- + 0.5\ O_2 \rightarrow 1/8\ S_8 + OH^- \tag{1}$$
$$HS^- + 2\ O_2 \rightarrow SO_4^{2-} + H^+ \tag{2}$$
$$HS^- + O_2 \rightarrow 0.5\ S_2O_3^{2-} + 0.5\ H_2O \tag{3}$$
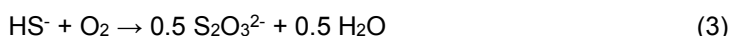
The dominant sulfur oxidizing bacteria (SOB) in full-scale haloalkaline biodesulfurization reactors were identified as *Thioalkalivibrio sulfidophilus* [10]. These microorganisms are highly suitable to be applied in the biological H_2S oxidation, because of their high dissolved salt and pH tolerance [11,12]. Based on the genome of *Thioalkalivibrio sulfidophilus*, Muyzer et al. [8] proposed a hypothetical pathway for sulfide oxidation in which various enzymes oxidize sulfide to sulfate with (in)organic polysulfide anions and sulfite as intermediates. For SOB, product selectivity was found to be dependent on the degree of reduction of the cytochrome pool, where along with a decrease in ORP, further oxidation of sulfur is hampered due to a limitation in the electron transfer capacity of the sulfur/sulfite couple [13].

Nevertheless, later studies with haloalkaliphilic SOB, dominating in the reactors at higher pH, also suggested presence of different mechanism [10].

A thiol's sulfhydryl group (-SH), can disrupt the intermolecular disulfide bonds and alter enzyme structures or bind to the active site of enzymes leading to catalytic inactivity [14]. As an example of this, Van den Bosch et al. [15] observed SOB inhibition by VOSCs that were added to an H_2S-oxidizing bioreactor. In a previous study, we investigated the effect of methanethiol (MT) on the biological conversion of H_2S under different redox conditions in a novel integrated setup consisting of a gas absorber and a bioreactor. Our experiments showed that MT inhibits biological sulfate formation already at concentration of 0.6 µM, whilst biological oxidation of sulfide to sulfur is hardly affected up to this concentration [16]. However, at higher MT loading rates the effect of thiols under conditions favorable for sulfur formation (i.e. at low redox) is not known. The assessment of the inhibitory effect of VOSCs on sulfide oxidation by SOB can be determined by measuring the IC_{50} concentration at which biotic oxidation of sulfide is inhibited by 50%. The IC_{50} value at $[Na^+ + K^+] = 2$ M, pH = 9 and T = 35 °C for MT was found to be 0.05 mM, whereas inhibition of dimethyl disulfide (DMDS) and dimethyl trisulfide (DMTS) is much less severe, with IC_{50} values of 1.5 and 1.0 mM, respectively [17].

Toxicity parameters like IC_{50} values, kinetic parameters and the inhibition mode of SOB are usually determined by measuring the rate of oxygen consumption, also referred to as biological oxygen monitoring (BOM) tests [16,17]. However, SOB can oxidize sulfide in up to three consecutive steps [8] and therefore results from BOM tests are not always unambiguous. For example, we found in previous studies that in BOM tests for sulfide oxidation, up to three different oxygen consumption rates can be found in a single experiment [16,17]. Consequently, the estimated kinetic parameters based on such an experiment can be a mixture of two or three different (simplified) reactions, such as Eq. 1 and 2. Besides that, and as mentioned before, product selectivity of SOB depends on the redox state of the involved enzymes [13]. Therefore, by changing the initial sulfide concentration, which is a strong reducing compound, the product selectivity changes significantly. To avoid these effects, the BOM test shall be replaced by an alternative test, such as the biological sulfide monitoring (BSM) test, in which consumption of sulfide is measured instead of oxygen consumption. Such method is new and has never

4

been used to measure the activity of SOB in the presence of organic sulfur compounds.

The aim of the current study is to investigate the effect of MT concentrations in the feed gas on the biological sulfur production from the oxidation of HS⁻ in a bench scale system that consists of a gas absorber and a bioreactor, and that is operated under haloalkaline conditions. Moreover, a novel BSM test for the estimation of kinetic parameters of the process has been developed and validated. The kinetic parameters obtained from the BSM test and the results from the bioreactor experiments were used to validate a mathematical model describing the biological H_2S oxidation process in the presence of MT. Finally, we propose and examine a solution to mitigate the effects of MT in biological gas desulfurization systems.

4.2. Materials and methods

4.2.1. Analytical techniques

The biomass concentration was measured as the amount of organic nitrogen oxidized to nitrate by digestion with peroxodisulphate (LCK238, Hach Lange, the Netherlands). Before analysis, the cells were centrifuged twice at 20,000 x *g* for 10 minutes and washed with N-free medium. We did not attempt to remove sulfur particles, as its presence does not affect the results [18].

Sulfide was measured as total sulfide (S^{2-}_{tot}) using a methylene blue method with a standard cuvette test method (LCK653, Hach Lange, the Netherlands). Sulfide analysis was carried out immediately after sampling and filtration over a 0.22 μm syringe filter (Millex G5 filter unit, Merck, the Netherlands).

We determined the sulfate and thiosulfate concentrations by ion chromatography (Metrohm Compact IC 761, Switzerland) with an anion column (Metrohm Metrosep A Supp 5, 150/4.0 mm, Switzerland) equipped with a pre-column (Metrohm Metrosep A Supp 4/5 Guard, Switzerland). The ion chromatography system included a chemical suppressor (Metrohm, Switzerland), CO_2 suppressor (853, Metrohm, Switzerland) and conductivity detector (Metrohm, Switzerland). In addition, suppressors for eluent conductivity and carbon dioxide were used (Metrohm, Switzerland). The mobile phase flow rate was 0.7 mL min⁻¹. The mobile phase consisted of 3.2 mM sodium carbonate and 1 mM sodium bicarbonate solution

and 1% acetone. Before starting the analyses, we filtered the samples over a 0.22 μm syringe filter (Millex G5 filter unit, Merck, the Netherlands). To prevent any abiotic sulfide oxidation we mixed the filtered sample with 0.2 M zinc acetate (Sigma-Aldrich, the Netherlands) in a 1:1 ratio in order to remove all dissolved sulfide as ZnS. The samples were stored at 4 °C.

We calculated the elemental sulfur concentration by establishing the sulfur mass balance on the basis of sulfide, thiosulfate and sulfate analyses in four consecutive liquid samples as described elsewhere [15].

The gas phase (H_2S and O_2) was analyzed with a gas chromatograph (Varian CP4900 Micro GC, Agilent, USA) equipped with two separate column modules: a 10 m long Mol Sieve 5A PLOT (MS5) and a 10-m-long PoraPlot U (PPU). The limit of quantification was 0.1% for all compounds. Both column modules were connected to a thermal conductivity detector for data acquisition. Argon was used as a carrier gas with a flow rate of 1.47 ml min^{-1}. The temperature was 80 °C for the MS5, 65 °C for PPU column, and 105 °C at the injection port.

The gaseous MT and DMDS concentrations were measured with a gas chromatograph (Thermo scientificTM Trace GC Ultra with Trace GC Ultra valve oven, Interscience, Breda, the Netherlands) equipped with a Restek column (RT®-U-Bond, 30 m x 0.53 mm di x 20 μm df). The limits of quantification were 0.8 ppm(v) and 0.7 ppm(v), respectively. The analysis of sulfur compounds was carried out using a flame photometric detector (150 °C) and thermal conductivity detector (160 °C). Inlet temperature was 190 °C. Oven temperature of the first 2 min was 70 °C, followed by a gradient increase of 40 °C min^{-1}, to final temperature of 190 °C and subsequently hold for 5 min. Helium was used as carrier gas with a flow rate of 10 mL min^{-1}. Loop temperature was 50 °C and the injection volume was 250 μL, where a total sample volume of 2.5 mL was used to flush thoroughly. All tubing was of the type Sulfinert®, to prevent absorption and reaction of the sulfur compounds.

Dissolved oxygen (DO) was measured with an optical trace oxygen sensor for inline measurements (OIM-PSt6, PreSens GmbH, Regensburg, Germany). The oxygen concentration was recorded by the data logger (Fibox 4 trace, PreSens GmbH, Regensburg, Germany) which was corrected for temperature and salinity.

Table 1. Dimensions and process conditions of gas absorber for H_2S and methanethiol (MT) removal in our study.

Dimensions and process conditions	
Column diameter [m]	0.011
Column height [m]	0.8
Specific gas-liquid interfacial area [m^2 m^{-3}]	396
Total gas flow [Nm^3 s^{-1}]	2.8×10^{-6}
Empty bed retention time [s]	27
H_2S loading [Nm^3 s^{-1}]	2.5×10^{-8}
MT loading [Nm^3 s^{-1}]	$0.3 - 6 \times 10^{-10}$
Liquid flow [Nm^3 s^{-1}]	2.8×10^{-6}

4.2.2. Experimental setup

The experimental setup consisted of a falling film gas absorber and a fed-batch bioreactor, both without packing material. For a schematic representation of the setup we refer to Roman et al. [19]. Table 1 shows the dimensions and the operating conditions of the gas absorber. The liquid volume of the bioreactor was 2.2 L and the volume of the gas absorber was 0.2 L. The total liquid volume remained constant throughout each experimental run. Oxygen gas (99.995 vol.%) was supplied to the bioreactor by using a mass flow controller (type EL-FLOW, model F-201DV-AGD-33-K/E, 0-30 mL min^{-1}, Bronkhorst, the Netherlands) to control the ORP value. The same type of mass flow controller was used to feed H_2S (99.8 vol.%, 0-17 mL min^{-1}), MT (1 vol.% in N_2, 0-8 mL min^{-1}) and N_2 gas (99.995 vol.%, 0-350 mL min^{-1}) to the gas absorber. Carbon dioxide (99.99 vol.%) was fed to the inlet of the gas absorber with a solenoid valve (125318, Burkert, Germany) to control the pH. The oxygen and carbon dioxide supply were controlled with a multi-parameter transmitter (Liquiline CM442; Endress+Hauser, the Netherlands) based on real-time signals from the redox potential electrode (Ag/AgCl reference electrode, Orbisint CPS12D; Endress+Hauser) and a pH sensor (Orbisint CPS11D; Endress+Hauser), respectively. A gear pump (EW-74014-40, Metrohm Applikon, Schiedam, the Netherlands) recycled the liquid between the bioreactor and the gas

4

absorber. The gas phase from the bioreactor headspace was continuously send to the bottom of the bioreactor (34 L min^{-1}) with a gas compressor (N-840, KNF, Germany). The bioreactor and the gas absorber were kept at 35 °C with a thermostat bath (DC10-P5/U, Haake, Germany). We collected gaseous samples from sampling points placed in the inlet and outlet of the gas absorber and in the bioreactor headspace. Liquid samples were collected from a sampling point placed in the middle section of the bioreactor.

4.2.2.1. Medium composition

Two different carbonate buffers (0.5 and 1.5 M [Na$^+$ + K$^+$]) were used as the bioreactor medium. The 0.5 M [Na$^+$ + K$^+$] consisted of 0.27 M Na$^+$ and 0.23 M K$^+$ and the 1.5 M [Na$^+$ + K$^+$] consisted of 0.8 M Na$^+$ and 0.7 M K$^+$. Furthermore, the medium contained 1.0 g K$_2$HPO$_4$, 6.0 g NaCl, 0.20 g MgCl$_2$ × 6 H$_2$O, and 0.60 g urea, each per 1 L of Milli-Q water. A trace elements solution (1 mL L^{-1}) was added as described elsewhere [20]. The final pH of the medium was controlled at a value of 8.50 ± 0.01 at 35 °C.

4

4.2.2.2. Inoculum

The bioreactor was inoculated with cells obtained by centrifugation (30 min at 16,000 x *g*) of a 1-L culture collected from a full-scale gas biodesulfurization installation at Industriewater Eerbeek B.V., the Netherlands [21]. The dominant SOB species in this bioreactor is *Thioalkalivibrio sulfidophilus* [10]. The biomass concentration in every experiment was 46 ± 4 mg N L^{-1}. For each experiment, we used biomass that had previously not been exposed to MT and DMDS.

4.2.3. Experimental design

4.2.3.1. Effect of methanethiol on sulfur selectivity

The inhibitory effects of different MT-loadings on product selectivity were determined at both low salinity (0.5 M [Na$^+$ + K$^+$]) and high salinity (1.5 M [Na$^+$ + K$^+$]) buffers to assess the salt effect on biological sulfur formation. Eleven experimental runs were conducted at various MT loading rates (Table 2) and at sulfur-producing

conditions (ORP = -390 mV) in two identical experimental setups (described in Section 4.2.2). Each increase in MT loading rate was done alternately in the other setup to demonstrate that the perturbed setup itself had no influence on the results (Table 2). The H_2S loading rate was always kept constant at supply of 61.3 mM d^{-1} and before the start of each experiment ORP was constant (± 5 mV), indicating steady-state operation of the system. Each experiment lasted 24 hours during which four samples at regular time intervals were taken.

Table 2. Loading rate of methanethiol to the experimental setup for each experiment operated under constant H_2S loading rate (61.3 mM d^{-1}) and reduction-oxidation potential (-390 mV). Two identical lab-setups (setup 1 and setup 2) were used for the experiments.

Experiment number	1	2	3	4	5	6	7	8	9	10	11
Setup	1	2	1	2	1	2	1	2	1	2	1
Methanethiol loading rate [mM d^{-1}]	0.05	0.10	0.20	0.29	0.39	0.49	0.59	0.69	0.79	0.89	0.99

4.2.3.2. Biological sulfide measurement

Batch sulfide oxidation experiments were performed in order to investigate the SOB inhibition mechanism by MT in a saline medium ($[Na^+ + K^+]$ = 1.5 M, pH = 8.5) and estimate kinetic parameters of this reaction. Biological sulfide oxidation was monitored by measuring a decrease in the sulfide concentration measured using UV spectrophotometry at 230 nm (UV-1650PC, Shimadzu, Japan). The initial sulfide concentration in each experiment was based on the absorbance, with correction of absorption for biomass and medium. Moreover, any decrease of absorption was corrected for abiotic sulfide oxidation rate (test without cells). Activity was measured in quartz cuvette with screw cap in 2.5 mL liquid volume (Z801313, Sigma-Aldrich, the Netherlands). Reaction was started by injection of sulfide stock solution (98% pure nona-hydrate, Sigma Aldrich, the Netherlands) with a microliter syringe (Hamilton, USA). Sulfide concentrations ranged from 5 µM to 100 µM. After injection

and mixing by inversion, absorption was measured for 5 min at 230 nm. The biological sulfide oxidation rate was measured in both the absence and presence of MT (95% pure sodium thiomethoxide, Sigma Aldrich, the Netherlands) added just before injection of sulfide solution. All experiments were performed at room temperature.

Biomass used in BSM tests was obtained from the lab-scale H_2S oxidizing bioreactor operated at sulfur-forming conditions (ORP = -390 mV). The sulfur-free biomass solution was prepared by centrifugation of 700 mL of the sulfide-oxidizing culture and a washing step after re-suspension of the pellet in 25 mL 1.5 M [$Na^+ + K^+$] medium. The biomass concentration in the batch experiments was always kept at 1 mg N L^{-1}.

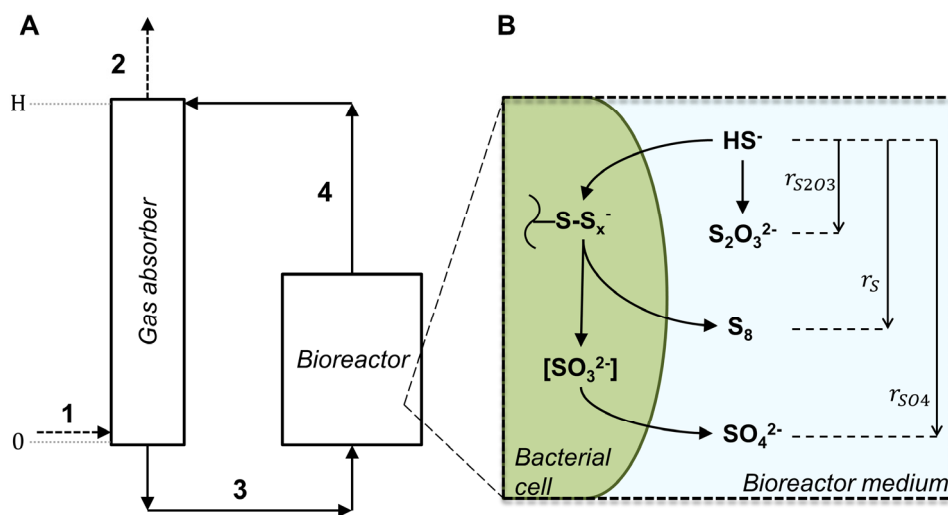**Figure 1. A.** Flow scheme of the experimental setup: *1.* Absorber gas inlet ($C_{H2S,MT}^{G}(0)$, mol m^{-3}); *2.* Absorber gas outlet ($C_{H2S,MT}^{G}(H)$, mol m^{-3}); *3.* Bioreactor liquid inlet ($C_{H2S,MT}^{R,in}$, mol m^{-3}); *4.* Bioreactor liquid outlet ($C_{H2S,MT}^{R}$, mol m^{-3}). **B.** Reactions that occur in the bioreactor related to the sulfide oxidation.

4.2.4. Integrated absorber and bioreactor model

A mathematical model for the two-step biodesulfurization process with simultaneous removal of MT and H2S, under alkaline conditions, has been developed. As mentioned before, the setup consists of two sections: a gas absorber, where H2S and MT are washed from the gas mixture, and a fed-batch sulfide oxidizing bioreactor (Fig. 1A). In what follows, material balances for each section, assuming steady state conditions, are presented.

In the setup, liquid from the bioreactor is recycled over the gas absorber (Fig. 1A). General spatially distributed H2S mass balances for the gas and liquid phase in the gas absorber are represented by Eq. 4 and 5 [22]:

$$\phi_G \frac{dC^G_{H2S}(z)}{dz} = -k^{H2S}_{ov} aS \left(C^G_{H2S}(z) - \frac{C^L_{H2S}(z)}{m_{H2S}} \right) \tag{4}$$

$$\phi_L \frac{dC^L_{H2S}(z)}{dz} = k^{H2S}_{ov} aS \left(C^G_{H2S}(z) - \frac{C^L_{H2S}(z)}{m_{H2S}} \right) \tag{5}$$

where

$$k^{H2S}_{ov} = \frac{1}{k_{G,H2S}^{-1} + (m_{H2S} \, k_{L,H2S})^{-1}} \tag{6}$$

Analogous expressions can be derived for MT. The overall mass transfer coefficient (k_{ov}) is determined by the gas-side and liquid-side mass transfer coefficients (Eq. 6). The general mass balances for the gas and liquid phase in the gas absorber are solved with the following boundary conditions $z = H$:

$$C^G_{H2S}(z) = C^{G,H}_{H2S} \tag{7}$$

$$C^L_{H2S}(z) = C^R_{H2S} \tag{8}$$

The biological oxidation of sulfide by *Thioalkalivibrio* is governed by subsequent reactions in which sulfide is first transformed into an intracellular polysulfur compound ($\{S_x\}$) [23], and then to elemental sulfur (Eq. 1), which is secreted outside the cell. The polysulfur compound is also transformed to sulfite followed by the conversion to sulfate (Eq. 2) [8]. A schematic representation of these reactions is given in Figure 1B. From two substrates (sulfide and oxygen), the oxygen was excluded from the equations describing biological reactions because there is no direct cause and effect relationship on the product formation in the presence of MT [16]. Therefore, in order to model the effect of MT concentration on the sulfur production, the reaction term in the sulfide mass balance

over the bioreactor is only based on the rate of sulfide consumption. Hence, the sulfide mass balance, under steady-state conditions, is given by:

$$0 = \phi_L(C_{H2S}^{R,in} - C_{H2S}^R) + V_r R_{H2S} \tag{9}$$

where the molar sulfide consumption rate is described by:

$$R_{H2S} = -r_{SO4}m_b F_{SO4} - r_S m_b F_S - r_{S2O3} \tag{10}$$

The selectivity factors for sulfate (F_{SO4}) and sulfur (F_S) account for the product selectivity under the most optimal conditions for sulfur formation.

Besides biological sulfide oxidation, the overall mass balance also includes the abiotic oxidation of sulfide (Fig. 1B), which is described by Eq. 11 [7,24].

$$r_{S2O3} = k_{S2O3}C_{O2}^{R\ 0.8}C_{H2S}^{R\ 1.02} \tag{11}$$

The reaction rates for sulfide consumption for sulfur and sulfate production are described by "Michaelis-Menten" equations (Eq. 12-13) for a competitive inhibition of SOB inhibition by MT [16], that is:

$$r_S = \frac{r_{max}^{H2S}C_{H2S}^R}{K_M^{H2S}\left(1+\frac{C_{MT}^R}{k_i^{S8}}\right)+C_{H2S}^R} \tag{12}$$

$$r_{SO4} = \frac{r_{max}^{H2S}C_{H2S}^R}{K_M^{H2S}\left(1+\frac{C_{MT}^R}{k_i^{SO4}}\right)+C_{H2S}^R} \tag{13}$$

It should be noted that, the above reaction rates differ only in their inhibition constants. It was found that reactions leading to sulfur and sulfate formation have different susceptibilities to MT, which can be related to different enzyme systems used during the formation of these products [16].

The model also includes the chemical reaction between MT and biologically produced sulfur particles, in which dimethyl polysulfanes are formed [25]. The kinetics of this reaction were described by Van Leerdam et al. [26]. This enables us to articulate the steady-state mass balance for MT in the bioreactor as follows:

$$0 = \phi_L(C_{MT}^{R,in} - C_{MT}^R) + V_r R_{MT} \tag{14}$$

where

$$R_{MT} = -kC_{MT}^{R\ 2.1}C_S^{R\ 0.76} \tag{15}$$

4.3. Results and discussion

4.3.1. Identification of overall inhibition using the BSM test

We developed the BSM test to study the inhibition of biological sulfide oxidation by MT. The millimolar extinction coefficient at maximum absorbance of sulfide (230 nm) was found to be 8300 M^{-1} cm^{-1} based on Beer-Lambert law, which is exactly the same value as has been reported by Fischer et al. [27]. The spectrophotometric measurement at wavelength of 230 nm is limited to low concentrations of H_2S (up to 0.1 mM), because of the maximum absorbance of 1 Abs. However, a change of the wavelength to 255 nm allows extending the range of applicability to 4 mM.
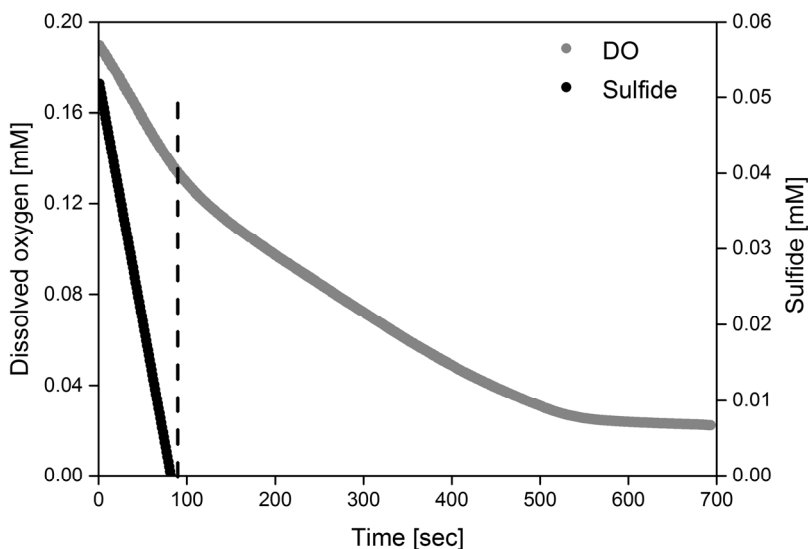
Figure 2. An example of dissolved oxygen (DO) and sulfide consumption over time for the O_2/H_2S ratio of 0.4 mol mol^{-1}. The DO consumption rate was obtained from the biological oxygen measurement at a temperature of 35 °C, medium [Na^+ + K^+] = 1.5 M and biomass concentration = 10 mg N L^{-1} (see Roman et al. [16]). The sulfide consumption rate was obtained from the biological sulfide measurement at a temperature of 25 °C, medium [Na^+ + K^+] = 1.5 M and biomass concentration of 1 mg N L^{-1}, which was recalculated to a temperature of 35 °C and the biomass concentration of 10 mg N L^{-1}.

The BSM test is a direct method to assess the biological oxidation rate of sulfide, i.e. the first step in the pathway for oxidation of sulfur compounds by SOB. Subsequently, we overlaid the BOM results from a preceding study [16] with the BSM results from this work after recalculation to the same biomass concentration and temperature (Fig. 2). A temperature correction was made in accordance with Van't Hoff Law.

It can be observed from Figure 2 that after all sulfide is consumed, the oxygen consumption rate still changes. Only after 500 s. the oxygen concentration stabilizes at 22 µM. It has been assumed that other intracellular processes, related to further oxidation of sulfide derivatives ($\{S_x\}$), are responsible for the continuous oxygen consumption which determines the second oxygen consumption rate. Thus, kinetic parameters estimated based on the second part of the oxygen consumption rate (from approx. 90 to 530 s.) most likely will be related to other enzymatic processes.

Figure 3. Lineweaver-Burk plot obtained from a kinetic study of biological sulfide oxidation in the absence and presence of methanethiol, C_{H2S} is the concentration of sulfide and r_S is the reaction rate. Temperature = 25 °C, pH = 8.5, and [Na$^+$ + K$^+$] = 1.5 M.
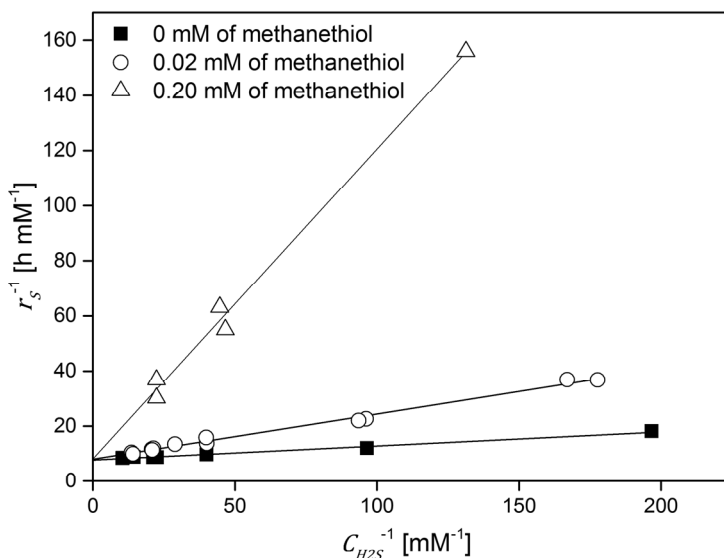
The results obtained from the BSM test were validated by assessing the inhibition mode of MT on SOB by preparing a Lineweaver-Burk plot (Fig. 3) [28]. From this plot, it follows that MT is a competitive inhibitor as at increasing substrate, i.e. sulfide, concentrations the inhibition by MT is mitigated. This is in agreement with our previous findings [16].

4.3.2. Effect of methanethiol on biological sulfur production

Process performance of biological sulfide oxidation, in 1.5 M [Na^+ + K^+] medium and at different MT loadings, was monitored in terms of DO, oxygen in the bioreactor headspace and O_2/H_2S consumption ratio (Fig. 4A). Based on these results, it can be seen that the bioreactor was stable up to a MT loading rate of 0.3 mM d^{-1}, as the selectivity for sulfur and thiosulfate formation remained fairly constant. Stable bioreactor operation becomes apparent from a constant sulfur production (75 - 82 mol%) and constant selectivity for thiosulfate which is around 20 mol% (Fig. 4B). These observations suggest that MT has negligible effect on sulfur production below a loading rate of 0.3 mM d^{-1}, which is in good agreement with our previous findings [16]. Moreover, biological production of sulfur is well correlated with the O_2/H_2S ratio (0.61 ± 0.02 mol mol^{-1}), which corresponds to literature values [6,18]. Through all experiments, the sulfate selectivity (Eq. 2) remained constant (2 ± 1 mol%). Along with a further increase of the MT loading rate, the selectivity for sulfur production decreases. This is caused by inhibition of the biological activity, resulting in sulfide accumulation. The increasing sulfide concentrations result in a decrease of the ORP at constant oxygen supply rates. However, because the system is operated at an ORP setpoint value of -390 mV, the oxygen supply rate increases once the ORP value is below the setpoint value. Because the additional O_2 is not consumed by the bacteria an increase of the DO and P_{O_2} in the bioreactor headspace was found (Fig. 4A). As a result, the biotic sulfide oxidation rate is overtaken by its abiotic oxidation under the formation of $S_2O_3^{2-}$ (Eq. 3). It can be seen that thiosulfate formation becomes significant at MT loading rates above 0.5 mM d^{-1}. Moreover, any process deterioration is also obvious from the increased standard deviation of product selectivity and oxygen related parameters (Fig. 4A). The situation in which sulfide accumulates due to inhibition of SOB and when it is not possible to maintain a constant redox by dosing oxygen

to the gas recycling loop is in what follows referred to as the "collapse" of the bioreactor. For experiments with a medium salinity of 1.5 M [Na^+ + K^+], the bioreactor collapsed under MT loading of 0.59 mM d^{-1} (Fig. 4B). In a previous study, where SOB were exposed to MT, the decrease in sulfur production was never observed [15], because these experiments were performed at significantly lower MT loading rates ($\leq$ 79.3 µM d^{-1}).
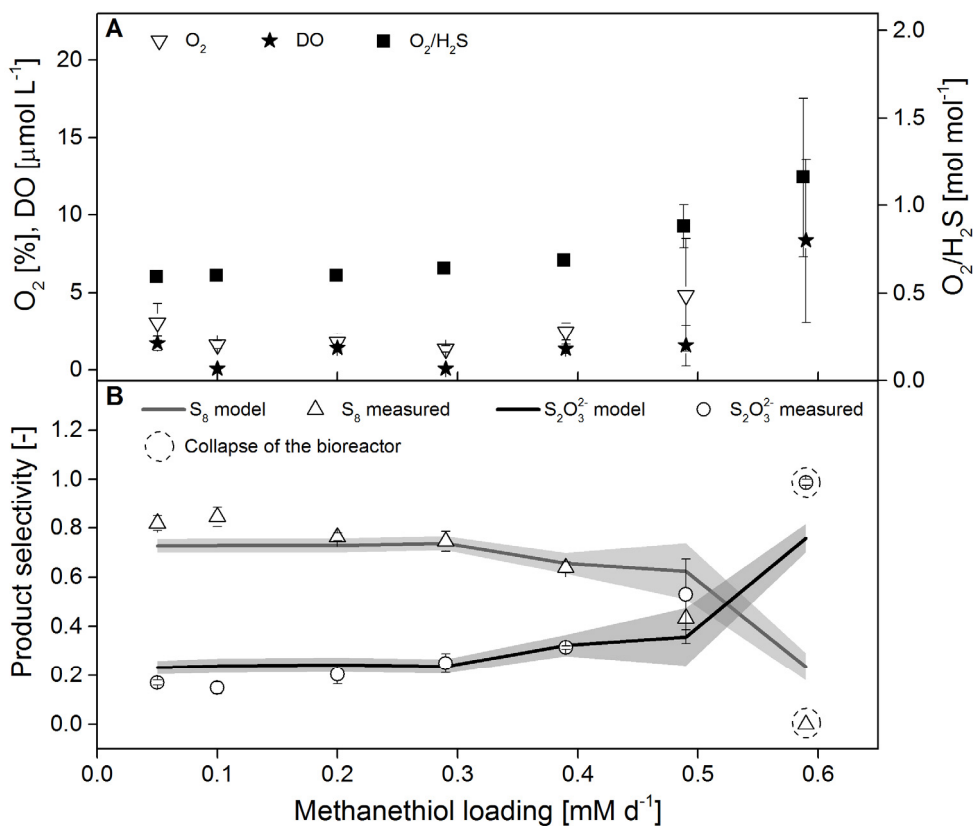
Figure 4. Bioreactor performance of experimental runs at different methanethiol loadings. **A.** Oxygen in the headspace of the bioreactor, dissolved oxygen (DO) and molar O_2/H_2S supply. H_2S loading rate = 61.3 mM d^{-1}, pH = 8.5 and [Na^+ + K^+] = 1.5 M. **B.** Sulfur and thiosulfate selectivity with corresponding model predictions. The sulfate selectivity was constant during all experiments (2 ± 1 %). The grey area corresponds to model output uncertainties as a result of variations in DO concentrations.

4.3.3. Mathematical model of integrated absorber and bioreactor

4.3.3.1. Estimation of the unknown parameters

The unknown parameters (Table 3) were estimated using a non-linear least-squares method (the Levenberg-Marquardt algorithm) as described by Keesman [29], unless otherwise stated. For instance, the distribution coefficient of MT (m_{MT}) in 1.5 M [Na^+ + K^+] medium was estimated based on static headspace measurements, as described elsewhere by Iliuta and Larachi [30]. The overall mass transfer coefficient for MT (K_{ov}^{MT}) was estimated based on absorption measurements (Supporting Information). A similar approach could not be applied for the estimation of K_{ov}^{H2S}, because in all performed experiments H2S was always below the detection limit due to high absorption rate. Therefore, K_{ov}^{H2S} and m_{H2S} were respectively assumed to be $3.5 \cdot 10^{-3}$ m^2 s^{-1} and 1.78 [31], for which a complete absorption occurred. To evaluate the sensitivity of these parameters choices, the assumed values were evaluated on a range of nominal value ± 10%. Within this range no significant effects on the model outputs were observed and thus, in what follows, these parameter values were fixed. The selectivity factors for sulfate (F_{SO4}) and sulfur (F_S) account for the product selectivity under the most optimal conditions for sulfur formation. The estimates of F_{SO4} and F_S were found from the fed-batch experiments, as presented in Roman et al. [16]. The rate constant k in Eq. 15 for the reaction between MT and biosulfur at pH = 8.7 and T = 35 °C was determined graphically and is given by $k = 0.0373$ $m^{5.58}$ $mol^{-1.86}$ s^{-1}, according to Van Leerdam et al. [26]. The maximum reaction rate of biotic sulfide oxidation (r_{max}^{H2S}), Michaelis constant (K_M^{H2S}) and inhibition constant for sulfur formation (k_i^{S8}) were estimated from data obtained from the BSM tests (Section 4.3.1). The Michaelis-Menten constant (K_M^{H2S} = 6 ± 1 µM) and the inhibition constant (k_i = 7.6 ± 0.8 µM) were found to be comparable to the parameter estimated from the BOM tests (K_M^{H2S} = 3.6 ± 0.3 µM and k_i = 3.1 ± 0.5 µM) for the same biomass and medium, but at 35 °C [16]. Although the BSM tests were performed at 25 °C and BOM tests at 35 °C, we still can compare obtained estimates K_M and k_i. This holds because SOB can be considered as eurythermal species [12], which are known to have a stable K_m and k_i value [32,33]. In contrast to k_i^{S8}, it was not possible to estimate the inhibition constant for sulfate formation (k_i^{SO4}) from data of the BSM experiments, as this test only includes the first (sulfide oxidation) step. Therefore, k_i^{SO4} was estimated based

on the data from the preceding study [16]. The estimate of k_I^{SO4} was found to be 33 times lower than k_I^{S8}, which is in agreement with the assumption that the selectivity for sulfur and sulfate have different susceptibility to MT. On the basis of the same study, we also estimated the thiosulfate reaction constant (k_{S2O3}).

Table 3. Parameter estimates with corresponding standard deviations.

Symbol	Value	Unit
F_S	0.78 ± 0.09	-
F_{SO4}	0.192 ± 0.08	-
k_I^{S8}	7.6 ± 0.8	µM
k_I^{SO4}	0.23 ± 0.05	µM
K_M^{H2S}	6 ± 1	µM
$K_{ov,MT}$	1.856E-03 ± 3E-06	$m^2\ s^{-1}$
k_{S2O3}	21 ± 1	$m^{2.46}\ mol^{-0.82}\ s^{-1}$
$m_{DMDS}^{0.5M}$	5.0 ± 0.3	-
$m_{DMDS}^{1.5M}$	4.0 ± 0.2	-
$m_{MT}^{0.5M}$	2.8 ± 0.3	-
$m_{MT}^{1.5M}$	2.00 ± 0.05	-
r_{max}^{H2S}	3.5E-05 ± 1E-06	$mol\ m^{-3}\ s^{-1}\ mgN^{-1}$

4.3.3.2. Validation of the bioreactor model

The estimated parameters in Table 3, obtained from literature and lab-scale experiments, were used to validate the bioreactor model. Only limited literature data were available to describe biological sulfide oxidation in the presence of MT. Hence, the model (Eq. 4-15) with parameter values from Table 3, was validated with data obtained from the bioreactor experiments described in section 4.3.2.

In the integrated reactor system, dimethyl disulfide (DMDS) is the end-product from the abiotic oxidation of MT. In order to validate the model assumption that the gas absorber and the bioreactor are in equilibrium, we measured the DMDS

concentration in the absorber outlet and in the bioreactor headspace (Fig. 5). Results obtained at stable bioreactor operation (all points except for an MT loading of 0.59 mM d^{-1}) show that the DMDS concentrations are indeed the same in the bioreactor headspace and in the absorber outlet. This observation confirms that the liquid and gas phase are in equilibrium. The DMDS concentration in the bioreactor headspace increased significantly after the bioreactor collapsed because of an increase in the oxygen concentration (Fig. 4A), which subsequently resulted in an intensified oxidation of MT to DMDS.
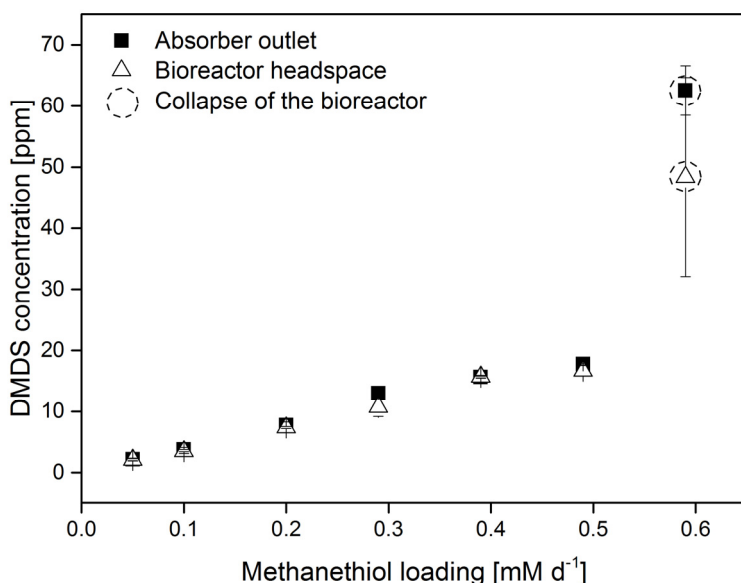
Figure 5. Concentration of dimethyl disulfide (DMDS) in headspace of the bioreactor and absorber outlet at different methanethiol loadings. Reactor system operated at H$_2$S loading rate = 61.3 mM d^{-1}, temperature = 35 °C, pH = 8.5, and [Na$^+$ + K$^+$] = 1.5 M.

Results of the model are expressed in terms of the selectivity for sulfur and thiosulfate formation in mol% (Fig. 4B). The model also predicts selectivity for sulfate, but these results are not included in the graph as they remained fairly constant, at a level of 2 ± 1 mol%, which are close to the measured value. For the other two selectivities, the model fit is in very good agreement with the experimental data (Fig. 4B). It can be seen that the model predicts a stable

bioreactor operation up to MT loading rate of 0.3 mM d^{-1}. Above this value, inhibition of biological reactions is predicted and observed, leading to an increase of abiotic oxidation of sulfide to form thiosulfate. At MT loading rates above 0.5 mM d^{-1}, model output uncertainties increase significantly due to an increased instability of the process, e.g. high fluctuations of DO (Fig. 4A). For the highest loading of MT (0.6 mM d^{-1}), i.e. the condition under which the bioreactor collapsed, the model does not predict the observed complete inhibition of biotic sulfide oxidation. However, a strong decline in biological activity is predicted.

The proposed model structure with corresponding parameter values allow to summarize the experimental results presented in the current study in mathematical terms. Furthermore, the model can be used to predict the product selectivity of the biological oxidation of sulfide and corresponding uncertainty bounds under conditions different from that were measured. Also, given the model, the biomass concentration that maintains the production of sulfur at a desired level in the presence of a specific concentration of MT can be calculated.

4.3.4. Mitigation of the methanethiol inhibition

Members of the genus *Thioalkalivibrio* have a wide salt tolerance ranging from 0.3 to 4 M total [Na$^+$ + K$^+$] with an optimum concentration between 0.4 and 2 M [34]. Within this broad range of salinity conditions, bacteria produce compatible solutes, such as glycine betaine, to control their osmotic pressure [8,35]. The concentration of individual compatible solutes increases at increasing salt concentrations and may constitute up to 9% of the total dry weight depending on the salinity [36]. Synthesis of these compounds consumes extra energy. Therefore, we hypothesized that after the reduction of the medium salinity from 1.5 to 0.5 M [Na$^+$ + K$^+$], bacteria will be under lower salt stress and might have more energy available to cope with MT. Especially, under sulfur-forming condition SOB generate limited amount of energy, and therefore, even a small change in energy generation might be vital for the SOB. Another advantage of lowering the medium salinity is an increase in oxygen solubility [37]. This increase can result in improved access of bacteria to oxygen, assuring stable operation of the bioreactor.

The effect of a lower salinity medium (0.5 M [Na$^+$ + K$^+$]) was investigated under identical conditions as experiments with the 1.5 M [Na$^+$ + K$^+$] medium,

described in section 4.3.2. Lowering the salt concentration resulted in a process less vulnerable to MT inhibition, which can be seen by the last stable operation of the bioreactor (related to the last stable data point in the graph) at almost two times higher loading of MT (0.49 *v.* 0.89 mM d^{-1}) (Fig. 4B and 6A). The bioreactor collapsed at an MT loading rate of 0.99 mM d^{-1}. Unfortunately, neither these nor intermediate measurements are available. For each experiment, i.e. under low and high salinity conditions, the MT and DMDS concentrations were measured in the bioreactor headspace (data not shown). Based on these measurements and estimation of the distribution coefficients for MT and DMDS, as described elsewhere [30,38], it was possible to calculate the concentration of these compounds in the bioreactor liquid (Fig. 6 B-C). From Figures 6B-C, it follows that at 0.5 M [Na$^+$ + K$^+$], the system can tolerate 2-3 times higher MT and DMDS concentrations compared to salinity 1.5 M [Na$^+$ + K$^+$].

Figure 6A and 4B show that 50% inhibition of sulfur production in medium 0.5 and 1.5 M [Na$^+$ + K$^+$] occurs at an MT loading rate of ~0.75 and ~0.49 mM d^{-1}, respectively. Under these conditions, the DMDS concentration in the bioreactor liquid is 2.5 times higher at 0.5 than at 1.5 M [Na$^+$ + K$^+$] medium (7.0 μM *v.* 2.8 μM), while the MT concentrations are comparable (2.5 and 3.2 μM) for the same conditions (Fig. 6 B-C). This means that the sulfur production is inhibited by 50% at similar MT concentrations. Moreover, the DMDS concentrations in the bioreactor liquid are 300 - 500 times lower for both saline media, than the IC$_{50}$ concentration (1500 μM) found by Van den Bosch et al. [17], while the MT concentrations are only 17 times lower (~2.9 *v.* 50 μM). Considering that MT is responsible for the sulfur inhibition in our experiments, the lower value of IC$_{50}$ can be explained by assuming that MT is a competitive inhibitor. Therefore, MT competes with sulfide in binding to the active place of the enzymes and the binding rate depends on the concentration of both of these compounds. The IC$_{50}$ concentration for MT found by Van den Bosch et al. [17] was determined for a sulfide concentration of 8 mg L^{-1}. Thus, lower values of the IC$_{50}$ concentrations for MT in our experiments are related to lower sulfide concentrations in the bioreactor, which were below the detection limit (0.1 mg L^{-1}). Based on these observations it can be deduced that from two dominant organic sulfur compounds (MT and DMDS) present in the bioreactor, MT is the one responsible for the sulfur inhibition.

4
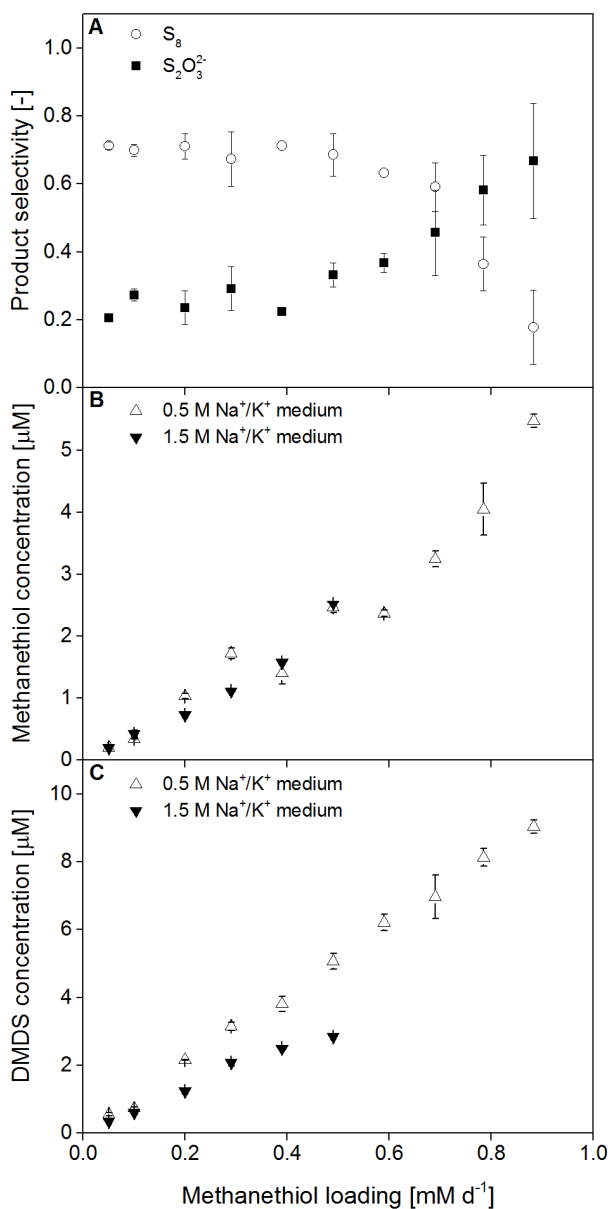
Figure 6. **A.** Product selectivities of stable bioreactor performance at different methanethiol loadings operated at H_2S loading rate = 61.3 mM d^{-1}, pH = 8.5 and $[Na^+ + K^+]$ = 0.5 M. **B, C.** Methanethiol and dimethyl disulfide (DMDS) concentrations respectively, in the liquid phase of the bioreactor at $[Na^+ + K^+]$ = 0.5 M and $[Na^+ + K^+]$ = 1.5 M. Experimental data for an MT loading 0.99 mM d^{-1} are not shown; impossible to measure.

4.4. Conclusions

In this paper it was shown for the first time that the biological oxidation of sulfide to sulfur was inhibited by MT. The inhibition occurs at an MT concentration of 1 µM and above, at MT a loading rate of 0.3 mM d^{-1} and an H$_2$S loading rate of 61.3 mM d^{-1}. Furthermore, a mathematical model has been proposed to describe the experimental results. This model is based on recent findings concerning the mode of SOB inhibition by MT and kinetic parameters found from BSM tests. With this model it is possible to calculate the maximum MT/H$_2$S supply ratio for which no inhibition occurs. This ratio also depends on the ORP and biomass concentration. The negative effect of MT on the biological formation of elemental sulfur can be mitigated by lowering the salinity of the bioreactor medium. Another positive effect of a lower salinity is an increased oxygen solubility which lowers the energy requirements to aerate the bioreactor. Our results also show that the toxic effect of MT can be mitigated by the chemical oxidation of MT to DMDS.

Based on the current work it can be concluded that the combined removal of H$_2$S and MT can be performed in the conventionally applied three-step process: (1) Absorption of sulfur compounds, (2) Oxidation of sulfur compounds and (3) Separation of the produced biosulfur particles. However, when the MT toxicity level is exceeded a separate absorption of H$_2$S and MT can be considered. A split absorber design could be applied in order to remove the majority of the H$_2$S in the first absorber and MT in the second absorber with an alkaline solution. It should be noted that the partial absorption of MT in the first absorber should be low to not exceed any toxic levels in the bioreactor. This can be achieved by adjusting the wash water flow over the absorber column. The absorbed MT from the second absorber could be transformed to diorgano polysulfanes by a reaction with biosulfur. Under anaerobic conditions the formed organosulfur compounds can be converted to sulfide and recycled to the sulfide oxidizing bioreactor. The proposed treatment process would allow for a complete removal of H$_2$S and thiols.

4

Acknowledgements

References

1. Adib H, Sharifi F, Mehranbod N, Kazerooni NM, Koolivand M. Support Vector Machine based modeling of an industrial natural gas sweetening plant. *J. Nat. Gas Sci. Eng.* Elsevier; 2013;14:121–131.

2. Smet E, Lens PNL, Langenhove HV. Treatment of waste gases contaminated with odorous sulfur compounds. *Crit. Rev. Env. Sci. Tec.* Taylor & Francis; 1998;28:89–117.

3. Cline C, Hoksberg A, Abry R, Janssen AJH. Biological Process for H_2S Removal from Gas Streams: The Shell-Paques/THIOPAQ™ Gas Desulfurization Process. *Proceedings of the Laurance Reid Gas Conditioning Conference.* 2003. p. 1–18.

4. Buisman CJN, Geraats BG, IJspeert P, Lettinga G. Optimization of sulphur production in a biotechnological sulphide-removing reactor. *Biotechnol. Bioeng.* Wiley Online Library; 1990;35:50–56.

5. Janssen AJH, Meijer S, Bontsema J, Lettinga G. Application of the redox potential for controling a sulfide oxidizing bioreactor. *Biotechnol. Bioeng.* Wiley Online Library; 1998;60:147–155.

6. Klok JBM, van den Bosch PLF, Buisman CJN, Stams AJM, Keesman KJ, Janssen AJH. Pathways of sulfide oxidation by haloalkaliphilic bacteria in limited-oxygen gas lift bioreactors. *Environ. Sci. Technol.* ACS Publications; 2012;46:7581–7586.

7. Klok J, de Graaff M, van den Bosch PLF, Boelee NC, Keesman KJ, Janssen AJH. A physiologically based kinetic model for bacterial sulfide oxidation. *Water Res.* Elsevier; 2013;47(2):483–492.

8. Muyzer G, Sorokin DY, Mavromatis K, Lapidus A, Clum A, Ivanova N, Pati A, d' Haeseleer P, Woyke T, Kyrpides NC. Complete genome sequence of "*Thioalkalivibrio sulfidophilus*" HL-EbGr7. *Stand. Genomic. Sci.* Genomic Standards Consortium; 2011;4:23.

9. Chen KY, Morris JC. Kinetics of oxidation of aqueous sulfide by oxygen. *Environ. Sci. Technol.* ACS Publications; 1972;6:529–537.

10. Sorokin DY, Muntyan MS, Panteleeva AN, Muyzer G. *Thioalkalivibrio sulfidiphilus* sp. nov., a haloalkaliphilic, sulfur-oxidizing gammaproteobacterium

from alkaline habitats. *Int. J. Syst. Evol. Microbiol.* Soc General Microbiol; 2012;62:1884–1889.

11. Sorokin D, van den Bosch PLF, Abbas B, Janssen AJH, Muyzer G. Microbiological analysis of the population of extremely haloalkaliphilic sulfur-oxidizing bacteria dominating in lab-scale sulfide-removing bioreactors. *Appl. Microbiol. Biotechnol.* Springer; 2008;80:965–975.

12. Sorokin DY, Kuenen JG. Haloalkaliphilic sulfur-oxidizing bacteria in soda lakes. *FEMS Microbiol. Rev.* Wiley Online Library; 2005;29:685–702.

13. Visser JM, Robertson LA, Van Verseveld HW, Kuenen JG. Sulfur production by obligately chemolithoautotrophic thiobacillus species. *Appl. Environ. Microbiol.* Am Soc Microbiol; 1997;63:2300–2305.

14. Finkelstein A, Benevenga NJ. The effect of methanethiol and methionine toxicity on the activities of cytochrome c oxidase and enzymes involved in protection from peroxidative damage. *J. Nutr.* 1986;116:204–215.

15. Van den Bosch PLF, Fortuny-Picorell M, Janssen AJH. Effects of methanethiol on the biological oxidation of sulfide at natron-alkaline conditions. *Environ. Sci. Technol.* ACS Publications; 2009;43:453–459.

16. Roman P, Bijmans MFM, Janssen AJH. Influence of methanethiol on biological sulfide oxidation in gas treatment system. *Environ. Tech.* 2015.

17. Van den Bosch PLF, de Graaff M, Fortuny-Picornell M, van Leerdam RC, Janssen AJH. Inhibition of microbiological sulfide oxidation by methanethiol and dimethyl polysulfides at natron-alkaline conditions. *Appl. Microbiol. Biotechnol.* Springer; 2009;83:579–587.

18. Van den Bosch PLF, van Beusekom OC, Buisman CJN, Janssen AJH. Sulfide oxidation at halo-alkaline conditions in a fed-batch bioreactor. *Biotechnol. Bioeng.* Wiley Online Library; 2007;97:1053–1063.

19. Roman P, Bijmans MFM, Janssen AJH. Quantification of individual polysulfides in lab-scale and full-scale desulfurisation bioreactors. *Environ. Chem.* CSIRO; 2014;11:702–708.

20. Pfennig N, Lippert KD. Über das vitamin B_{12}-bedürfnis phototropher Schwefelbakterien. *Arch. Microbiol.* Springer; 1966;55:245–256.

21. Janssen AJH, Lens PNL, Stams AJM, Plugge CM, Sorokin DY, Muyzer G, Dijkman H, Van Zessen E, Luimes P, Buisman CJN. Application of bacteria involved in the biological sulfur cycle for paper mill effluent purification. *Sci. Total Environ.* Elsevier; 2009;407:1333–1343.

22. Blauwhoff P, Van Swaaij W. Simultaneous mass transfer of H_2S and CO_2 with complex chemical reactions in an aqueous di-isopropanolamine solution. *Chem. Eng. Process.* Elsevier; 1985;19:67–83.

23. Prange A, Chauvistré R, Modrow H, Hormes J, Trüper HG, Dahl C. Quantitative speciation of sulfur in bacterial sulfur globules: X-ray absorption spectroscopy reveals at least three different species of sulfur. *Microbiology*. Soc General Microbiol; 2002;148:267–276.

24. O'Brien DJ, Birkner FB. Kinetics of oxygenation of reduced sulfur species in aqueous solution. *Environ. Sci. Technol.* ACS Publications; 1977;11:1114–1120.

25. Steudel R. The chemistry of organic polysulfanes RS (n)-R (n> 2). *Chem. Rev.* 2002;102:3905.

26. Van Leerdam RC, Bosch PLF, Lens PNL, Janssen AJH. Reactions between methanethiol and biologically produced sulfur. *Environ. Sci. Technol.* 2011;45:1320–1326.

4

27. Fischer H, Schulz-Ekloff G, Wöhrle D. Oxidation of aqueous sulfide solutions by dioxygen part I: autoxidation reaction. *Chem. Eng. Technol.* Wiley Online Library; 1997;20:462–468.

28. Sharma R. Enzyme Inhibition: Mechanisms and Scope. R. Sharma, editor. InTech; 2012.

29. Keesman KJ. System identification: an Introduction. Springer, Verlag, UK; 2011.

30. Iliuta MC, Larachi F. Gas-liquid partition coefficients and Henry's law constants of methyl mercaptan in aqueous solutions of Fe (II)-CDTA chelate complex. *Fluid Phase Equilib.* Elsevier; 2007;253:124–129.

31. Wilhelm E, Battino R, Wilcock RJ. Low-pressure solubility of gases in liquid water. *Chem. Rev.* ACS Publications; 1977;77:219–262.

32. Griffith SM, Brewer TG, Steiner JJ. Thermal Dependence of the Apparent Km of Glutathione Reductase from Three Wetland Grasses and Maize. *Ann. Bot.* Elsevier; 2001;87:599–603.

33. Somero GN. Proteins and temperature. *Annu. Rev. Physiol.* Annual Reviews 4139 El Camino Way, PO Box 10139, Palo Alto, CA 94303-0139, USA; 1995;57:43–68.

34. Sorokin DY, Banciu H, Robertson LA, Kuenen JG, Muntyan MS, Muyzer G. Halophilic and haloalkaliphilic sulfur-oxidizing bacteria. In: Rosenberg E. et al., editor. *The Prokaryotes*. Springer-Verlag: Berlin-Heidelberg; 2013. p. 529–554.

35. Banciu H, Sorokin DY, Kleerebezem R, Muyzer G, Galinski EA, Kuenen JG. Growth kinetics of haloalkaliphilic, sulfur-oxidizing bacterium *Thioalkalivibrio versutus* strain ALJ 15 in continuous culture. *Extremophiles*. Springer; 2004;8:185–192.

36. Banciu H, Sorokin DY, Rijpstra WIC, Sinninghe Damsté JS, Galinski EA, Takaichi S, Muyzer G, Kuenen JG. Fatty acid, compatible solute and pigment composition of obligately chemolithoautotrophic alkaliphilic sulfur-oxidizing bacteria from soda lakes. *FEMS Microbiol. Lett.* Wiley Online Library; 2005;243:181–187.

37. Millero FJ, Huang F, Laferiere AL. Solubility of oxygen in the major sea salts as a function of concentration and temperature. *Mar. Chem.* Elsevier; 2002;78:217–230.

38. Iliuta MC, Larachi F. Solubility of dimethyldisulfide (DMDS) in aqueous solutions of Fe (III) complexes of trans-1, 2-cyclohexanediaminetetraacetic acid (CDTA) using the static headspace method. *Fluid Phase Equilib.* Elsevier; 2005;233:184–189.

4

Nomenclature

Symbol	Parameter	Unit
Φ_G	Gas volumetric flow rate	$m^3\ s^{-1}$
Φ_L	Liquid volumetric flow rate	$m^3\ s^{-1}$
a	Gas-liquid interfacial area	$m^2\ m^{-3}$
$C_{H2S}^{G,z}$	Concentration of sulfide in the gas phase	$mol\ m^{-3}$
$C_{MT}^{G,z}$	Concentration of methanethiol in the gas phase	$mol\ m^{-3}$
$C_{H2S}^{L,z}$	Concentration of sulfide in the liquid phase	$mol\ m^{-3}$
$C_{MT}^{L,z}$	Concentration of methanethiol in the liquid phase	$mol\ m^{-3}$
C_{H2S}^{R}	Concentration of sulfide in the liquid outlet	$mol\ m^{-3}$
C_{O2}^{R}	Oxygen concentration in bioreactor	$mol\ m^{-3}$
C_{MT}^{R}	Concentration of the methanethiol in the liquid outlet	$mol\ m^{-3}$
$C_{H2S}^{R,in}$	Concentration of sulfide in the liquid inlet	$mol\ m^{-3}$
$C_{MT}^{R,in}$	Concentration of the methanethiol in the liquid inlet	$mol\ m^{-3}$
C_{S}^{R}	Sulfur concentration in bioreactor	$mol\ m^{-3}$
F_S	Sulfur selectivity coefficient	-
F_{SO4}	Sulfate selectivity coefficient	-
H	Column height	m
k	Reaction rate constant (reaction between methanethiol and biologically produced sulfur)	$m^{5.58}\ mol^{-1.86}\ s^{-1}$
$k_{G,H2S}$	Gas side mass transfer coefficient for sulfide	$m\ s^{-1}$
$k_{G,MT}$	Gas side mass transfer coefficient for methanethiol	$m\ s^{-3}$
k_I^{S8}	Inhibition constant for sulfur production	μM
k_I^{SO4}	Inhibition constant for sulfate production	μM
$k_{L,H2S}$	Liquid side mass transfer coefficient for sulfide	$m\ s^{-2}$
$k_{L,MT}$	Liquid side mass transfer coefficient for methanethiol	$m\ s^{-2}$
K_M^{H2S}	Michaelis constant	μM
$K_{ov,MT}$	Overall mass transfer coefficient for methanethiol	$m^2\ s^{-1}$
$K_{ov,H2S}$	Overall mass transfer coefficient for sulfide	$m^2\ s^{-1}$
k_{S2O3}	Reaction rate constant (chemical oxidation of sulfide)	$m^{2.46}\ mol^{-0.82}\ s^{-1}$
m_{H2S}	Distribution coefficient between gas and liquid for sulfide	-
m_{MT}	Distribution coefficient between gas and liquid for methanethiol	-
m_b	Total amount of biomass in the bioreactor	mgN
R_{H2S}	Molar consumption rate of sulfide	$mol\ m^{-3}\ s^{-1}$
r_{max}^{H2S}	Maximal reaction rate of sulfide oxidation	$mol\ m^{-3}\ s^{-1}\ mgN^{-1}$
R_{MT}	Molar consumption rate of sulfide	$mol\ m^{-3}\ s^{-1}$
r_S	Sulfide consumption rate for sulfur production	$mol\ m^{-3}\ s^{-1}\ mgN^{-1}$
r_{S2O3}	Sulfide consumption rate for thiosulfate production	$mol\ m^{-3}\ s^{-1}$
r_{SO4}	Sulfide consumption rate for sulfate production	$mol\ m^{-3}\ s^{-1}\ mgN^{-1}$
S	Column cross sectional area	m^2
V_r	Volume of the bioreactor	m^3
z	Height of column element	m

4

Supporting Information. The measured methanethiol concentration in the inlet and outlet of the gas absorber used for the estimation of the overall mass transfer coefficient ($K_{ov}{}^{MT}$).

4
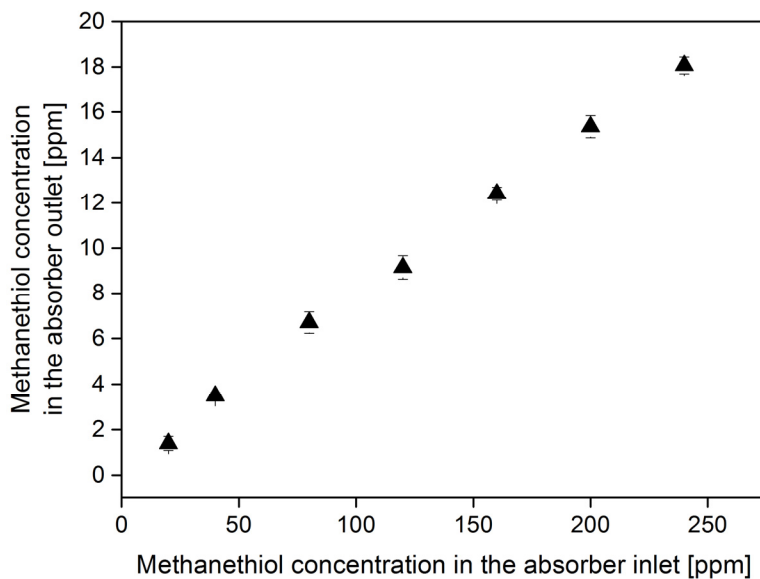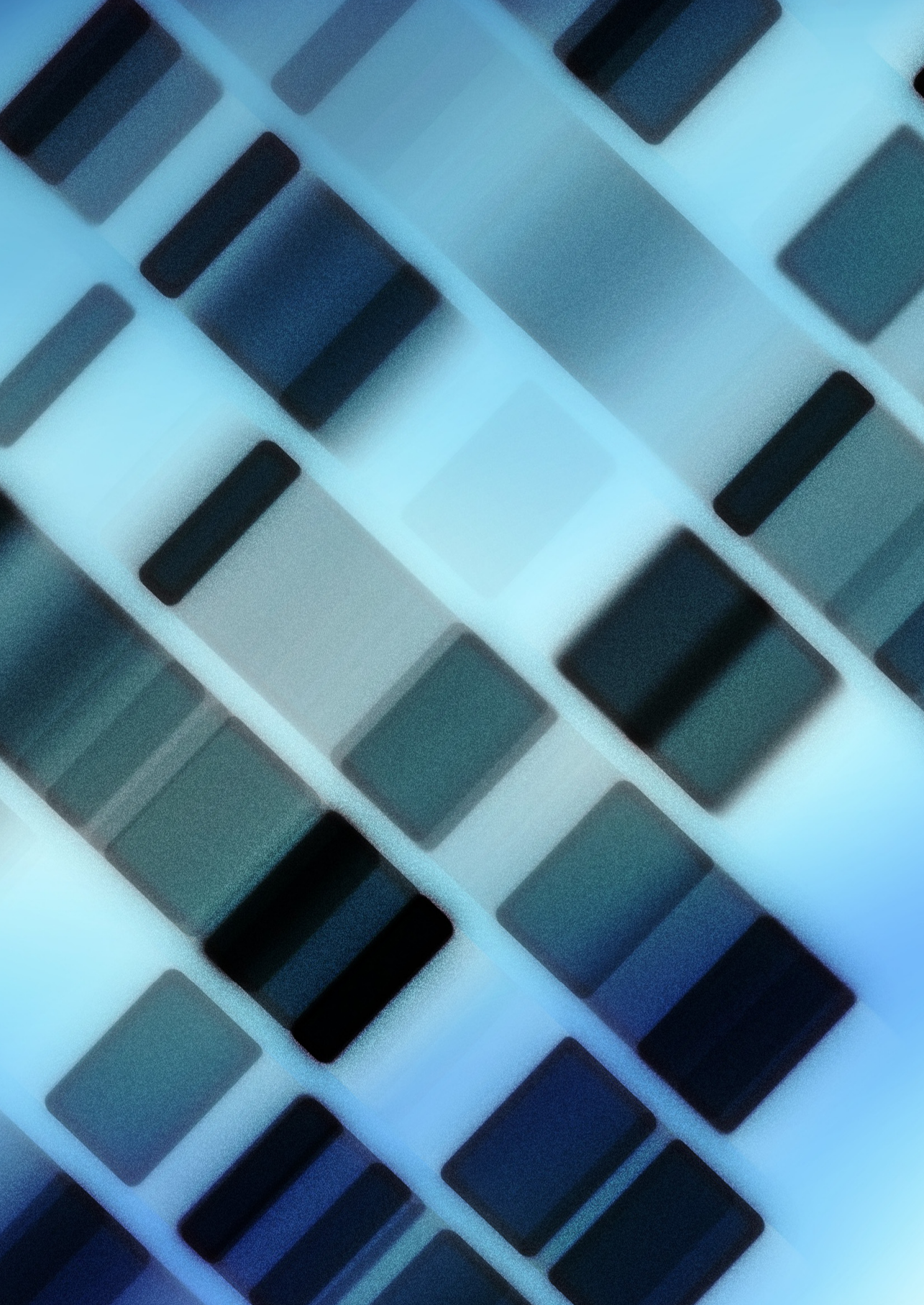
Chapter 5

Inhibition of a biological sulfide oxidation under haloalkaline conditions by thiols and diorgano polysulfanes

5

Abstract

A novel approach has been developed for the simultaneous description of sulfur and sulfate formation from the biological oxidation of hydrogen sulfide (H_2S) using a quick, sulfide-dependent respiration test. Next to H_2S, thiols are commonly present in sour gas streams. We investigated the inhibition mode and the corresponding inhibition constants of six thiols and diorgano polysulfanes on the biological oxidation of H_2S. A positive and negative linear relationship was found between the calculated IC_{50} values and the lipophilicity of thiols and diorgano polysulfanes, respectively. Moreover, a mathematical model was proposed to estimate the biomass activity in the absence and presence of sulfurous inhibitors. The biomass used in the respiration tests originated from a full-scale biodesulfurization reactor. A microbial community analysis of this biomass revealed that two groups of microorganism are abundant, viz. *Ectothiorhodospiraceae* and *Piscirickettsiaceae*.

5.1. Introduction

Biological processes to remove hydrogen sulfide (H_2S) from gas streams have become increasingly attractive in recent years as an alternative to physicochemical technologies [1,2]. Key drivers to select biotechnological solutions for the treatment of sour gas streams instead of physicochemical processes are the higher H_2S removal efficiencies, lower operational cost and, most importantly, the simpler operating procedures [3]. After the first commercial applications in the oil and gas industry, the need has arisen to broaden the operating window of these bioprocesses by enabling the removal of thiols next to H_2S as these volatile organosulfur compounds are regularly present in sour natural gas streams.

Thiols are considerably more toxic to sulfur oxidizing bacteria (SOB) than dissolved sulfide [4,5]. In the presence of oxygen thiols are rapidly oxidized to organic disulfides (Eq. 1) [6]. Thiols also react with biologically produced sulfur particles to form diorgano polysulfanes (Eq. 2). These organosulfur compounds (with n > 3) are unstable and quickly decompose to stable di- and trisulfides [7], according to Eq. 3.

$$2\ RSH + 0.5\ O_2 \rightarrow RS_2R + H_2O \qquad\qquad (1)$$

$$2\ RSH + S_8 \rightarrow RS_nR + S_x^{2-} + 2\ H^+,\ \text{with } n+x = 10 \qquad (2)$$

$$2\ RS_nR \leftrightarrow RS_{n-1}R + RS_{n+1}R,\ \text{with } n > 3 \qquad\qquad (3)$$
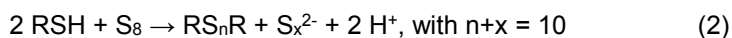
Diorgano di- and trisulfides are found to be the most predominant organosulfur compounds in a bioreactor operating at haloalkaline conditions [4]. Clearly, a better understanding of the toxic effects of these compounds on SOB is of key importance to ensure a stable reactor performance.

It was shown that *Thioalkalivibrio sulfidophilus* is the most dominant SOB in full-scale Thiopaq installations that are operated at haloalkaline conditions, i.e. at pH 9, 1 M total Na^+ and at a redox potential below -250 mV to ensure sulfur-producing conditions [8]. Based on a complete genome analysis Muyzer et al. (2011) [9] reconstructed a sulfur oxidation pathway in *Tv. sulfidophilus*. In this pathway SOB oxidize sulfide to sulfate via zero-valent sulfur as an intermediate. In the first step *Tv. sulfidophilus* oxidizes sulfide to a polysulfur-containing compound(s), hereafter referred to as $\{S_x\}$. $\{S_x\}$ can be secreted from the periplasm as elemental sulfur globules at low redox conditions or oxidized to sulfate via intermediate sulfite

at elevated redox values (Fig. 1). The reactions describing the formation of both products can be written in the following simplified form:

$$HS^- + 0.5\ O_2 \rightarrow 1/8\ S_8 + OH^- \tag{4}$$

$$HS^- + 2\ O_2 \rightarrow SO_4^{2-} + H^+ \tag{5}$$

A more detailed description of the underlying principles of biological sulfide oxidation was presented by Klok et al. (2012) [10].

Reaction kinetics of the biological sulfide oxidation processes can be studied by performing biological oxygen monitoring (BOM) tests, which are based on monitoring the decrease of the dissolved oxygen concentration. Recently it was found that for biomass samples in which representatives of the genus *Thioalkalivibrio* were identified as the dominating SOB, the oxygen consumption rate can be described by two different reaction rates [4]. The first and fast rate (R1) is related to the partial oxidation of sulfide to {S_x}, while the second and much lower rate (R2) is related to the further oxidation of {S_x} to sulfate ions (Fig. 1) [11].
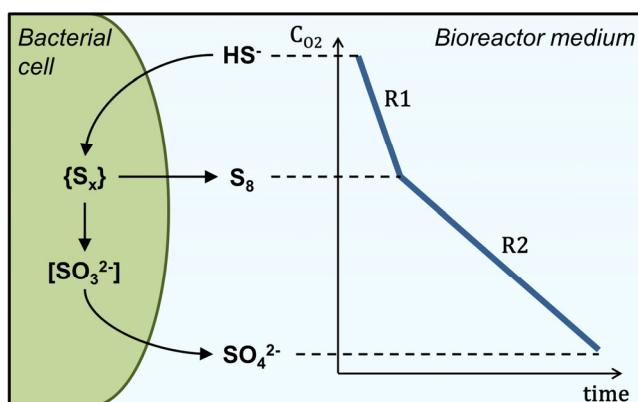
Figure 1. Schematic overview of the reaction that occurs in the bacterial cell related to sulfide oxidation and the corresponding oxygen concentration profile from biological oxygen measurements.

We have also shown that by understanding the inhibition mode for a single thiol, it is possible to model the performance of the biodesulfurization process in lab-scale reactors [4]. The aim of the current study is to investigate the inhibitory effects of the most common thiols i.e. MT, ethanethiol (ET), 1-propanothiol (PT) and the products of their chemical oxidation (Eq. 1-3): DMDS, diethyl disulfide (DEDS) and dipropyl disulfide (DPDS) on the biological oxidation rate of dissolved sulfide.

The identified modes of inhibition and the associated kinetic parameters will be used in a set of mathematical equations to describe the prevailing reaction kinetics in integrated systems for the treatment of sulfide and thiols containing gas streams. Several authors have presented kinetic models to characterize the aerobic biological sulfide oxidation process [12–14]. However, the inhibition by organic sulfur compounds was never taken into account despite the fact that thiols are a commonly present in sour gas streams [15–17]. Our mathematical model builds on a genomic model proposed by Muyzer et al. (2011) [9]. The presented model can be used as a tool for designing industrial biodesulfurization installations.

Table 1. Chemicals used to prepare solutions in the current study. All chemicals were purchased from Sigma-Aldrich, the Netherlands.

Compound name	CAS no.	Chemical formula	Solvent
Sodium sulfide hydrate	1313-84-4	$Na_2S \cdot 9\ H_2O$	Water
Sodium thiomethoxide	5188-07-08	CH_3SNa	Water
Ethanethiol	75-08-1	C_2H_5SH	Methanol
1-Propanethiol	107-03-9	$CH_3CH_2CH_2SH$	Methanol
Dimethyl disulfide	624-92-0	$CH_3S_2CH_3$	Methanol
Diethyl disulfide	110-81-6	$(C_2H_5)_2S_2$	Methanol
Dipropyl disulfide	629-19-6	$(CH_3CH_2CH_2)_2S_2$	Methanol

5

5.2. Materials and methods

5.2.1. Experimental setup

Respiration tests were performed to assess the kinetic parameters of biological sulfide oxidation and the mode of inhibition by thiols and diorgano polysulfanes (Table 1) in an air-saturated medium. We used a similar setup as described elsewhere [18], which consisted of a glass mini-reactor (60 mL) equipped with a magnetic stirrer. The reactor was closed with a Teflon piston to avoid any oxygen ingress. We added stock solutions containing the inhibitors and sulfide to the reactor with a syringe passing through the piston. The sulfide oxidation rate was determined by measuring the oxygen consumption rate with a dissolved-oxygen (DO) sensor (Oxymax COS22D, Endress+Hauser). Signals from the DO sensor were

recorded using a multiparameter transmitter (Liquiline CM442; Endress+Hauser, the Netherlands). All experiments were performed at 35 °C (DC10-P5/U thermostat bath, Haake, Germany).

5.2.2. Medium composition

The reactor medium included a carbonate/bicarbonate buffer of 0.1 M Na_2CO_3 and 0.8 M $NaHCO_3$ (1 M total Na^+). Furthermore, the medium contained 1.0 g K_2HPO_4, 0.20 g $MgCl_2 \times 6\ H_2O$, and 0.60 g urea, each per 1 L of Milli-Q water. A trace elements solution (1 mL L^{-1}) was added as described elsewhere [19]. The final pH of the medium was 9.00 ± 0.01 at 35 °C.

5.2.3. Biomass

In the respiration tests we used biomass sampled from a full-scale gas biodesulfurization installation, located at Industriewater Eerbeek B.V., the Netherlands which is operated at oxygen-limiting conditions and low redox potential values [1].

A sulfur-free biomass suspension was prepared by centrifugation (30 min at 16,000 x *g*) of the sulfide-oxidizing culture followed by a washing step after re-suspending the pellet in the same medium as described in section 5.2.2.

DNA extraction from biomass samples taken from a full-scale gas biodesulfurization installation were performed as follows. First, the samples were washed twice with a buffer of pH 9 and 0.5 M Na^+ to prevent the occurrence of an osmotic shock. Then, the washing was performed by (1) centrifuging the samples at 20,000 x *g* for 5 min; (2) removal of the supernatant; and (3) addition of fresh buffer and mixing with a vortex to re-suspend the pellet. Afterwards, Total Genomic DNA was extracted from the washed biomass using the PowerBiofilm™ DNA Isolation Kit (MoBio, USA) following the manufacturer's instructions. All the above procedures were performed in duplicate.

For biomass samples from the full-scale gas biodesulfurization installation the 16S rRNA gene profiling was performed as following. Illumina 16S rRNA gene amplicon libraries were generated and sequenced at BaseClear BV (Leiden, the Netherlands). In short, barcoded amplicons from the V3-V4 region of 16S rRNA

genes were generated using a 2-step PCR. 10-25 ng genomic DNA was used as template for the first PCR with a total volume of 50 µl using the 341F (5'-CCTACGGGNGGCWGCAG-3') and the 785R (5'-GACTACHVGGGTATCTAATCC-3') primers appended with Illumina adaptor sequences. PCR products were purified and the size of the PCR products were checked on a Bioanalyzer (Agilent, CA, USA) and quantified by fluorometric analysis. Purified PCR products were used for the 2nd PCR in combination with sample-specific barcoded primers. Subsequently, PCR products were purified, checked on a Bioanalyzer (Agilent, CA, USA) and quantified, followed by multiplexing, clustering, and sequencing on an Illumina MiSeq with the paired-end 250 cycles protocol and indexing. The sequencing run was analyzed with Illumina CASAVA pipeline (v1.8.3) with demultiplexing based on sample-specific barcodes. The raw sequencing data produced was processed by removing the sequence reads of too low quality (only "passing filter" reads were selected) and discarding reads containing adaptor sequences or PhiX control with an in-house filtering protocol. A quality assessment on the remaining reads was performed using the FASTQC quality control tool version 0.10.0.

5.2.4. Respiration tests

Sulfide-dependent O_2-consumption rates were measured in a thermostated reactor (Section 5.2.1). The biomass concentration was always kept at 10 mg N L^{-1}, measured as the amount of organic nitrogen oxidized to nitrate by digestion with peroxodisulphate (LCK238, Hach Lange, the Netherlands) in triplicate. The medium with biomass was aerated as described elsewhere [5]. Measurements commenced after sulfide was injected and lasted for 5 to 14 minutes. All solutions containing sulfurous compounds were freshly prepared before each series of experiments. Methanol was used as a solvent for hydrophobic inhibitors (Table 1), which had no effect on the oxygen consumption rate (data not shown). For all other inhibitors, we used Milli-Q water as a solvent. In order to prevent any oxidation of thiols all solvents were first purged with 99.99% nitrogen gas for at least 15 min.

A wide range of sulfide concentrations was applied to estimate the kinetic parameters for both biological sulfide oxidation rates (R1 and R2, Fig.1). Sulfide concentrations ranging between 0.02 and 0.3 mM were used to estimate kinetic parameters related to R1. In this concentration range R2 was more or less constant and ranges around

its maximum value. Hence, a reliable estimation of its value was not possible. In order to estimate kinetic parameters related to R2 significantly lower sulfide concentrations (0.005 - 0.012 mM) were applied. For these ranges of sulfide concentrations, we experimentally verified that the contribution of chemical sulfide oxidation to biological sulfide oxidation is insignificantly small, and can therefore be neglected.

We performed a series of experiments in the absence of any inhibitor to estimate the maximum biological sulfide oxidation (r_{max}) rate and the associated Michaelis constant (K_M). The sulfide concentration for R1 varied from 0.2 to 4.0 K_M and for R2 from 2.0 to 8.0 K_M to obtain reliable estimates of K_M and r_{max} [20]. The methylene blue method (Cuvette test LCK653, Hach Lange, the Netherlands) was used to verify the sulfide concentration in stock solution. All measurements were performed in triplicate. We performed respiration tests in the presence of an inhibitor to identify the mode of inhibition and the parameters for inhibitors that bind to free enzyme (K_i) and enzyme-substrate complex (K_{ies}). In these tests first the inhibitor was added and then the substrate. Each series of experiments was carried out in duplicate. We tested all inhibitors for both oxidation steps (R1 and R2) at 35 °C with an incubation time between 1 and 60 min to determine the time required for biomass incubation with an inhibitor at a certain concentration.

5.2.5. Modelling biological sulfide oxidation pathway

A mathematical model for describing the biological sulfide oxidation with SOB has been developed on the basis of material balances for sulfide, {S_x} and O_2. It has been assumed that in the absence of inhibitors SOB oxidize sulfide (Eq. 6-7) to {S_x} (Eq. 8). The formed {S_x} is transformed to sulfate which results in an additional oxygen consumption (Eq. 9).

$$\frac{dc_{HS}}{dt} = -c_b \gamma^{R1} \frac{r_{max}^{R1} c_{HS}}{K_M^{R1} + c_{HS}} \tag{6}$$

$$\frac{dc_{O2}^{R1}}{dt} = -c_b \frac{r_{max}^{R1} c_{HS}}{K_M^{R1} + c_{HS}} \tag{7}$$

$$\frac{dc_{Sx}}{dt} = c_b \gamma^{R1} \frac{r_{max}^{R1} c_{HS}}{K_M^{R1} + c_{HS}} - c_b \gamma^{R2} \frac{r_{max}^{R2} c_{Sx}}{K_M^{R2} + c_{Sx}} \tag{8}$$

$$\frac{dc_{O2}^{R2}}{dt} = -c_b \frac{r_{max}^{R2} c_{Sx}}{K_M^{R2} + c_{Sx}} \tag{9}$$

The superscripts $R1$ and $R2$ refer to the first and second oxidation rate, as shown in Figure 1. The model also includes the endogenous oxygen consumption (r_{eg}) [5], which was calculated as follows:

$$\frac{dc_{O2}^{eg}}{dt} = -r_{eg} \tag{10}$$

Biomass growth is not included in the model equations as we assume that it remains constant during the relatively short time frame (<14 min) of the respiration experiments [21]. It should be noted that the terms used for describing the sulfide and {S_x} consumption rates have the same unit, because sulfide is transformed to {S_x}. The yield coefficients for sulfide (γ^{R1}, mM HS- (mM O₂)-1) and {S_x} consumption (γ^{R2}, mM HS- (mM O₂)-1) account for the conversion of r_{max} for oxygen consumption to sulfide consumption. It is not possible to estimate $\gamma^{R1,R2}$ and $r_{max}^{R1,R2}$ independently, as they always appear as the algebraic product $\gamma \cdot r_{max}$. Therefore, the values for $\gamma^{R1,R2}$ were chosen from the stoichiometric equations 4 and 5 and in, what follows, only $r_{max}^{R1,R2}$ and the affinity constants in Eq. 6-9 were estimated from the experimental data. Furthermore, it is assumed that oxygen is not a limiting factor as the medium is air-saturated i.e. there is an excess amount of oxygen available and the affinity constant for oxygen-respiring SOB are in the range of a few µM [22]. BOM tests with sulfide as substrate showed values of 1.5-2.5 µM O₂ for the representatives of the genus *Thioalkalivibrio* (unpublished results). The general mass balances for the substrates and {S_x} are solved for the following range of initial experimental conditions:

$$c_{HS}(0) \in [0.003, 0.3] \tag{11}$$

$$c_{Sx}(0) = 0 \tag{12}$$

$$c_{O2}^{R1}(0) \in [0.01, 0.022] \tag{13}$$

$$c_{O2}^{R2}(0) = 0 \tag{14}$$

Furthermore, c_{HS}, c_{Sx} and c_{O2} are the concentrations (in mM) of sulfide, {S_x} and oxygen, respectively. The total oxygen consumption is given by:

$$c_{O2}^{tot} = c_{O2}^{R1} + c_{O2}^{R2} + c_{O2}^{eg} \tag{15}$$

An uncertainty assessment of the predicted model output was performed by using a Monte Carlo simulation technique with parameters sampled from the distribution space of the estimated parameters. For each estimated parameter 100 samples were drawn, leading to 100 sampled parameter vectors. For each

vector, we calculated the corresponding model output trajectory. Based upon the 100 model output trajectories, the mean and the time-varying standard deviation of the model output were calculated.

5.2.6. Estimation of kinetic parameters

We estimated the kinetic parameters in Eq. 6-9 by using a static approach in which a stepwise method was taken to minimize the residual error [20]. Firstly, we estimated r_{max} and K_M from experimental data in the absence of an inhibitor for both R1 and R2. Secondly, the estimated parameters (r_{max} and K_M) were substituted into a modified "Michaelis-Menten" equation that describes the mode of inhibition, to estimate the inhibition constants (K_i and K_{ies}).

To estimate the kinetic parameters related to R2, we had to assume the initial sulfide concentrations instead of {S_x} concentrations as it is not possible to measure the intracellularly bonded {Sx}. To evaluate the effect of this choice we additionally estimated parameters (r_{max}, K_M, and when applicable the inhibition constants: K_i and K_{ies}) using a dynamic approach which relies on solving the relevant set of differential equations (Eq. 6-10) iteratively. In this approach the {S_x} concentration is implicitly calculated from the proposed and validated model (Section 5.3.4). In particular, we solved the following optimization problem:

$$\min \sum (c_{O2}^{tot}(t) - \widehat{c_{O2}^{tot}}(t,\theta))^2 \tag{16}$$

with $\widehat{c_{O2}^{tot}}$ the calculated total oxygen concentration (Eq. 15), given the solutions to Eq. 6-10 for the set of kinetic parameters (θ: r_{max}, K_M). In the presence of inhibitors (Eq. 17-19) the set of parameters is extended with the inhibition constants: K_i and K_{ies}. Given the observations of c_{O2}^{tot}, the kinetic parameters were estimated using a non-linear least-squares method (Levenberg-Marquardt algorithm), as described by Keesman (2011) [23].

5.3. Results and discussion

5.3.1. Microbial diversity in a full-scale gas biodesulfurization installation

Microbial community analysis of biomass collected from a full-scale gas biodesulfurization installation in Eerbeek (the Netherlands) showed that the bacterial composition (Supplementary Information, Fig. S1) is similar to what has been described previously [8]. The dominant bacterial group (approximately 50% of the 16S rRNA sequences analyzed) belongs to the family *Ectothiorhodospiraceae*. Within this group, 99% of the 16S rRNA sequences belonged to the genus *Thioalkalivibrio*. Also bacteria related to the family *Piscirickettsiaceae* are abundant, 24.8% and 26.1% in both replicates. Within this group, approximately 80% of the 16S rRNA sequences are closely related to the *Thiomicrospira pelophila* / *Thioalkalimicrobium* species, which are often present in the full-scale Thiopaq installations [24].

5.3.2. Determination of incubation time

A complete saturation of enzymes with an inhibitor is required in order to properly determine the inhibition constants (K_i and K_{ies}). Zhang et al. (2001) [25] indicated that in the presence of an inhibitor the incubation time needed to reach complete saturation is related to the inhibitor concentration which, in turn, is related to the degree of inhibition. Due to different susceptibilities of R1 and R2 to the inhibitors [21] it was necessary to apply different inhibitor concentrations, i.e. a higher and a lower one for respectively R1 and R2 (Fig.1). The concentration of each inhibitor was chosen such that only partial inhibition was achieved. An appropriate incubation time for each concentration of each inhibitor had to be determined whilst taking into account that too long incubation times for thiols shall be avoided in order to prevent any chemical oxidation to disulfides (Eq. 1).

From the results shown in Figure 2 it follows that R1 and R2 require different incubation times to reach a complete saturation of the enzymes in the presence of an inhibitor. Table 2 shows the inhibitor concentrations and incubation times that were selected in the remainder of this study.

5
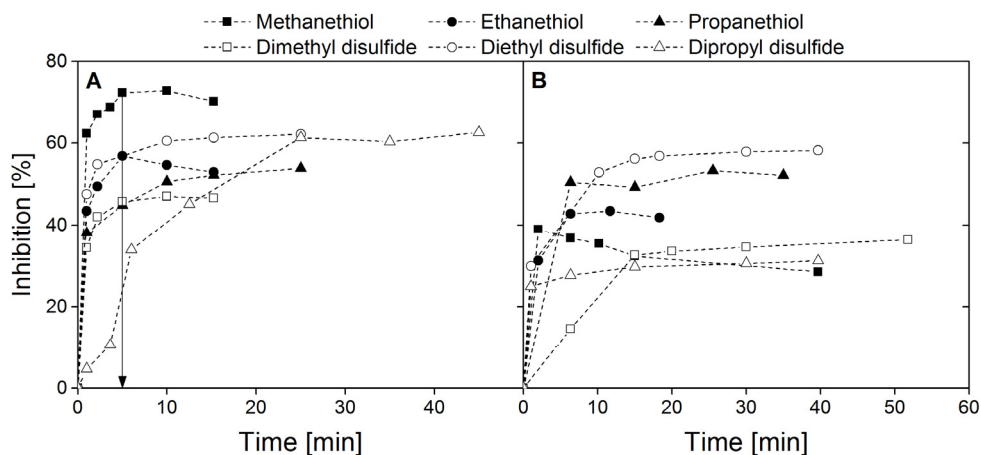
Figure 2. Incubation test performed to investigate time needed for complete saturation of enzymes with inhibitor. **A.** Inhibition results for the first rate of the oxygen consumption rate. Concentrations of methanethiol, ethanethiol, propanethiol, dimethyl disulfide, diethyl disulfide, dipropyl disulfide were equal to 0.0243, 0.06, 0.08, 0.96, 1.2 and 2.5 mM respectively. The arrow indicates the incubation time used in tests with methanethiol. **B.** Inhibition results for the second rate of the oxygen consumption rate. Concentrations of methanethiol, ethanethiol, propanethiol, dimethyl disulfide, diethyl disulfide, dipropyl disulfide were equal to 0.04, 0.01, 0.04, 0.1, 0.1 and 0.42 mM respectively. In all experiments the biomass concentration was 10 mgN L^{-1}, [Na$^+$ + K$^+$] = 1 M, pH = 9 and T = 35 °C.

Table 2. Concentration of inhibitors (C_i) and incubation time (T) used in sulfide-dependent respiration tests for assessing the oxygen consumption rates R1 and R2.

Inhibitor	R1		R2	
	C_i [mM]	T [min]	C_i [mM]	T [min]
Methanethiol	0.024	5	0.005	2
Ethanethiol	0.061	5	0.025	6
Propanethiol	0.080	15	0.017	15
Dimethyl disulfide	0.960	10	0.100	20
Diethyl disulfide	1.200	10	0.100	15
Dipropyl disulfide	0.850	25	0.420	10

5.3.3. Determination of inhibition mode and kinetic parameters

The results from sulfide-dependent respiration tests were plotted in double-reciprocal plots (Supplementary Information, Fig. S2) to identify the inhibition mode related to R1 and R2. From this plot it clearly follows that MT, ET and PT act as competitive inhibitors for R1. Therefore, the mode of inhibition can be described by a modified "Michaelis-Menten" equation:

$$r_i^{R1} = \frac{r_{max}^{R1} c_{HS}}{K_M^{R1}\left(1+\frac{c_i}{K_i^{R1}}\right)+c_{HS}} \tag{17}$$

where c_i is an inhibitor concentration. This mode of inhibition is in agreement with our previous findings viz. that MT acts as a competitive inhibitor for sulfide oxidation by SOB [21]. According to Wilms et al. (1980) [26], this can be explained by the structural similarity between sulfide (HS⁻) and MT (CH₃S⁻). In contrast, diorgano disulfides are non-competitive inhibitors for R1 and their inhibitory effects can be described as follows:

$$r_i^{R1} = \frac{r_{max}^{R1} c_{HS}}{K_M^{R1}+c_{HS}\left(1+\frac{c_i}{K_{ies}^{R1}}\right)} \tag{18}$$

This type of inhibition is common in multi-substrate reactions (Eq. 4-5) in contrast to single-substrate reactions [27].

To establish the effect of thiols and diorgano polysulfanes on R2, double reciprocal plots were prepared which show a mixed type of inhibition (Supplementary Information, Fig. S2), indicating that the inhibitors are able to bind at the active and allosteric site of enzymes. The corresponding specific reaction rate is given by:

$$r_i^{R2} = \frac{r_{max}^{R2} c_{HS}}{K_M^{R2}\left(1+\frac{c_i}{K_i^{R2}}\right)+c_{HS}\left(1+\frac{c_i}{K_{ies}^{R2}}\right)} \tag{19}$$

It is obvious that equations 17-19 only describe a phenomenological characterization of the experimental observation but do not provide any underlying mechanisms. However, in section 5.3.4, we will describe that the lipophilicity effects of the inhibitors influence the inhibition of sulfide oxidation. Then, the specific reaction rates (Eq. 17-19) can substitute the generic rates mentioned (Eq. 6-9) to predict the biomass activity in the presence of thiols and diorgano polysulfanes.

Table 3. Estimated specific maximal reaction rate (r_{max}), Michaelis-Menten constant (K_M) and inhibition constants (K_i and K_{ies}) with their corresponding standard deviation (σ) for the first (R1) and second (R2) oxygen consumption rate.

Reaction rate	Inhibitor	Mode of inhibition	Parameter	Estimated value	σ	Unit
R1 **(HS⁻ → {Sₓ})**	Not inhibited reaction		r_{max}	600	30	µM O$_2$ (mg N h)$^{-1}$
			K_M	79	9	µM
	MT	competitive	K_i	23	2	µM
	ET		K_i	46	5	µM
	PT		K_i	50	6	µM
	DMDS	uncompetitive	K_{ies}	1000	90	µM
	DEDS		K_{ies}	710	60	µM
	DPDS		K_{ies}	440	20	µM
R2 **({Sₓ} → SO₄²⁻)**	Not inhibited reaction		r_{max}	103	4	µM O$_2$ (mg N h)$^{-1}$
			K_M	1.9	0.4	µM
	MT	mixed	K_i	5	2	µM
			K_{ies}	14	3	µM
	ET		K_i	8.2	0.8	µM
			K_{ies}	40	3	µM
	PT		K_i	10	2	µM
			K_{ies}	70	10	µM
	DMDS	mixed	K_i	49	6	µM
			K_{ies}	260	20	µM
	DEDS		K_i	61	6	µM
			K_{ies}	230	20	µM
	DPDS		K_i	100	10	µM
			K_{ies}	220	10	µM

5

After identification of the inhibition mode for each inhibitor on R1 and R2, it was possible to estimate the kinetic parameters in equations 17-19. Estimated values of r_{max}, K_M, K_i and K_{ies} and the corresponding standard deviations are shown in Table 3. From these parameter estimations it follows that MT is the most toxic thiol as it has the lowest K_i value. This is in agreement with our hypothesis that the inhibitory effect decreases with increasing steric hindrance of the thiols [21]. Estimated values of K_{ies} for R1 and diorgano polysulfanes are strongly correlated with their molecular weight (R^2 = 0.999). Similar strong correlations are observed for K_i and K_{ies} of thiols and for K_i of diorgano polysulfanes for R2. However, K_{ies} of diorgano polysulfanes is more or less constant (approximately 0.24 mM), indicating that the same non-competitive inhibition mechanism applies. Because the diorgano

polysulfanes in our tests only differ in their aliphatic chain length while the number of sulfur atoms remains the same, it can be hypothesized that non-competitive inhibition (K_{ies}) is related to the sulfur-sulfur bond.

The results from the parameter estimations show that there is no significant difference between the estimated values obtained via the dynamic and the static approach (data not shown). However, the dynamic approach yields K_m values with a higher level of uncertainty in the estimate because the data contained less information.

5.3.4. Calculation of IC$_{50}$ and its correlation with lipophilicity

The IC$_{50}$ value represents the inhibitor concentration at which 50% inhibition occurs of an enzymatic reaction at a specific substrate concentration. A mathematical relation between the inhibition constants and the IC$_{50}$ value is described by Yung-Chi and Prusoff (1973) [28]. Equations describing this relationship for competitive, uncompetitive and mixed inhibition are given by:

$$\text{IC}_{50} = K_i(1 + \frac{c_{HS}}{K_M}) \tag{20}$$

$$\text{IC}_{50} = K_{ies}(1 + \frac{K_M}{c_{HS}}) \tag{21}$$

$$\text{IC}_{50} = \frac{c_{HS} + K_M}{\frac{K_M}{K_i} + \frac{c_{HS}}{K_{ies}}} \tag{22}$$

Based on the estimated values for the kinetic parameters and the corresponding uncertainties (Table 3), we calculated IC$_{50}$ values with uncertainty bounds for both oxygen consumption rates (R1 and R2) and for each of the inhibitors (Fig. 3 A-C). Taking into account that the IC$_{50}$ value is dependent on the substrate concentration, results are plotted in the range of 0-3 mM sulfide. To compare our results with available literature data, the IC$_{50}$ values for MT and DMDS for R1 have been reviewed (Table 4). The values for both inhibitors are very similar to previously reported data. It can be seen that thiols become less toxic with increasing substrate concentrations (Fig. 3A), while the IC$_{50}$ values for diorgano polysulfanes stabilize at around 1 mM for substrate concentrations above 0.5 mM (Fig. 3B). Moreover, it can be observed that R2 is more susceptible to the inhibitors at almost all sulfide concentrations (Fig. 3C) because of much lower IC$_{50}$ values. These results support our previous findings from lab-scale reactor experiments that biological production of sulfate is more vulnerable to inhibitors than the biological production of sulfur [4,21].
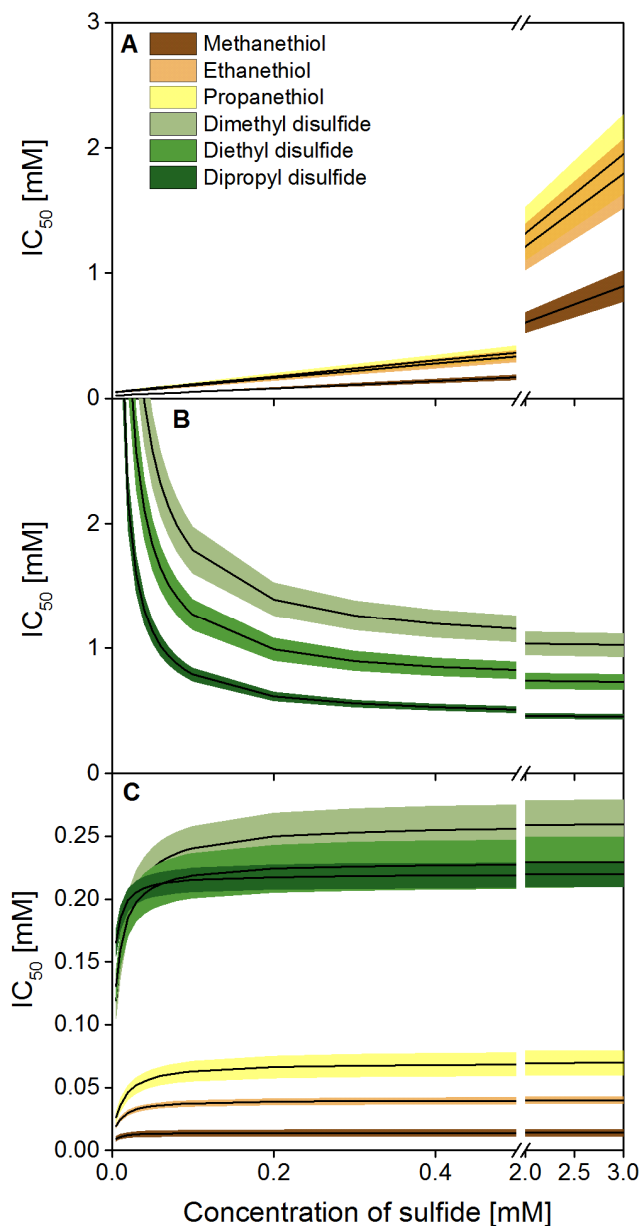
Figure 3. Calculated IC$_{50}$ values with corresponding uncertainty bounds at increasing concentration of sulfide. **A.** Methanethiol, ethanethiol and propanethiol for the first oxygen consumption rate (R1). **B.** Dimethyl disulfide, diethyl disulfide and dipropyl disulfide (R1). **C.** All aforementioned inhibitors for the second oxygen consumption rate (R2).

Table. 4. Calculated IC_{50} values for methanethiol and dimethyl disulfide, and comparison with literature data at sulfide concentration of 0.2 mM.

IC$_{50}$ [mM]		pH	[Na$^+$ + K$^+$]	Reference
Methanethiol	**Dimethyl disulfide**			
0.08 ± 0.01	1.4 ± 0.1	9	1	current study
0.05	1.5	9	2	[5]
0.11 ± 0.02	N.A.	8.5	1.5	[21]
0.2 ± 0.6	1.4 ± 0.2	9.5	0.8	[33]

N.A. - not available

It is known that the biological activity of inhibitors can be directly related to their physicochemical properties [29]. Hence, we compared their lipophilicity expressed as logarithm of octanol-water partition coefficient (log(P)), with the measured IC_{50} values. The estimation of log(P) for the various inhibitors was calculated using ALOGPS 2.1 software [30,31]. For thiols the log(P) values ranged from 0.4 to 1.2 and for diorgano polysulfanes ranged from 1 to 3. To determine whether lipophilicity is correlated with IC_{50} values at sulfide concentration of 0.2 mM, the relationship between log(P) and IC_{50} values for the particular group of inhibitors for both oxidation rates (R1 and R2) was assessed by linear regression (Fig. 4 A-B). A clear and positive correlation was found between log(P) and the IC_{50} values for thiols for both R1 and R2, with coefficients of determination of 0.848 and 0.999, respectively (Fig. 4A). These correlations show that hydrophobic thiols are less toxic to SOB compared to the more hydrophilic ones. This might also indicate that inhibition by thiols is related to the hydrophilic interaction in the inhibition mechanisms. For diorgano polysulfanes, we found large negative correlations between log(P) and the IC_{50} values with coefficients of determination of 0.995 and 0.994 for R1 and R2, respectively (Fig. 4B). In contrast to thiols, toxicity of diorgano polysulfanes increases with their lipophilicity which suggests involvement of hydrophobic interaction in the inhibition mechanisms. This could mean that diorgano polysulfanes are affecting enzymes that are embedded in the cell membrane which is in agreement with another observation that diorgano polysulfanes toxicity is not competitive for R1 because the substrate, i.e. sulfide, reacts with enzymes located outside the cell membrane in the periplasm or on the external surface of the cell membrane [32].
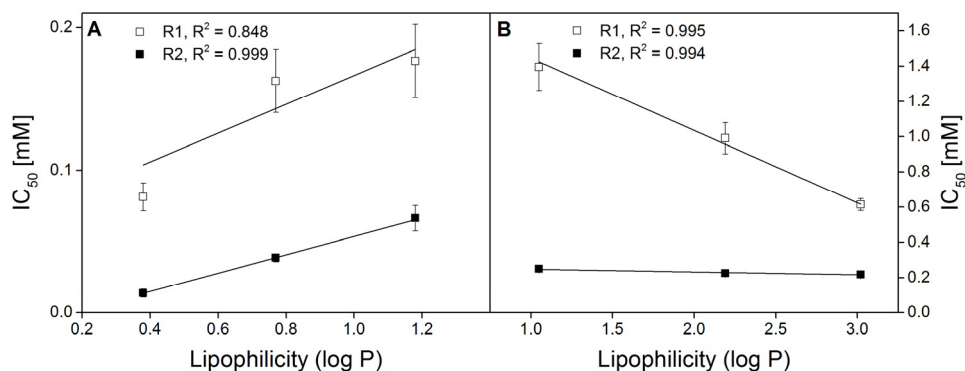
5

Figure 4. Relationship between lipophilicity and IC_{50} values at sulfide concentration of 0.2 mM. **A.** Methanethiol, ethanethiol, propanethiol for the first (R1) and the second (R2) oxygen consumption rate. **B.** Dimethyl disulfide, diethyl disulfide, dipropyl disulfide for R1 and R2.

5.3.5. Comparison of the model results with experimental data

The estimated kinetic parameters in Table 3 were obtained from sulfide-dependent respiration tests and then used in the above described mathematical model (Eq. 6-15). The model predictions were compared with a set of independent respirometric results. The biomass used for the validation experiments was taken from the same full-scale reactor but two months after biomass sampling for the parameter estimation tests.

The model was experimentally validated in the absence of an inhibitor with the initial sulfide concentration ranging from 0.005 to 0.2 mM (Fig. 5A-F). From these results, it can be seen that the proposed model predicts the oxygen consumption reasonably well for haloalkaliphilic SOB cultivated under O_2-limiting conditions. For the highest sulfide concentrations the deviation between experimental measurements and model predictions increases somewhat which can be attributed to a lag phase of the SOB. Nevertheless, an error analysis of r^{R1} showed that the coefficient of variation was always below ± 25%, which is a reasonable margin if one takes into account the measurement errors in the dissolved oxygen, sulfide, biomass concentrations, liquid volumes and influence of the error propagation. Furthermore, the measured and predicted reaction rates seem to correspond (Supplementary Information, Fig. S3). The uncertainty in the model output resulting

from uncertainties in the estimates for the kinetic parameters (Table 3) is rather small because of strong correlations between the identifiable parameter estimates, as also follows from the covariance and correlation matrix of the estimates (Supplementary Information, S2). In addition, respiration tests with biomass concentration of 1 mg N L^{-1} were performed to validate the model. Although these tests were performed with ten times lower biomass concentration than tests used for the parameter estimation, no significant differences between the model output and the measured oxygen consumption rate were observed, i.e. the coefficient of variation was below ± 27%.

Figure 5. Comparison between measured and predicted dissolved oxygen (DO) consumption rate and model predictions of sulfide (HS$^-$) and polysulfur compound {S$_x$} concentrations, in absence of an inhibitor. Results of the simulation are based on estimates from Table 3. The sample interval is 1 s for both measured and predicted results. The initial sulfide concentration was 0.005, 0.01, 0.06, 0.08, 0.12, 0.2 mM in figures A-F, respectively. The biomass concentration was 10 mgN L^{-1}, [Na$^+$ + K$^+$] = 1 M, pH = 9 and T = 35 °C.
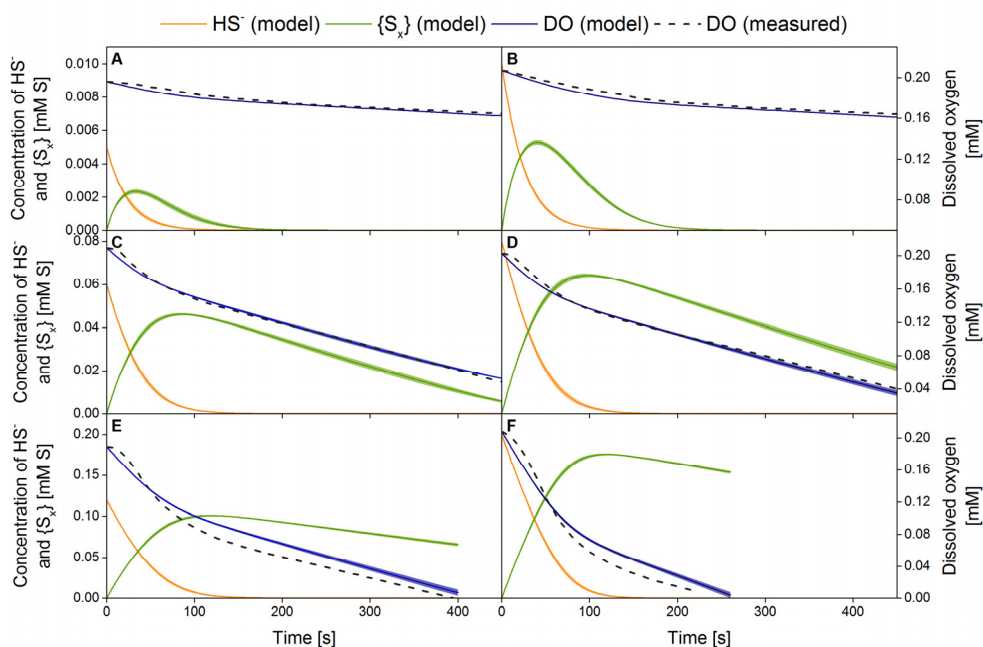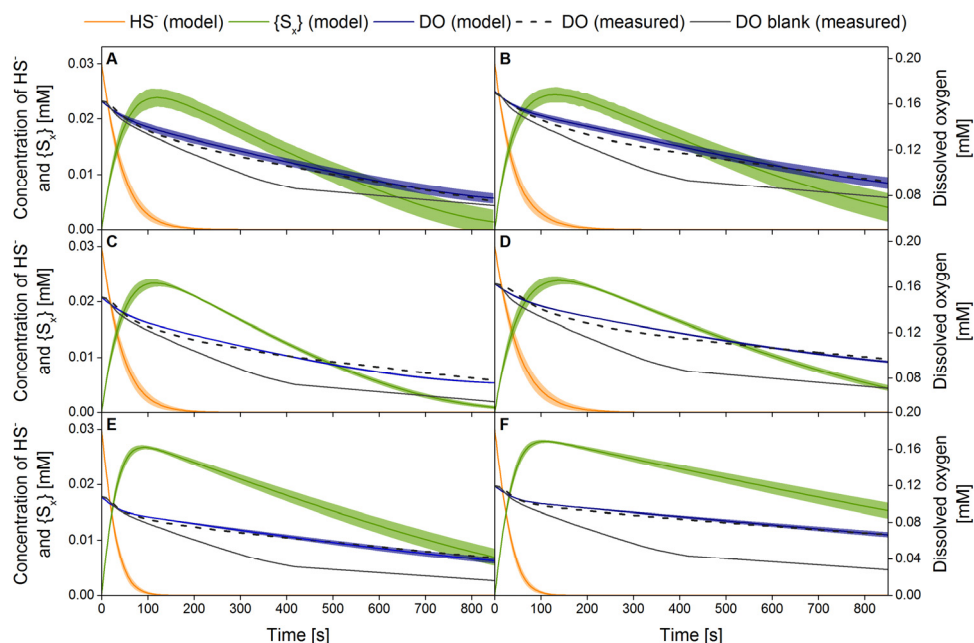
Figure 6. Comparison between measured and predicted dissolved oxygen (DO) consumption rate and model predictions of sulfide (HS⁻) and polysulfur compound {S_x} concentration with corresponding model output uncertainties as a result of variations in estimated parameters. Results of the simulation are based on estimates from Table 3. The sample interval is 1 s for measured results. Respiration tests were performed at different concentration of various inhibitors: **A.** Methanethiol, 0.02 mM. **B.** Methanethiol, 0.04 mM. **C.** Ethanethiol, 0.04 mM. **D.** Ethanethiol, 0.08 mM. **E.** Dimethyl disulfide, 0.5 mM. **F.** Dimethyl disulfide, 1 mM. DO blank refers to an experiment performed without inhibitor. The biomass concentration was 10 mgN L⁻¹, [Na⁺ + K⁺] = 1 M, pH = 9 and T = 35 °C.

Hereafter, the model was validated with tests performed at constant initial sulfide concentration (0.03 mM) in the presence of MT, ET and DMDS at different concentrations (Fig. 6A-F). For this purpose, equations describing the model (Eq. 6-15) were adjusted with modified "Michaelis-Menten" equations (Eq. 17-19) depending on the type of inhibitor. For all measurements, model predictions are in a good agreement with the experimental results (on average the difference is 14 ± 4 % for R1 and 7 ± 6 % for R2). This allows for an explicit mathematical description

and supports double sulfide-dependent oxygen consumption rates by SOB. Consequently, the model can be used to predict the biomass activity and to predict the accumulation rate of intracellularly produced $\{S_x\}$.

From Figure 6 it can be seen that for biological oxidation of sulfide inhibited by MT and ET, the experimental results and the model predictions show almost two times lower sulfide consumption rates and significantly lower oxidation rates of $\{S_x\}$ compared to uninhibited reactions. For reactions inhibited by DMDS, the oxidation of sulfide is inhibited only slightly (8%, Fig. 6E) and moderately (23%, Fig. 6F), while the oxidation of $\{S_x\}$ is almost completely blocked (Fig. 6E-F). These results clearly show that the sulfide oxidation is significantly less vulnerable to these sulfurous inhibitors than $\{S_x\}$ oxidation is. In the presence of an inhibitor model output uncertainties increased due to the uncertainty of inhibition constants (Figure 5).

5.4. Conclusions

In this study, a novel approach for the simultaneous description of biological sulfur and sulfate formation using a quick sulfide-dependent respiration test has been presented. By applying this approach, the inhibition of haloalkaliphilic SOB by the most common thiols and their corresponding diorgano polysulfanes was described. We found that IC_{50} values are correlated with the lipophilicity of the inhibitors. Thiols interfere with the oxidation of sulfide by hydrophilic interaction while hydrophobic interaction is the most important mechanism for diorgano polysulfanes. This can be related to the ionic and non-ionic form of the various inhibitors. For each inhibitor, we identified the inhibition mode and the corresponding inhibition constants. Understanding the inhibitory properties of thiols on the biological oxidation of sulfide allows designing full-scale systems in which any inhibition is prevented e.g. by increasing the biomass or/and substrate concentration.

Moreover, a mathematical model has been described to calculate the biological sulfide oxidizing capacity in the absence or presence of inhibitory thiols and their corresponding diorgano polysulfanes. The proposed model can be used to design full-scale installations to remove H_2S from gas streams in which thiols and diorgano polysulfanes are present.

5

Acknowledgements

This work was performed within the cooperation framework of Wetsus, European Centre of Excellence for Sustainable Water Technology (www.wetsus.nl). Wetsus is co-funded by the Netherlands' Ministry of Economic Affairs and Ministry of Infrastructure and the Environment, the European Union's Regional Development Fund, the Province of Fryslân, and the Northern Netherlands Provinces. The authors thank the participants of the research theme "Sulfur" and Paqell for fruitful discussions and financial support.

5

References

1. Janssen AJH, Lens PNL, Stams AJM, Plugge CM, Sorokin DY, Muyzer G, Dijkman H, Van Zessen E, Luimes P, Buisman CJN. Application of bacteria involved in the biological sulfur cycle for paper mill effluent purification. *Sci. Total Environ.* Elsevier; 2009;407:1333–1343.
2. Schieder D, Quicker P, Schneider R, Winter H, Prechtl S, Faulstich M. Microbiological removal of hydrogen sulfide from biogas by means of a separate biofilter system: experience with technical operation. *Water Sci. Technol.* 2003;48:209–212.
3. Cline C, Hoksberg A, Abry R, Janssen AJH. Biological Process for H_2S Removal from Gas Streams: The Shell-Paques/THIOPAQ™ Gas Desulfurization Process. *Proceedings of the Laurance Reid Gas Conditioning Conference*. 2003. p. 1–18.
4. Roman P, Veltman R, Bijmans MFM, Keesman K, Janssen AJH. Effect of methanethiol concentration on sulfur production in biological desulfurization systems under haloalkaline conditions. *Environ. Sci. Technol.* ACS Publications; 2015;49:9212–9221.
5. Van den Bosch PLF, de Graaff M, Fortuny-Picornell M, van Leerdam RC, Janssen AJH. Inhibition of microbiological sulfide oxidation by methanethiol and dimethyl polysulfides at natron-alkaline conditions. *Appl. Microbiol. Biotechnol.* Springer; 2009;83:579–587.
6. Van Leerdam RC, Bosch PLF, Lens PNL, Janssen AJH. Reactions between methanethiol and biologically produced sulfur. *Environ. Sci. Technol.* 2011;45:1320–1326.
7. Steudel R. The chemistry of organic polysulfanes RS (n)-R (n> 2). *Chem. Rev.* 2002;102:3905.
8. Sorokin DY, Muntyan MS, Panteleeva AN, Muyzer G. Thioalkalivibrio sulfidiphilus sp. nov., a haloalkaliphilic, sulfur-oxidizing gammaproteobacterium from alkaline habitats. *Int. J. Syst. Evol. Microbiol.* Soc General Microbiol; 2012;62:1884–1889.
9. Muyzer G, Sorokin DY, Mavromatis K, Lapidus A, Clum A, Ivanova N, Pati A, d' Haeseleer P, Woyke T, Kyrpides NC. Complete genome sequence of "Thioalkalivibrio sulfidophilus" HL-EbGr7. *Stand. Genomic. Sci.* Genomic Standards Consortium; 2011;4:23.

10. Klok JBM, van den Bosch PLF, Buisman CJN, Stams AJM, Keesman KJ, Janssen AJH. Pathways of sulfide oxidation by haloalkaliphilic bacteria in limited-oxygen gas lift bioreactors. *Environ. Sci. Technol.* ACS Publications; 2012;46:7581–7586.

11. Sorokin D, van den Bosch PLF, Abbas B, Janssen AJH, Muyzer G. Microbiological analysis of the population of extremely haloalkaliphilic sulfur-oxidizing bacteria dominating in lab-scale sulfide-removing bioreactors. *Appl. Microbiol. Biotechnol.* Springer; 2008;80:965–975.

12. Mora M, López LR, Lafuente J, Pérez J, Kleerebezem R, van Loosdrecht MC, Gamisans X, Gabriel D. Respirometric characterization of aerobic sulfide, thiosulfate and elemental sulfur oxidation by S-oxidizing biomass. *Water Res.* Elsevier; 2016;89:282–292.

13. Klok J, de Graaff M, van den Bosch PLF, Boelee NC, Keesman KJ, Janssen AJH. A physiologically based kinetic model for bacterial sulfide oxidation. *Water Res.* Elsevier; 2013;47(2):483–492.

14. Roosta A, Jahanmiri A, Mowla D, Niazi A. Mathematical modeling of biological sulfide removal in a fed batch bioreactor. *Biochem. Eng. J.* Elsevier; 2011;58:50–56.

15. Cui H, Turn SQ, Reese MA. Removal of sulfur compounds from utility pipelined synthetic natural gas using modified activated carbons. *Catal. Today*. Elsevier; 2009;139:274–279.

16. Lee S, Xu Q, Booth M, Townsend TG, Chadik P, Bitton G. Reduced sulfur compounds in gas from construction and demolition debris landfills. *Waste Manage.* Elsevier; 2006;26:526–533.

17. Kim K-H, Choi Y, Jeon E, Sunwoo Y. Characterization of malodorous sulfur compounds in landfill gas. *Atmos. Environ.* Elsevier; 2005;39:1103–1112.

18. Kleinjan WE, Keizer A de, Janssen AJ. Kinetics of the chemical oxidation of polysulfide anions in aqueous solution. *Water Res.* Elsevier; 2005;39:4093–4100.

19. Pfennig N, Lippert KD. Über das vitamin B$_{12}$-bedürfnis phototropher Schwefelbakterien. *Arch. Microbiol.* Springer; 1966;55:245–256.

20. Marangoni AG. Enzyme kinetics: a modern approach. John Wiley & Sons; 2003.

21. Roman P, Bijmans MFM, Janssen AJH. Influence of methanethiol on biological sulfide oxidation in gas treatment system. *Environ. Tech.* Taylor & Francis; 2015;1–42.

22. Zannoni D, others. Respiration in archaea and bacteria. Springer; 2004.

23. Keesman KJ. System identification: an Introduction. Springer, Verlag, UK; 2011.

24. Sorokin DY, Kuenen JG, Muyzer G. The microbial sulfur cycle at extremely haloalkaline conditions of soda lakes. *Frontiers in Microbiology, 2 (article 44), March 2011*. Frontiers; 2011.

25. Zhang S, Zhao H, John R. A theoretical model for immobilized enzyme inhibition biosensors. *Electroanalysis*. Wiley Online Library; 2001;13:1528–1534.

26. Wilms J, Lub J, Wever R. Reactions of mercaptans with cytochrome c oxidase and cytochrome c. *Biochim. Biophys. Acta, Bioenerg.* Elsevier; 1980;589:324–335.

27. Segal I. Enzyme Kinetics: Behavior and Analysis of Rapid Equilibrium and Steady-State Enzyme Systems. Wiley, New York, USA; 1993. p. 957.

28. Yung-Chi C, Prusoff WH. Relationship between the inhibition constant (K$_i$) and the concentration of inhibitor which causes 50 per cent inhibition (I$_{50}$) of an enzymatic reaction. *Biochem. Pharmacol.* Elsevier; 1973;22:3099–3108.

5

29. Cronin MT. Predicting chemical toxicity and fate. CRC press; 2004.
30. ALOGPS 2.1 software [Internet]. [cited 2015]. Available from: http://www.vcclab.org/lab/alogps.
31. Tetko IV, Tanchuk VY. Application of associative neural networks for prediction of lipophilicity in ALOGPS 2.1 program. *J. Chem. Inf. Comp. Sci.* ACS Publications; 2002;42:1136–1145.
32. Gregersen LH, Bryant DA, Frigaard N-U. Mechanisms and evolution of oxidative sulfur metabolism in green sulfur bacteria. *Front. Microbiol.* Frontiers Media SA; 2011;2.
33. Graaff C de. Biological treatment of sulfidic spent caustics under haloalkaline conditions using soda lake bacteria. Thesis Wageningen University; 2012.

5

Supplementary Information

S1. Figures:
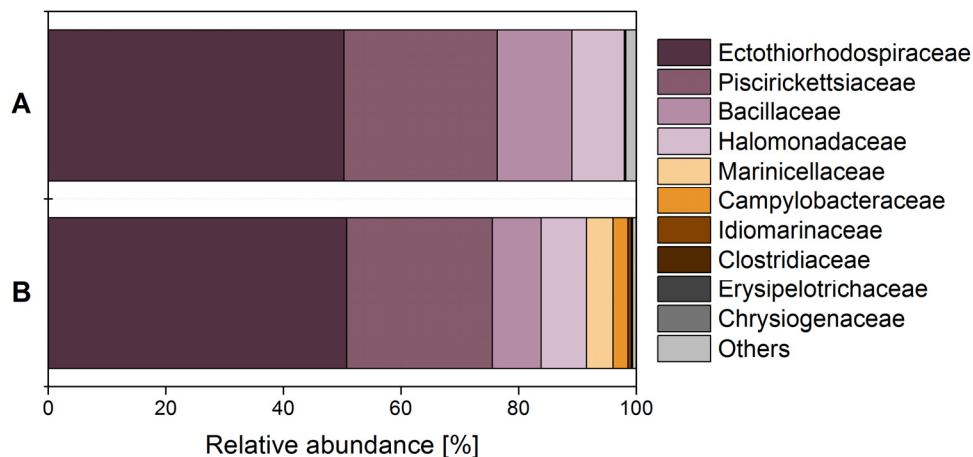
Figure S1. Relative abundance of the microbial composition based on the 16S rRNA gene for the biomass from a full-scale gas biodesulfurization installation [1]. Only bacteria with a relative abundance higher than 0.5% are listed (remaining bacteria are grouped into "Others"). A and B represents two replicates.

5
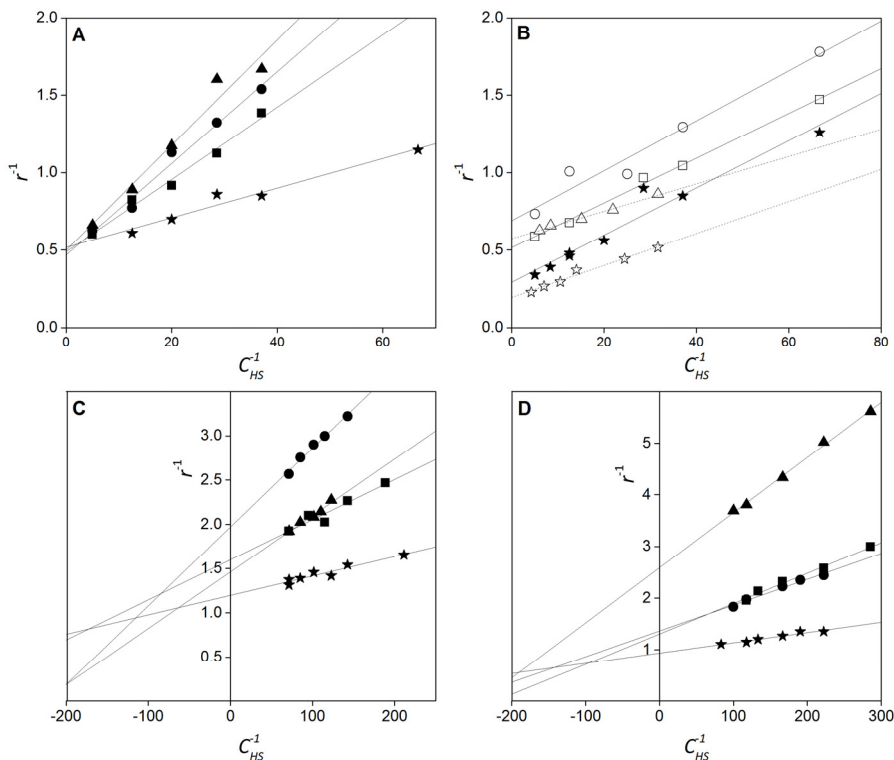
Figure S2. An example of results from sulfide-dependent respiration tests plotted on double-reciprocal plots for the first (A and B) and the second (C and D) oxygen consumption rate, where r is the reaction rate [mM O_2 (mg N h)$^{-1}$] and C_{HS} is the sulfide concentration [mM]. The inhibitor concentrations for each oxygen consumption rate are given in Table 2. The biomass concentration was 10 mg N L^{-1}, pH = 9 and T = 35 °C.
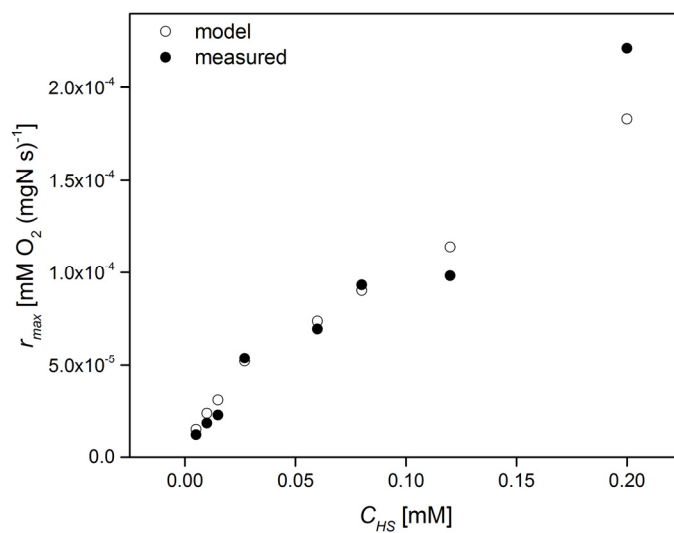
Figure S3. Comparison between measured and predicted reaction rate for the first rate of the oxygen consumption rate at different initial sulfide concentrations.

5

S2. Covariance and correlation matrix of the estimates

The parameter estimates related to the first oxygen consumption rate (R1) are given by:

$$\hat{\theta}_{R1} = \begin{pmatrix} r_{max}^{R1} \\ K_m^{R1} \end{pmatrix} = \begin{pmatrix} 0.6 \\ 0.079 \end{pmatrix}$$

with corresponding covariance and correlation matrices:

$$COV\hat{\theta}_{R1} = \begin{pmatrix} 0.0012 & 0.0003 \\ 0.0003 & 0.0001 \end{pmatrix}$$

$$R_{\hat{\theta}_{R1}} = \begin{pmatrix} 1 & 0.866 \\ 0.866 & 1 \end{pmatrix}$$

Similarly, parameters estimates related to the second oxygen consumption rate (R2) are described by:

$$\hat{\theta}_{R2} = \begin{pmatrix} r_{max}^{R2} \\ K_m^{R2} \end{pmatrix} = \begin{pmatrix} 0.103 \\ 0.0019 \end{pmatrix}$$

$$COV\hat{\theta}_{R2} = \begin{pmatrix} 0.0000148 & 0.0000019 \\ 0.0000019 & 0.0000003 \end{pmatrix}$$

$$R_{\hat{\theta}_{R2}} = \begin{pmatrix} 1 & 0.864 \\ 0.864 & 1 \end{pmatrix}$$

5
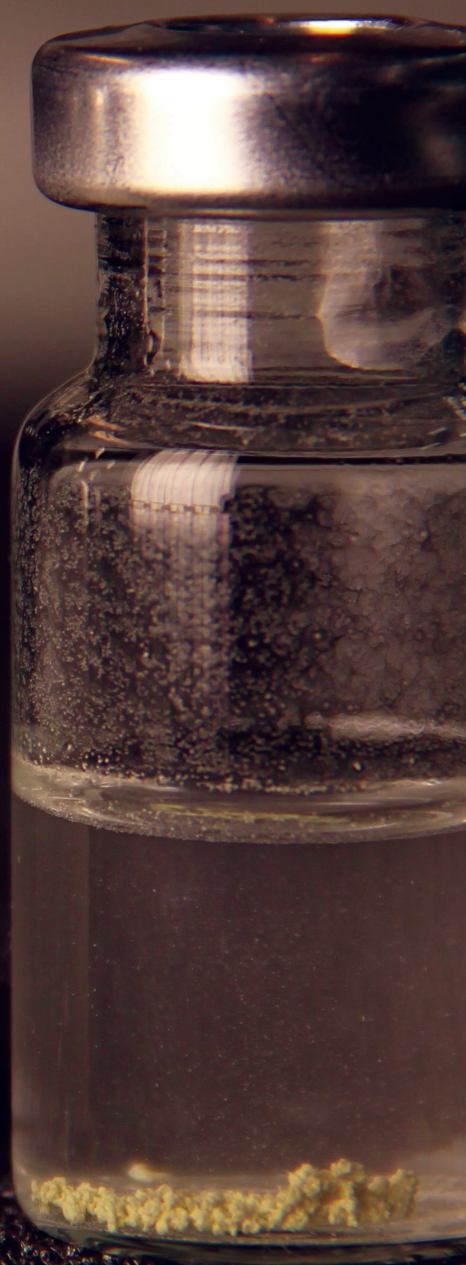
Chapter 6

Removal of H$_2$S and thiols from sour gas streams under haloalkaline conditions

Abstract

Deployment of biological processes to remove hydrogen sulfide (H_2S) from sour gas streams has been one of the most innovative developments in industrial gas treating processes in recent years. After the first commercial applications for treating low pressure biogas containing H_2S, the need arose to broaden the operating window to also enable the removal of organosulfur compounds from high pressure sour gases. The current work describes the effect of elevated loading rates (2.1 - 9.1 mM d^{-1}) of methanethiol, ethanethiol, and propanethiol on the biological conversion of dissolved sulfide to biosulfur. Experiments were performed in an integrated laboratory-scale setup consisting of a gas absorber and bioreactor operated under haloalkaline conditions. In contrast to our previous studies, we used biomass originating from a full-scale desulfurization installation that was fed with high pressure natural gas containing H_2S and thiols. The effect of thiols on the microbial community was investigated by using next-generation sequencing of the 16S rRNA gene which showed a shift in the microbial community from Halomonadaceae to Halothiobacillaceae members. We also found that absorption of thiols can be enhanced by a reaction with biosulfur. The inhibitory effects of thiols on the sulfide-oxidizing biomass can be mitigated by removing these compounds from the bioreactor medium via gas stripping and via a chemical reaction with biosulfur particles. Finally, it was found that a conventional method to control the oxygen supply to the bioreactor, i.e. by maintaining a redox potential set-point value, was ineffective when thiols were present in the biodesulfurization reactor.

6

6.1. Introduction

Thiols are analogues of alcohols with a general formula of RSH, where R represents an aliphatic chain. These unwanted organosulfur compounds c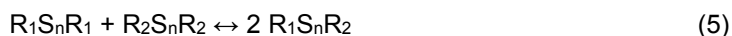an be present in many sour gas streams such as landfill gas, liquefied petroleum gas, and natural gas [1–3]. The presence of thiols in gas streams is associated with hydrogen sulfide (H_2S). Both are corrosive and acidifying compounds that contribute to air pollution and are toxic to humans. Hence, H_2S and thiols need to be removed from sour gas streams by applying either physicochemical or biological desulfurization processes [4]. Hydrogen sulfide can be removed by sulfur oxidizing bacteria (SOB) [5–7], however, thiols already inhibit SOB at ~0.6 µM [8,9].

Gas biodesulfurization processes are preferably performed under haloalkaline conditions, i.e. elevated pH values (>8.5) and carbonate concentrations (~1 M) to ensure high H_2S absorption rates by reaction with hydroxyl and (bi)carbonate ions. It is known that haloalkaliphilic SOB are a suitable group of microorganisms for sulfide oxidation because of their high sulfide-oxidizing capacity at elevated salt and pH levels [5,10].

Short chain thiols such as methanethiol (MT), ethanethiol (ET), and propanethiol (PT) have pK_a values around 10.4 [11,12]. As a result, the combined removal of thiols and H_2S from contaminated gas streams is feasible (Eq. 1) under alkaline conditions and after which the dissociated species are sent to the bioreactor. Dissociated thiols (RS^-) are strong nucleophiles, and therefore, very reactive [13]. For example, a reaction between MT and biologically produced sulfur particles results in the formation of diorgano polysulfanes (Eq. 2-3) [14]. The first reaction product is diorgano pentasulfide, which immediately undergoes interconversion reactions to form a mixture of organosulfur compounds (Eq. 4). Sulfides originated from different thiols can exchange the organic groups to form asymmetric sulfides (Eq. 5) Moreover, thiols can be easily oxidized to diorgano disulfides (Eq. 6), where the oxidation rate of thiols decreases with increasing molecular weight [15].

$$RSH + OH^- \rightarrow RS^- + H_2O \qquad\qquad (1)$$

$$RSH + S_8 \rightarrow RS_9^- + H^+ \qquad\qquad (2)$$

$$RSH + RS_9^- \rightarrow RS_nR + S_x^{2-} + H^+, \text{ with } n+x = 10 \qquad\qquad (3)$$

$$2\ RS_nR \leftrightarrow RS_{n-1}R + RS_{n+1}R, \text{ with } n>3 \qquad\qquad (4)$$

$$R_1S_nR_1 + R_2S_nR_2 \leftrightarrow 2\ R_1S_nR_2 \qquad\qquad (5)$$

$$2\ RSH + 0.5\ O_2 \rightarrow RS_2R + H_2O \qquad\qquad (6)$$
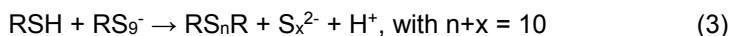
Literature about the effect of thiols on biodesulfurization processes is scarce and the growing need to expand the application window of existing biodesulfurization systems for thiol removal necessitates more research. This paper describes the effect of an increasing loading rate (2.5 - 9.1 mM d^{-1}) of the most common thiols (MT, ET, and PT) on the overall performance of gas biodesulfurization processes. According to the best of our knowledge, the effect of higher thiols (ET and PT) on biological H$_2$S removal process has not yet been studied. In order to find an appropriate inoculum for our bench-scale bioreactor we collected biomass from a full-scale installation. In this plant a natural gas condensate containing H$_2$S and thiols is treated. In the following section, we provide a detailed description of this desulfurization plant. SOB have been adapted to MT loading rates of ≤ 9 mM d^{-1} for a period of 70 days. The adaptation and the effect of MT, ET and PT on the microbial population were monitored by using next-generation sequencing of the 16S rRNA gene. Moreover, the toxic effect of thiols has been mitigated by stripping them from the bioreactor medium, thereby mimicking full-scale biodesulfurization installations in which the vent-air from the bioreactors is sent to atmosphere after passing a compost filter [16].

6.2. Description of full-scale plant for desulfurization of a natural-gas condensate

A small oilfield situated in Southern Illinois, North America, covers less than 40 km^2 and contains more than 300 small production wells. The oilfield produces approximately 1500-2000 barrels of oil per day. When crude oil reaches the surface, dissolved gases are released which have been flared for more than 70 years because gathering and processing was economically not feasible. However, because of rising energy costs the presence of extensive amounts of valuable condensable hydrocarbon liquids and the desire to reduce CO$_2$ and SO$_2$ emission levels triggered the choice to install a liquefied petroleum gas (LPG) recovery system. The main hurdle in recovering the LPG is the requirement to remove H$_2$S and volatile organic sulfur compounds (VOSC) from the associated gas. The latter are predominantly

thiols (methyl-, ethyl-, propyl-, and butylthiols). Around 2005, a biological desulfurization process (Thiopaq O&G) was taken into service.
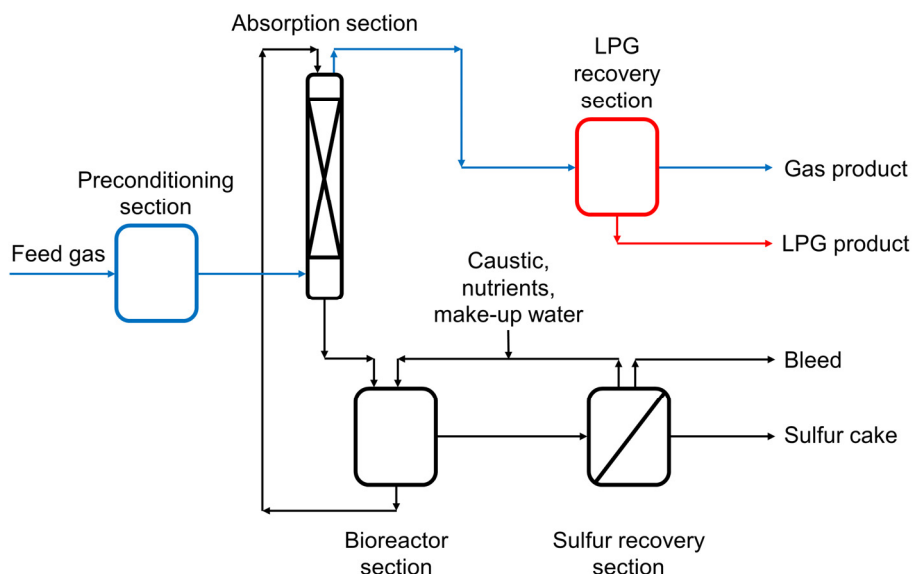
Figure 1. The full-scale plant scheme indicating the flow of gas (blue), desulfurization unit (black), and the mechanical refrigeration unit (red).

Table 1. Inlet and outlet gas composition of the full-scale installation used to desulfurize a natural-gas condensate. VOSC - volatile organic sulfur compounds.

Component	Inlet gas	Outlet gas
H_2S	1-5 vol.%	<4 ppm(v)
VOSCs	50-200 ppm(v)	<1 ppm(v)
CO_2	1-3 vol.%	<2 vol.%
CH_4	40-50 vol.%	40-50 vol.%
C_2H_6	15-20 vol.%	15-20 vol.%
C_3H_8	12-17 vol.%	12-17 vol.%
C_4+	10-15 vol.%	10-15 vol.%
H_2O	<2 vol.%	saturated

6

Table 2. Composition of the process solution in the full-scale bioreactor used in desulfurization process of a natural-gas condensate.

Ion	C_{av} [mM]
Na^+	834
CO_3^{2-}	21
HCO_3^-	463
SO_4^{2-}	35
$S_2O_3^{2-}$	119

In the oil field, pipelines have been installed to collect the associated gas, ranging from approximately 800 up to 1100 Nm^3 h^{-1}. This low pressure gas is first preconditioned to prevent hydrocarbon liquids from entering the desulfurization process. Subsequently, the remaining gas is directed to the two step Thiopaq O&G desulfurization process (Fig. 1). In the first step, sour-gas components such as CO_2 and H_2S are absorbed in a mildly alkaline process solution (pH = 9.0, (bi)carbonates = 0.5 M) in a gas absorber. The inlet and outlet gas compositions are shown in Table 1 and the composition of the process solution is shown in Table 2. The governing chemical equilibrium reactions in the gas absorber are as follows [5]:

$$H_2S_{(G)} \leftrightarrow H_2S_{(L)} \tag{7}$$
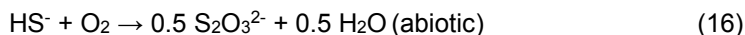
$$H_2S_{(L)} + OH^- \leftrightarrow HS^- + H_2O \tag{8}$$

$$H_2S_{(L)} + HCO_3^- \leftrightarrow HS^- + CO_2 + H_2O \tag{9}$$

$$H_2S_{(L)} + CO_3^{2-} \leftrightarrow HS^- + HCO_3^- \tag{10}$$

$$CO_2_{(G)} \leftrightarrow CO_2_{(L)} \tag{11}$$

$$CO_2_{(L)} + H_2O \leftrightarrow HCO_3^- + H^+ \tag{12}$$

$$HCO_3^- \leftrightarrow CO_3^{2-} + H^+ \tag{13}$$
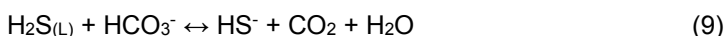
It can be seen that absorption of H_2S in the solution is accompanied by consumption of hydroxyl ions. After leaving the gas absorber, the treated gas contains less than 10 ppm(v) of total sulfur compounds (Table 1). The loaded aqueous solvent is sent from the bottom section of the absorber column to an atmospheric bioreactor. In the bioreactor section, hydroxyl ions are regenerated by SOB under oxygen limiting and sulfur forming conditions:

$$HS^- + 0.5\ O_2 \rightarrow 1/8\ S_8 + OH^-\ \text{(biotic)} \tag{14}$$

In addition, sulfate [5,7] and thiosulfate (through polysulfide anions [17]) are biologically and abiotically produced, respectively:

$$HS^- + 2\ O_2 \rightarrow SO_4^{2-} + H^+ \text{ (biotic)} \qquad\qquad (15)$$

$$HS^- + O_2 \rightarrow 0.5\ S_2O_3^{2-} + 0.5\ H_2O \text{ (abiotic)} \qquad\qquad (16)$$
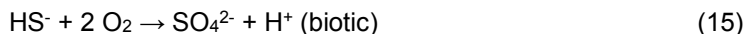
To remove elemental sulfur particles from the system a small fraction of the circulating process solution is continuously routed to a decanter centrifuge wherefrom the recovered sulfur cake is disposed in a landfill whilst the clear filtrate is returned to the bioreactor section. The desulfurized gas stream (Table 1) is then directed to the LPG recovery section in which the process gas is pressurized to approximately 35 bar and then chilled to a temperature of -28 °C in a conventional mechanical refrigeration unit. After stabilizing the liquids, the LPG product is stored. The clean gas, mainly consisting of methane (~60%) and ethane (~30%), is sold to the local distribution grid.

6.3. Materials and methods

6.3.1. Experimental setup

The experimental setup consisted of a falling film gas absorber and a fed-batch air-lift bioreactor (Fig. 2). A falling-film absorber was chosen to avoid any sulfur plugging issues as previously encountered with a packed column. Table 3 shows the dimensions and process conditions of the gas absorber. The liquid volume of the bioreactor was 2.2 L and the volume of the gas absorber was 0.2 L. The total liquid volume remained constant throughout each experimental run. Oxygen gas (99.995 vol.%) was supplied to the bioreactor by a mass flow controller (type EL-FLOW, model F-201DV-AGD-33-K/E, 0-30 mL min⁻¹, Bronkhorst, the Netherlands) to control the oxidation reduction potential (ORP) value. The same type of mass flow controller was used to feed H_2S (99.8 vol.%, 0-17 mL min⁻¹), MT, ET, PT (1 vol.% in N_2, 0-30 mL min⁻¹), and N_2 gas (99.995 vol.%, 0-350 mL min⁻¹) to the gas absorber and the bioreactor. Carbon dioxide (99.99 vol.%) was fed to the inlet of the gas absorber with a solenoid valve (125318, Burkert, Germany) to control the pH of the bioreactor medium. The oxygen and carbon dioxide supply rates were controlled with a multiparameter transmitter (Liquiline CM442; Endress+Hauser, the Netherlands) based on real-time signals from the redox potential electrode (Ag/AgCl reference electrode, Orbisint CPS12D;

6

Endress+Hauser) and a pH sensor (Orbisint CPS11D; Endress+Hauser), respectively. A gear pump (EW-74014-40, Metrohm Applikon, Schiedam, the Netherlands) recycled the liquid between the bioreactor and the gas absorber. The gas phase from the bioreactor headspace was continuously sent to the bottom of the bioreactor (34 L min^{-1}) with a gas compressor (N-840, KNF, Germany). The bioreactor and the gas absorber were kept at 35 °C with a thermostat bath (DC10-P5/U, Haake, Germany). Gaseous samples were collected from sampling points placed at the inlet and outlet of the gas absorber and in the bioreactor headspace (Fig. 2). Liquid samples were collected from a sampling point located in the middle section of the bioreactor (Fig. 2).
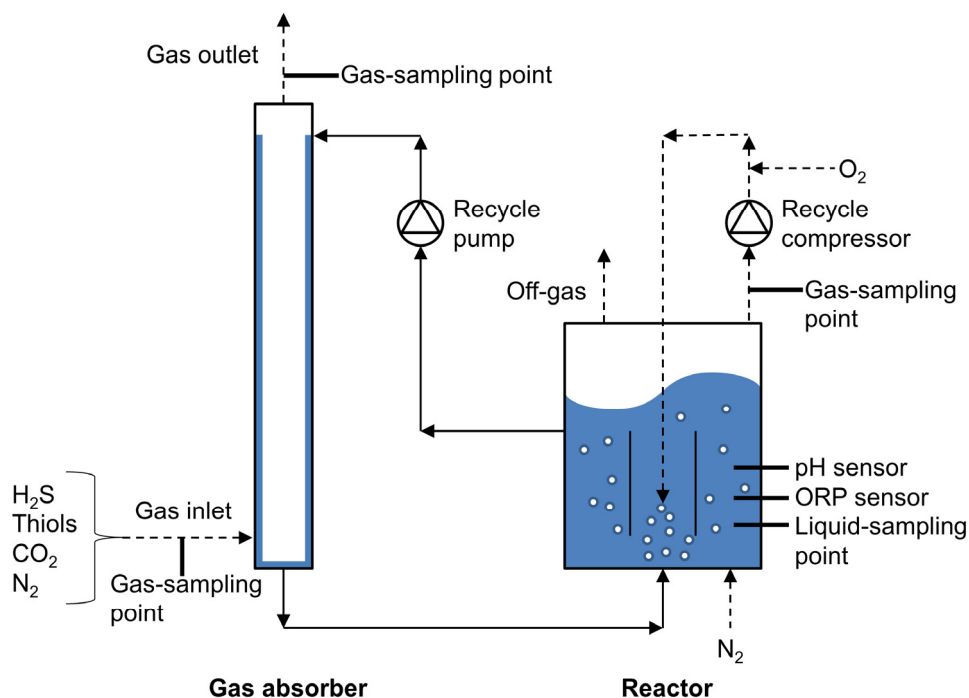

Figure 2. Flow scheme of experimental setup used for fed-batch experiments.

Table 3. Dimensions and process conditions of the gas absorber for H$_2$S and thiols removal.

Dimensions and process conditions	
Column diameter [m]	0.011
Column height [m]	0.8
Total gas flow [Nm^3 s^{-1}]	2.8 × 10^{-6}
Empty bed retention time [s]	27
H$_2$S loading [Nm^3 s^{-1}]	4.2 × 10^{-8}
Thiols loading [Nm^3 s^{-1}]	1.7 - 6.2 × 10^{-9}
Liquid flow [Nm^3 s^{-1}]	2.8 × 10^{-6}

6.3.1.1. Medium composition

The reactor medium included a carbonate/bicarbonate buffer of 0.1 M Na$_2$CO$_3$ and 0.8 M NaHCO$_3$. Furthermore, the medium contained 1.0 g K$_2$HPO$_4$, 0.2 g MgCl$_2$ × 6 H$_2$O, and 0.6 g urea per 1 L Milli-Q water. A trace elements solution was added (1 mL L^{-1}) as described elsewhere [18]. The final pH of the medium was kept constant at 9.00 ± 0.01 at 35 °C.

6.3.1.2. Inoculum

The bioreactor was inoculated with cells obtained by centrifugation (30 min at 16,000 x *g*) of a 2-L culture sample collected from a full-scale installation used to desulfurize a natural-gas condensate containing low concentrations of thiols (as described in Section 6.2).

6

Table 4. Loading rate of thiols to the experimental setup for each experiment operated under constant H_2S loading rate (61.3 mM d^{-1}) and reduction-oxidation potential (-390 mV).

Exp. number	Supplied thiol to the gas absorber	Thiol loading rate [mM d^{-1}]	N_2 flow over the bioreactor [NL h^{-1}]	Type of experiment
1	Methanethiol	9.1	0 (gas-tight reactor)	Biotic (biomass and sulfur present)
2			6	
3			12	
4			18	
5	Ethanethiol	9.1	0 (gas-tight reactor)	
6			6	
7			12	
8			18	
9	Propanethiol	4.5	0 (gas-tight reactor)	
10			6	
11			12	
12			18	
13	Methanethiol	2.5	0 (gas-tight reactor)	
	Ethanethiol	2.5		
	Propanethiol	2.5		
14	Methanethiol	2.5	18	
	Ethanethiol	2.5		
	Propanethiol	2.5		
15	Methanethiol	2.5	0 (gas-tight reactor)	Abiotic (biomass and sulfur absent)
	Ethanethiol	2.5		
	Propanethiol	2.5		

6

6.3.2. Experimental design

Unless stated otherwise, all experiments were performed in the experimental setup as described in section 6.3.1.

First, we adapted the microbial inoculum biomass originating form full-scale installation (described in Section 6.2) to MT, which is the most common and toxic of all thiol species. This adaptation was performed under a gradually increasing MT loading rate ranging from 0.1 to 9 mM d^{-1} over a period of 70 days (see Section 6.4.1, Fig. 4). During the adaptation period there was no N_2 flow over the bioreactor (Fig. 2).

Second, we studied the effect of stripping MT on the product selectivity and VOSCs distribution by sparging the bioreactor with N_2 gas (0-18 L h^{-1}). An overview of the operating conditions for these experiments is given in Table 4. The total MT and ET loading rate of the gas absorber was 9.1 mM d^{-1}, while the PT loading rate was 4.5 mM d^{-1} for experiments in which single thiols were supplied to the system. To avoid complete inhibition of the biomass, the loading rate of each thiol was lower (2.5 mM d^{-1}) when all three thiols were simultaneously supplied. All experimental runs were conducted under sulfur-producing conditions (ORP = -390 ± 5 mV). The H_2S loading rate was kept constant at 61.3 mM d^{-1}. Before the onset of each experiment the ORP was kept constant within ± 5 mV. Each experiment lasted for 24 hours, during which four gas and liquid samples were taken at regular time intervals. For experiments described in Table 4, the ionic charge balance was established by comparing equivalent amounts of cations and anions (see Section 6.3.3). The difference was 4 ± 3 % indicating that there was no significant gap in the sulfur balance.

6.3.3. Analytical techniques

Liquid sample preparation and chemical analysis of sulfur compounds (sulfur, sulfate, and thiosulfate) and biomass concentration were performed as described previously [19]. In addition to sulfur containing anions, we also analyzed Na^+ and K^+ with ion chromatography as described for the anions [19] except that a Metrohm Metrosep C4 - 150/4.0 mm column was used with a mobile phase of 0.9 mL 3 mM HNO_3 min^{-1}.

6

To close the ionic charge balance, the carbonate and bicarbonate ion concentrations were calculated using the Henderson-Hasselbalch equation [20] on the basis of inorganic carbon determined using high temperature catalytic oxidation at 680 °C in a TOC-VCPH/CPN analyzer (Shimadzu, the Netherlands). Before starting the analyses, all solids were removed by filtration over a 0.22 μm syringe filter (Millex G5 filter unit; Millipore). The samples were subsequently stored at 4 °C.

Concentrations of gaseous compounds (H_2S, O_2, N_2 and VOSCs; i.e. MT, ET, n-PT, and their diorgano polysulfanes) were analyzed as described previously [19]. To identify VOSCs, we used gas chromatography (6890N, Agilent, the Netherlands) coupled with a triple quadrupole mass spectrometer (5975, Agilent, the Netherlands), equipped with an Agilent column (HP-5MS, 30 m x 0.25 mm x 0.25 μm, Agilent, the Netherlands). Initially, the oven temperature was 50 °C. After 2 min, a gradient of 12.5 °C min^{-1} was applied to reach 200 °C. We operated the mass spectrometer in SIM mode with a filament voltage of 70 eV and an electron multiplier voltage of 1200 to 2800 V. Helium was the carrier gas, with a flow rate of 1.3 mL min^{-1}. The injection volume was 1 mL.

The morphological and elemental analyses of the bioreactor suspension were performed using a scanning electron microscope (JSM 6480 LV, JEOL, the Netherlands). We preserved the samples by fixation with a 10% glutaraldehyde solution (Sigma-Aldrich, the Netherlands) and subsequent air drying for 24 h.

Biomass particle size was quantified using laser measurement in a particle size and shape analyzer (Eyetech, Doner technologies, Or Akiva, Israel) with the Dipa 2000 software (Doner technologies, Or Akiva, Israel). Measurements were done in triplicate for 120 s while stirring.

6

6.3.4. DNA extraction and 16S rRNA gene sequencing

Biomass samples were collected for microbial community analysis of respectively (1) the inoculum; (2) after adaptation to MT; and (3) at the end of each experimental run. The samples were washed twice with a buffer of pH 9 and 0.5 M Na^+ to prevent the occurrence of an osmotic shock. The washing was performed by (1) centrifuging the samples at 20,000 x *g* for 5 min; (2) removal of the supernatant; and (3) addition of fresh buffer and mixing with a vortex to re-

suspend the pellet. Afterwards, Total Genomic DNA was extracted from the washed biomass using the PowerBiofilm™ DNA Isolation Kit (MoBio, USA) following the manufacturer's instructions. All the above procedures were performed in duplicate for each sample.

For the original inoculum and MT adapted biomass the 16S rRNA gene profiling was performed as following. Illumina 16S rRNA gene amplicon libraries were generated and sequenced at BaseClear BV (Leiden, The Netherlands). In short, barcoded amplicons from the V3-V4 region of 16S rRNA genes were generated using a 2-step PCR. 10-25 ng genomic DNA was used as template for the first PCR with a total volume of 50 µl using the 341F (5'-CCTACGGGNGGCWGCAG-3') and the 785R (5'-GACTACHVGGGTATCTAATCC-3') primers appended with Illumina adaptor sequences. PCR products were purified and the size of the PCR products were checked on a Bioanalyzer (Agilent, CA, USA) and quantified by fluorometric analysis. Purified PCR products were used for the 2nd PCR in combination with sample-specific barcoded primers. Subsequently, PCR products were purified, checked on a Bioanalyzer (Agilent, CA, USA) and quantified, followed by multiplexing, clustering, and sequencing on an Illumina MiSeq with the paired-end 250 cycles protocol and indexing. The sequencing run was analyzed with Illumina CASAVA pipeline (v1.8.3) with demultiplexing based on sample-specific barcodes. The raw sequencing data produced was processed by removing the sequence reads of too low quality (only "passing filter" reads were selected) and discarding reads containing adaptor sequences or PhiX control with an in-house filtering protocol. A quality assessment on the remaining reads was performed using the FASTQC quality control tool version 0.10.0.

For biomass samples taken at the end of the experimental runs with different thiols, the 16S rRNA profiling was performed as following. A portion of the 16S rRNA gene was amplified using primers 341F and 805R [21] following a modified PCR protocol by Hugerth et al. (2014) [22]. Sequencing was carried out at Science for Life Laboratory, Sweden (www.scilifelab.se) on the Illumina platform [23]. Sequence data were processed using the UPARSE pipeline [24] and annotated against the SINA/SILVA database (SILVA 119) [25] before analysis in Explicet 2.10.5 [26].

6

6.3.5. Effect of diorgano polysulfanes on the redox potential

We investigated the effect of dimethyl-, diethyl-, and dipropyl polysulfanes on the ORP by using a setup consisting of a glass mini-reactor (60 mL) equipped with a magnetic stirrer as described elsewhere [27]. The reactor was closed with a Teflon piston. The ORP was measured with a redox potential electrode (Ag/AgCl reference electrode, Orbisint CPS12D; Endress+Hauser). A multiparameter transmitter (Liquiline CM442; Endress+Hauser, the Netherlands) was used to record the signals from the ORP sensor. All the experiments were performed at 35 °C (DC10-P5/U thermostat bath, Haake, Germany).

Solutions of dimethyl-, diethyl-, and dipropyl polysulfanes were prepared by addition of 6 g L^{-1} biosulfur to 1.2 mM MT, ET, or PT solutions and incubated on a shaker for 24 hours at room temperature to allow for complete reaction between thiol and biosulfur (Eq. 2-3). Complete conversion of thiols was verified with the GC analysis. Solutions of dimethyl and diethyl polysulfanes were injected separately to the mini-reactor filled with the medium using a glass syringe with the injection volume between 50-150 µL. Each concentration was analyzed in triplicate.

6.4. Results and discussion

6.4.1. Effect of MT on the microbial population dynamics

The microbial community in the full-scale bioreactor as described in this paper was most similar to that which served as biomass inoculation source, located at Industriewater Eerbeek B.V., the Netherlands [28] (Fig. 3). However, a slight shift in the population was observed as SOB belonging to Halomonadaceae family were dominant in the full-scale plant described in this paper, while the Ectothiorhosdospiraceae family was the most dominant one in the Eerbeek full-scale plant [29]. This difference in microbial community may be explained by the presence of organic compounds in the full-scale plant described in this paper (Table 1). The Halomonadaceae family includes heterotrophic sulfide oxidizing species which might use these organic compounds [30]. Moreover, these micro-organisms can oxidize sulfide to tetrathionate in an indirect manner [30]. Tetrathionate is unstable under alkaline conditions leading to elevated concentration of thiosulfate as observed for the full-scale bioreactor described in this work (Table 2) [31].
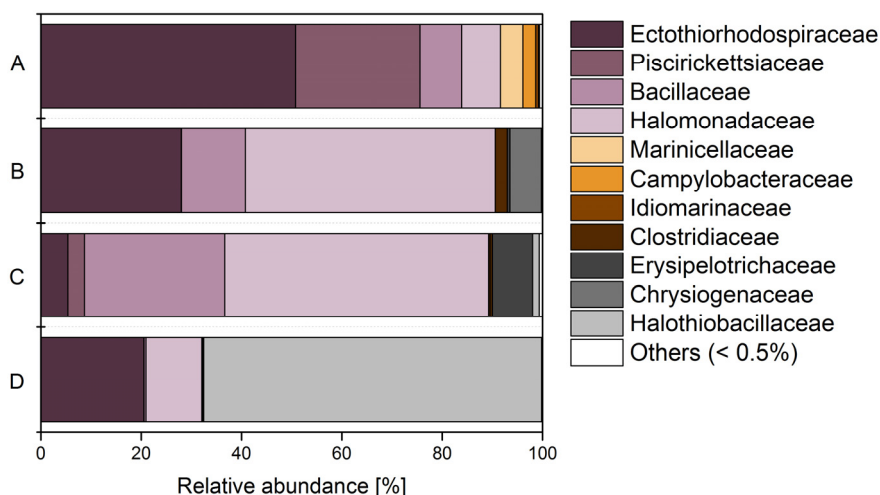
Figure 3. Relative abundance of the microbial composition based on the 16S rRNA gene. DNA was extracted and sequenced from biomass from the sulfide oxidizing bioreactors of the Thiopaq full-scale plant in Eerbeek (**A**) and in Southern Illinois (**B**); and from the laboratory reactor after 20 (**C**) and 61 days (**D**) during which the reactor was exposed to methanethiol (0.1 - 7 mM d^{-1}). The laboratory reactor was operated at oxidation reduction potential of -390 mV, pH = 9 and the H$_2$S loading rate was 61.3 mM d^{-1}. Only bacteria with a relative abundance higher than 0.5% are listed (remaining bacteria are grouped into "Others"). The results represent the average value between two replicas. The different replica values can be found in Table S1 in the supplementary material.

A clear shift in the original microbial community occurred after 3 weeks of incubation in the laboratory bioreactor (Fig. 3). At the end of the adaptation period, cells from the Halothiobacillaceae family became the dominant phylogenetic group, while cells from this family were not detected in the full-scale plant (Section 6.2, Fig. 3). A potential cause of this shift was the relatively high methanethiol loading applied to the bioreactor (up to 9.1 mM d^{-1}, Fig. 4), which might have given a competitive advantage to the SOB from Halothiobacillaceae family. After 8 weeks, it was found that the selectivity for sulfur formation was significantly higher compared to the original full-scale reactor biomass (day 17 *v.* 60, Fig. 4). This may have been caused by the shift in microbial community during adaptation to higher MT concentrations. A possible reason why this shift was already observed after 8 weeks

is the approximately 20 fold higher MT loading rate in comparison to the full-scale installation. Another difference was lower VOSC concentrations in the full-scale bioreactor due to gas stripping compared to the closed laboratory-scale bioreactor. Moreover, thiols present in the full-scale feed-gas mainly consisted of higher thiols that show less inhibition than MT (Chapter 5).
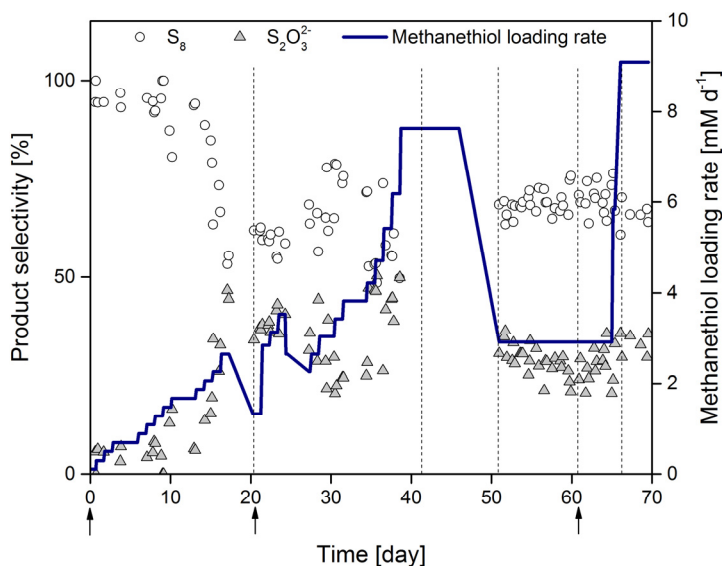

Figure 4. Product selectivity of biological and chemical oxidation of H_2S (61.3 $mM\,d^{-1}$) under different methanethiol loading rates. Arrows indicate sample collection for microbial community analysis and dashed lines represent centrifugation of the biomass and replacement with fresh medium. The reactor system was operated at oxidation reduction potential of -390 mV, pH = 9 and T = 35 °C.

6.4.2. Effect of MT, ET and PT on biological H_2S oxidation

6.4.2.1. Performance of the gas absorber

The scrubbing efficiency of H_2S and thiols in experiments 1 to 12 (Table 4) showed that in all experiments H_2S was almost completely absorbed from the inlet gas stream (>99.8%), while the scrubbing efficiency of thiols ranged between 40 and 70% (Fig. 5A). The difference in scrubbing efficiencies between H_2S and thiols was caused by the higher solubility of the former, resulting from a lower pK_a value than those of thiols (7 *v.* ~10.4) and higher Henry's law constant (0.41 *v.* ~0.15; values for water at 20 °C) [32].
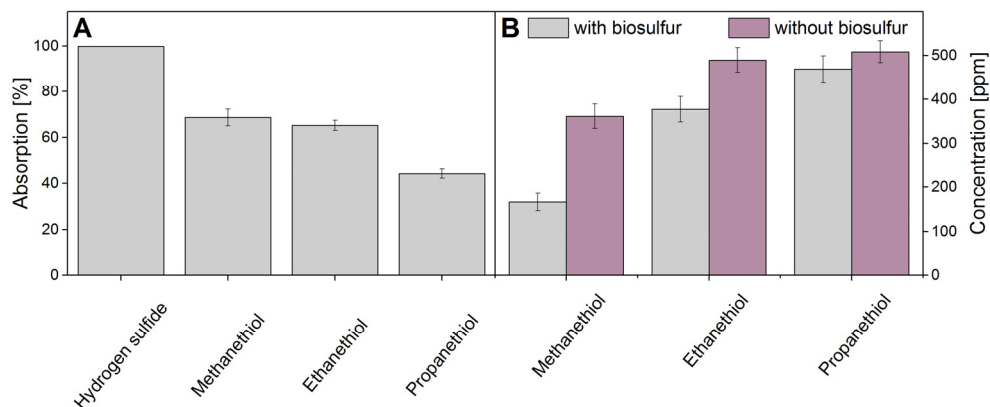
Figure 5. A. Absorption efficiency of hydrogen sulfide and thiols in a falling film gas absorber by an alkaline solution (pH = 9) with biosulfur. Gas flow was 2.8×10^{-6} Nm^3 s^{-1}. Liquid flow was 2.8×10^{-6} m^3 s^{-1}. **B.** Concentrations of organo-sulfur compounds in the outlet of the gas absorber during simultaneous removal of methanethiol, ethanethiol, and propanethiol in the presence and absence of biosulfur particles in the washing liquid. Reactor system operated at oxidation reduction potential of -390 mV, pH = 9 and thiols inlet concentration of 600 ppm(v). The error bars represent the standard deviation from triplicate samples.

An important factor influencing the absorption capacity of thiols is the reaction between thiols and biosulfur particles under the formation of diorgano polysulfanes (Eq. 1-5). In experiments 13 and 15 (Table 4), all thiols (MT, ET, and PT) were simultaneously supplied to the gas absorber in the presence and absence of biologically produced sulfur particles. When sulfur was present in the bioreactor, diorgano polysulfanes were formed according to Eq. 2 - 4 which are distributed between the gas, liquid, and solid (biosulfur) phases (Supplementary Information, Figure S1). Formation of diorgano polysulfanes enhanced absorption of thiols from a gas stream (Fig. 5B). In the presence of biologically produced sulfur particles, MT was absorbed with the highest efficiency (72%), while ET and PT absorptions were less efficient (37 and 22%, respectively). In the absence of biosulfur, thiol concentrations in the outlet of the gas absorber were higher, indicating that thiols were removed from the gas stream resulting from a homogeneous reaction with an alkaline solution (Eq. 1; Fig. 5B). The absorption efficiency of MT, ET,

and PT decreased to 40, 18, and 15%, respectively. Higher removal of MT was due to its higher solubility in water [33], i.e. thiols absorption decreased with increasing hydrophobicity. This result showed that the thiol removal efficiency from sour gas streams can be enhanced by heterogeneous reaction with biosulfur particles. As the experimental set-up (Fig. 2) does not have any other discharge than the gas outlet (experiments 13 - 15, Table 4), the removal efficiency reflects the reaction between thiols and sulfur with oxygen (Eq. 2 - 6). The sulfur is present in the bioreactor in a large excess (2.5 mM thiol d^{-1} of $v.$ 61.3 mM H_2S d^{-1}) and thus adding more sulfur will not result in a higher removal of the thiols. This, however, can be done by reducing the concentration of thiols in the bioreactor suspension, e.g. by stripping with gas.
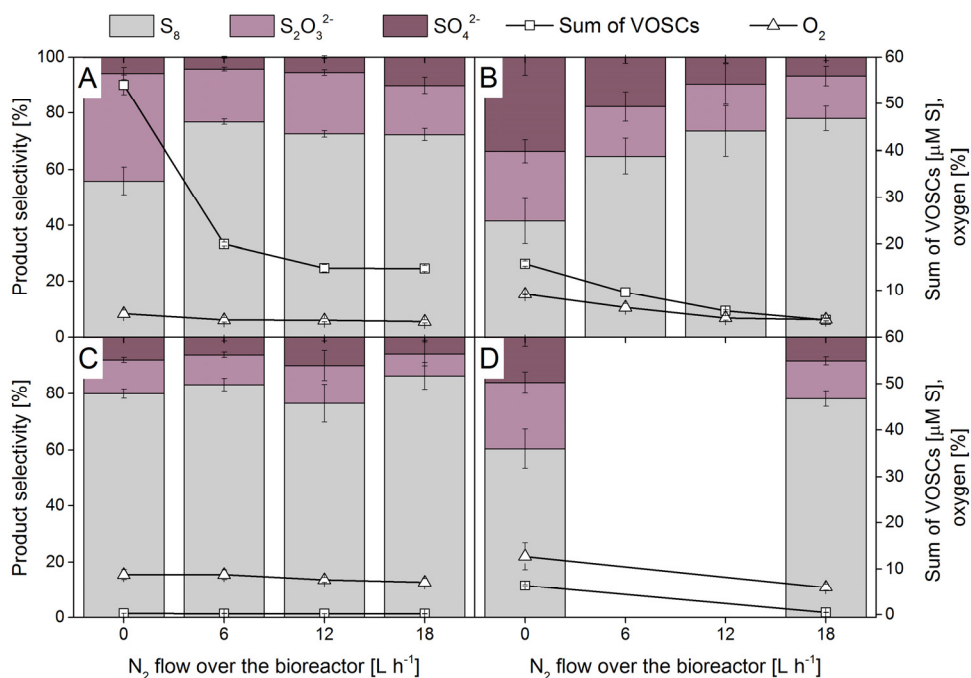

Figure 6. Performance of the gas biodesulfurization system fed with H_2S (61.3 mM d^{-1}) and: **A.** Methanethiol; loading rate was 9.1 mM d^{-1}. **B.** Ethanethiol; loading rate was 9.1 mM d^{-1}. **C.** Propanethiol; loading rate was 4.5 mM d^{-1}. **D.** Mixture of methanethiol, ethanethiol, and ethanethiol, loading rate was 2.5 mM d^{-1}, each. The reactor system was operated at oxidation reduction potential of -390 mV, pH = 9 and multiple flows of nitrogen over the bioreactor. The error bars represent the standard deviation from quadruple samples.

6.4.2.2. Effect of VOSCs stripping on bioreactor performance

N_2 gas was added to the bioreactor suspension as presented in Fig. 2 to assess the effect of thiols stripping on the bioreactor performance. The VOSC concentrations in the bioreactor decreased with increased N_2-flow rates (Fig. 6A-D) and showed that thiols can be effectively stripped by applying already a low volumetric flow rate of an inert gas. Moreover, it can be observed that the sum of VOSCs in the bioreactor headspace decreased with increasing thiol hydrophobicity (Fig. 6A-C) [32].

It was also demonstrated that stripping of VOSCs had a significant effect on the selectivity for sulfur product formation when the inlet gas stream was supplemented with MT (Fig. 6A). At the highest VOSCs concentration, the selectivity for biologically produced sulfur was the lowest (56 mol%) and more thiosulfate (38 mol%) was formed. However, at decreasing VOSCs concentration as a result of N_2 stripping, the selectivity for sulfur formation increased to about 74 mol% (Fig. 6A). Lower selectivity for sulfur production at higher VOSC concentrations resulted from the inhibitory effect of VOSCs on the biological oxidation of sulfide [9,19] which, in turn, leads to an enhancement of the chemical oxidation of sulfide to form thiosulfate [17,34]. Hence, the selectivity for chemically produced thiosulfate follows an exponential decay with decreasing concentrations of VOSCs.

Contrary to experiments with MT, experiments with ET (Experiments 5-8, Table 4) showed an increase in the selectivity of biologically produced sulfate with increasing VOSC concentrations, while the thiosulfate selectivity remained constant at around 18 mol% (Fig. 6B). We found that this unexpected change from sulfur to sulfate selectivity was a result of the influence of diethyl polysulfanes (Eq. 2-4) on the ORP. The principle of controlling biodesulfurization reactors is based on that the ORP is mainly determined by the sulfide concentration [35]. However, we found that in addition to sulfide, diethyl polysulfanes also lower the ORP, which resulted in an additional supply of oxygen to the bioreactor to keep a set point of -390 mV. This could be seen in an increased concentration of oxygen in the bioreactor (Fig. 6A *v.* Fig. 6B) and a doubling of the O_2/H_2S supply ratio (from 0.75 to 1.4 mol mol^{-1}) compared to experiments with MT and other studies [5,8]. This ratio is related to the total sulfide concentration [36] and the stoichiometry of the simplified bio-oxidation reactions (Eq. 14-15) [35].

6

Therefore, by increasing the O_2/H_2S supply ratio, the selectivity from sulfur to sulfate can be shifted [7,37]. In experiments with only MT, a clear change in product selectivity was not seen. An explanation for this observation was that diethyl polysulfanes lower the ORP by 36 ± 4 mV more than dimethyl polysulfanes that are formed from the abiotic oxidation of MT (Fig. 7). Moreover, diethyl polysulfanes are also less volatile than dimethyl polysulfanes [33], which results in a lower stripping rate from the bioreactor and thus higher concentrations in the bioreactor suspension (data not available).
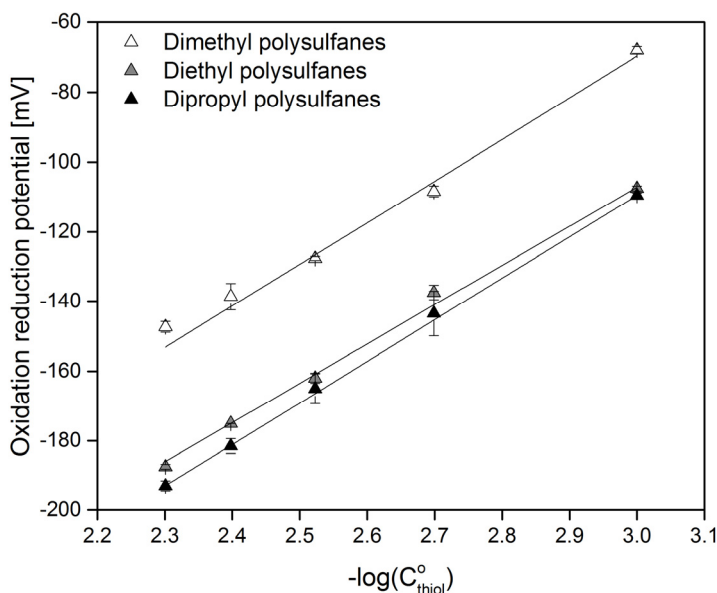

Figure 7. Relationship between the oxidation reduction potential and the initial thiol concentration (C°_{thiol}, mM) in a reaction between thiol and biosulfur leading to formation of diorgano polysulfanes. Measurements were performed in a medium with $[Na^+ + K^+]$ = 1 M, pH = 9 and T = 35°C.

The results show that the commonly used method to control the bioreactor by the ORP was insufficient as the ORP was no longer determined by the sulfide concentration alone. Therefore, to expand the application of biodesulfurization processes for gas streams containing ORP-lowering compounds, it is necessary to develop a new method to control the O_2 supply to biodesulfurization reactors. Such a method should not rely on indirect parameters, such as the ORP, but should be based on a straightforward measurement of the sulfide and VOSC concentration.

166

In experiments with PT, the loading rate was lowered from 9.1 to 4.5 mM d^{-1}, as the bioreactor appeared to be unstable under the former loading rate. Unstable operation of the bioreactor occurred when it was not possible to maintain a constant ORP value by dosing O$_2$ to the gas recycling loop (Fig. 2). The reason for the bioreactor instability was the same as described above: dipropyl disulfides are more reduced compounds than dimethyl disulfides, thereby more effective in lowering the ORP (Fig. 7). An additional factor can be higher hydrophobicity and lower volatility of dipropyl polysulfanes compared to dimethyl and diethyl polysulfanes [33] resulting in higher concentrations in the suspension of the bioreactor. Therefore, under a PT loading rate of 9.1 mM d^{-1}, dipropyl disulfides in the bioreactor reached a concentration at which it was no longer feasible to control the ORP at a constant value of -390 mV. After lowering the PT loading rate to 4.5 mM d^{-1}, no significant effects were observed on the product selectivity (Fig. 6C). The sulfur selectivity remained constant at about 80 mol% which was also found for a sulfide oxidation system that was not impacted by any thiol inhibition [38].

The effect of combined supply of all three of thiols (MT, ET, and PT) on the product selectivity was investigated by changing N$_2$-flow rates from 0 to 18 L h^{-1} (Fig. 6D). At the highest VOSC concentrations, we observed a decrease in sulfur selectivity with increased sulfate formation, which was in line with experiments in which thiols were individually supplied (Fig. 6A-B). Similarly to experiments in which only PT was supplied (Fig. 6C), no inhibitory effects were observed at the lowest VOSC concentration.

6.4.2.4. Effect of thiols on the adapted biomass

The microbial community analysis revealed that various thiols had a different impact on the microbial community composition (Fig. 8). The presence of thiols appeared to provide a competitive advantage to different populations when compared with previous studies with sulfide oxidizing bioreactors at haloalkaline conditions [29]. When MT and ET were supplied, the fraction of populations belonging to the family *Halothiobacillaceae* significantly increased, which was also observed in the biomass adaptation experiments. In this family, the only described haloalkaliphilic autotrophic sulfide oxidizing species is *Thioalkalibacter halophilus* [39]. The predominance of strains from the *Halothiobacillaceae* family was

in contrast with samples analyzed from full-scale biodesulfurization plants treating gas without thiols whereby species belonging to the genus *Thioalkalivibrio* (family *Ectothiorhodospiraceae*) are dominant [29]. There is no information available that explains why populations aligning within the *Halothiobacillaceae* family became more abundant in the presence of MT and ET. It might be that they have higher tolerance to thiols than the other haloalkaliphilic SOB species. However, in the presence of PT the increased dominance of SOB related to the *Halothiobacillaceae* was not observed. On the contrary, it became less abundant than in the inoculum. The fact that PT was supplied in lower concentrations compared to MT and ET might explain the difference. At these PT concentrations, other bacteria might still be tolerant to thiols, taking away the selective advantage of bacteria belonging to the *Halothiobacillaceae* family.
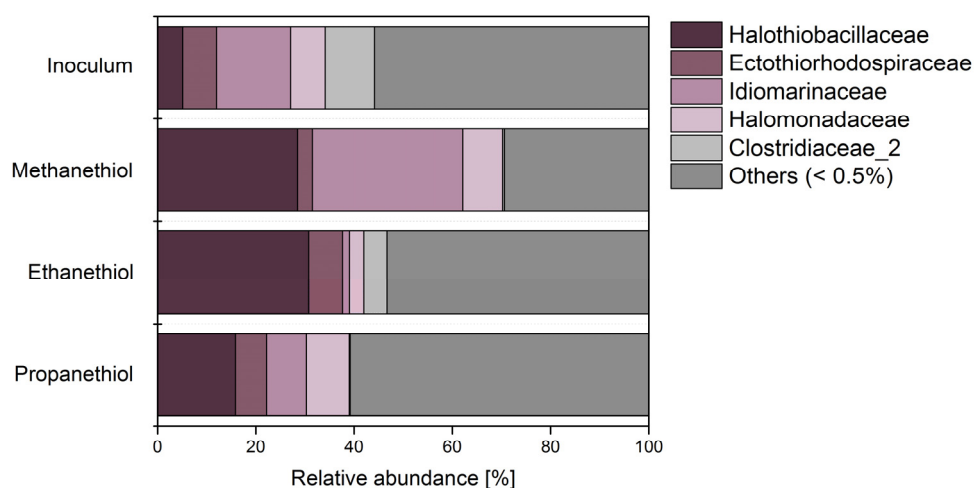

Figure 8. Relative abundance of the microbial composition based on the 16S rRNA gene. DNA was extracted and sequenced from the inoculum and biomass taken at the end of MT, ET, and PT experiments. The laboratory reactor was operated at oxidation reduction potential of -390 mV, pH = 9 and the H_2S loading rate was 61.3 mM d^{-1}. Only bacteria with a relative abundance higher than 0.5% are listed (remaining bacteria are grouped into "Others"). The results represent the average value between two replicas. The different replica values can be found in Table S2 in the supplementary material.

Another interesting observation was the increased abundance of bacteria related to the family *Idiomarinaceae* in the ET and PT experiments but not in the MT experiment. Within the *Idiomarinaceae* family, the only genus identified in this study was *Aliidiomarina* in which mainly heterotrophic aerobic bacteria are described [40]. To the best of our knowledge, there is no information available about their possible sulfide oxidizing capacity or use of VOSCs. Thus, the role of these bacteria and the reason for their increased dominance in the bioreactors where ET and PT was supplied remains unknown.

6.4.2.5. Coagulation of biosulfur in the presence of thiols

During the bioreactor operation with thiols, we have observed coagulation of colloidal biosulfur particles. Formed diorgano polysulfanes in reaction between thiols and biosulfur (Eq. 2 - 3) are hydrophobic. Therefore, these compounds adsorb onto somewhat hydrophobic biosulfur particles resulting in a coagulation of biosulfur and significantly increased particle size (Fig. 9A). Increased settling rate is important from the technological point of view as it allows easy separation of biosulfur from liquid. Also, we observed that coagulated sulfur forms hydrophobic aggregates which attract biomass (Fig. 9B). Attraction of biomass by biosulfur particles has a negative effect as it can lead to lowering the biomass concentration in bioreactor and therefore, lower process efficiency.
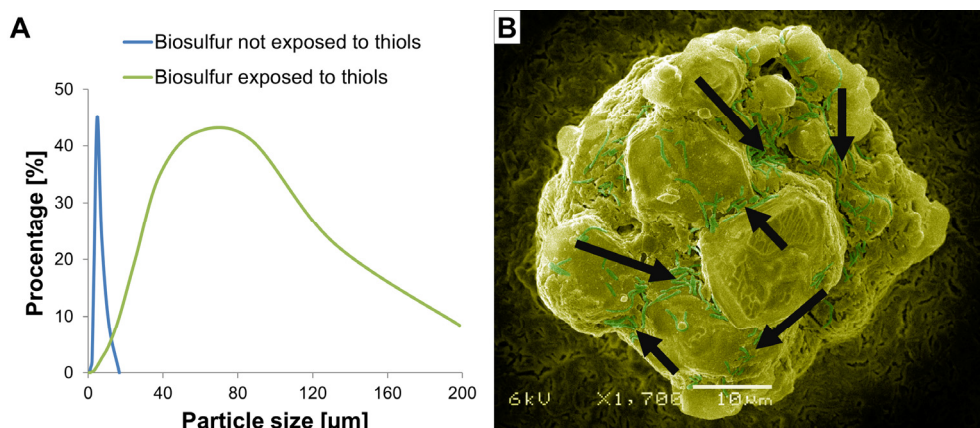
Figure 9. A. Biosulfur particle size distribution. **B.** Scanning electron microscope (SEM) picture of biosulfur aggregate exposed to thiols with attracted bacteria on its surface (indicated with arrows).

6.5. Conclusions

In this study we applied relatively high thiol loading rates compared to a full-scale plant (9.1 *v.* 0.4 mM d^{-1}) and other studies (0.079 mM d^{-1}) [38]. The obtained results showed that under such high loading rates it was possible to reach a stable operation of the bioreactor which demonstrates the high potential of such biodesulfurization systems. This study describes the combined removal of H$_2$S and thiols from gas streams at haloalkaline conditions. The effect of thiols on the biological oxidation of sulfide was minimized by the occurrence of a chemical reaction between thiols and biosulfur and gas stripping of the remaining thiols. The reaction between thiols and biosulfur leads to the formation of diorgano polysulfanes, which are less toxic than thiols, but these are stronger reductants and therefore interfere with the measured ORP that is an essential input parameter to control the oxygen supply rates. We recommend that future research focuses on finding alternatives to control the biodesulfurization processes. These could not only be based on the ORP but also on the actual sulfide and VOSC concentration. Also more research is needed to investigate the technological application of the reactions between thiols and biosulfur. An example of such direction can be looking at biological conversion of biosulfur with bounded diorgano polysulfanes.

Acknowledgements

References

1. Wang W, Turn SQ, Keffer V, Douette A. Study of process data in autothermal reforming of LPG using multivariate data analysis. *Chem. Eng. J.* Elsevier; 2007;129:11–19.
2. Kim K-H, Choi Y, Jeon E, Sunwoo Y. Characterization of malodorous sulfur compounds in landfill gas. *Atmos. Environ.* Elsevier; 2005;39:1103–1112.
3. Fredericks E, Harlow G. Determination of mercaptans in sour natural gases by gas liquid chromatography and microcoulometric titration. *Anal. Chem.* ACS Publications; 1964;36:263–266.
4. Song C. An overview of new approaches to deep desulfurization for ultra-clean gasoline, diesel fuel and jet fuel. *Catal. Today*. Elsevier; 2003;86:211–263.
5. Van den Bosch PLF, van Beusekom OC, Buisman CJN, Janssen AJH. Sulfide oxidation at halo-alkaline conditions in a fed-batch bioreactor. *Biotechnol. Bioeng.* Wiley Online Library; 2007;97:1053–1063.
6. Sercu B, Nunez D, Van Langenhove H, Aroca G, Verstraete W. Operational and microbiological aspects of a bioaugmented two-stage biotrickling filter removing hydrogen sulfide and dimethyl sulfide. *Biotechnol. Bioeng.* Wiley Online Library; 2005;90:259–269.
7. Alcántara S, Velasco A, Muñoz A, Cid J, Revah S, Razo-Flores E. Hydrogen sulfide oxidation by a microbial consortium in a recirculation reactor system: sulfur formation under oxygen limitation and removal of phenols. *Environ. Sci. Technol.* ACS Publications; 2004;38:918–923.
8. Roman P, Bijmans MFM, Janssen AJH. Influence of methanethiol on biological sulfide oxidation in gas treatment system. *Environ. Tech.* 2015.
9. Van den Bosch PLF, de Graaff M, Fortuny-Picornell M, van Leerdam RC, Janssen AJH. Inhibition of microbiological sulfide oxidation by methanethiol and dimethyl polysulfides at natron-alkaline conditions. *Appl. Microbiol. Biotechnol.* Springer; 2009;83:579–587.
10. Sorokin DY, Banciu H, Robertson LA, Kuenen JG, Muntyan MS, Muyzer G. Halophilic and haloalkaliphilic sulfur-oxidizing bacteria. In: Rosenberg E. et al., editor. *The Prokaryotes*. Springer-Verlag: Berlin-Heidelberg; 2013. p. 529–554.
11. Weast RC. CRC handbook of chemistry and physics. CRC Press, Boca Raton; 1986.
12. Crampton M. The Chemistry of the Thiol Group: Part 1. Patai, S., editor. Acidity and Hydrogen Bonding. New York, NY: John Wiley & Sons; 1974. p. 379–415.
13. Steudel R. The chemistry of organic polysulfanes RS (n)-R (n> 2). *Chem. Rev.* 2002;102:3905.
14. Van Leerdam RC, Bosch PLF, Lens PNL, Janssen AJH. Reactions between methanethiol and biologically produced sulfur. *Environ. Sci. Technol.* 2011;45:1320–1326.
15. Jocelyn PC. Biochemistry of the SH Group. Academic Press London; 1972.
16. Cline C, Hoksberg A, Abry R, Janssen AJH. Biological Process for H₂S Removal from Gas Streams: The Shell-Paques/THIOPAQ™ Gas Desulfurization Process. *Proceedings of the Laurance Reid Gas Conditioning Conference*. 2003. p. 1–18.
17. Chen KY, Morris JC. Kinetics of oxidation of aqueous sulfide by oxygen. *Environ. Sci. Technol.* ACS Publications; 1972;6:529–537.
18. Pfennig N, Lippert KD. Über das vitamin B₁₂-bedürfnis phototropher Schwefelbakterien. *Arch. Microbiol.* Springer; 1966;55:245–256.

6

19. Roman P, Veltman R, Bijmans MFM, Keesman K, Janssen AJH. Effect of methanethiol concentration on sulfur production in biological desulfurization systems under haloalkaline conditions. *Environ. Sci. Technol.* ACS Publications; 2015;49:9212–9221.

20. Po HN, Senozan N. The Henderson-Hasselbalch equation: its history and limitations. *J. Chem. Educ.* ACS Publications; 2001;78:1499.

21. Herlemann DP, Labrenz M, Jürgens K, Bertilsson S, Waniek JJ, Andersson AF. Transitions in bacterial communities along the 2000 km salinity gradient of the Baltic Sea. *ISME J.* Nature Publishing Group; 2011;5:1571–1579.

22. Hugerth LW, Wefer HA, Lundin S, Jakobsson HE, Lindberg M, Rodin S, Engstrand L, Andersson AF. DegePrime, a program for degenerate primer design for broad-taxonomic-range PCR in microbial ecology studies. *Appl. Environ. Microbiol.* Am Soc Microbiol; 2014;80:5116–5123.

23. Lindh MV, Figueroa D, Sjöstedt J, Baltar F, Lundin D, Andersson A, Legrand C, Pinhassi J. Transplant experiments uncover Baltic Sea basin-specific responses in bacterioplankton community composition and metabolic activities. *Front. Microbiol.* Frontiers Media SA; 2015;6.

24. Edgar RC. UPARSE: highly accurate OTU sequences from microbial amplicon reads. *Nat. Methods*. Nature Publishing Group; 2013;10:996–998.

25. Quast C, Pruesse E, Yilmaz P, Gerken J, Schweer T, Yarza P, Peplies J, Glöckner FO. The SILVA ribosomal RNA gene database project: improved data processing and web-based tools. *Nucleic. Acids. Res. 41*. Oxford Univ Press; 2012;D590–596.

26. Robertson CE, Harris JK, Wagner BD, Granger D, Browne K, Tatem B, Feazel LM, Park K, Pace NR, Frank DN. Explicet: graphical user interface software for metadata-driven management, analysis, and visualization of microbiome data. *Bioinformatics 29*. Oxford Univ Press; 2013;3100–3101.

27. Kleinjan WE, Keizer A de, Janssen AJH. Kinetics of the chemical oxidation of polysulfide anions in aqueous solution. *Water Res.* Elsevier; 2005;39:4093–4100.

28. Janssen AJH, Lens PNL, Stams AJM, Plugge CM, Sorokin DY, Muyzer G, Dijkman H, Van Zessen E, Luimes P, Buisman CJN. Application of bacteria involved in the biological sulfur cycle for paper mill effluent purification. *Sci. Total Environ.* Elsevier; 2009;407:1333–1343.

29. Sorokin DY, Muntyan MS, Panteleeva AN, Muyzer G. *Thioalkalivibrio sulfidiphilus* sp. nov., a haloalkaliphilic, sulfur-oxidizing gammaproteobacterium from alkaline habitats. *Int. J. Syst. Evol. Microbiol.* Soc General Microbiol; 2012;62:1884–1889.

30. Sorokin DY. Oxidation of inorganic sulfur compounds by obligately organotrophic bacteria. *Microbiology*. Springer; 2003;72:641–653.

31. Zhang H, Dreisinger DB. The kinetics for the decomposition of tetrathionate in alkaline solutions. *Hydrometallurgy*. Elsevier; 2002;66:59–65.

32. Matsis V, Georgantas D, Grigoropoulou H. Removal of n-butyl mercaptan using stripping with an inert gas: A nonequilibrium approach via mass balances. *Ind. Eng. Chem. Res.* ACS Publications; 2006;45:1766–1773.

33. Przyjazny A, Janicki W, Chrzanowski W, Staszewski R. Headspace gas chromatographic determination of distribution coefficients of selected organosulphur compounds and their dependence on some parameters. *J. Chromatogr. A*. Elsevier; 1983;280:249–260.

6

34. Janssen AJH, Sleyster R, Van der Kaa C, Jochemsen A, Bontsema J, Lettinga G. Biological sulphide oxidation in a fed-batch reactor. *Biotechnol. Bioeng*. Wiley Online Library; 1995;47:327–333.

35. Janssen AJH, Meijer S, Bontsema J, Lettinga G. Application of the redox potential for controling a sulfide oxidizing bioreactor. *Biotechnol. Bioeng.* Wiley Online Library; 1998;60:147–155.

36. Roman P, Bijmans MFM, Janssen AJH. Quantification of individual polysulfides in lab-scale and full-scale desulfurisation bioreactors. *Environ. Chem.* CSIRO; 2014;11:702–708.

37. Klok JBM, van den Bosch PLF, Buisman CJN, Stams AJM, Keesman KJ, Janssen AJH. Pathways of sulfide oxidation by haloalkaliphilic bacteria in limited-oxygen gas lift bioreactors. *Environ. Sci. Technol.* ACS Publications; 2012;46:7581–7586.

38. Van den Bosch PLF, Fortuny-Picornell M, Janssen AJH. Effects of methanethiol on the biological oxidation of sulfide at natron-alkaline conditions. *Environ. Sci. Technol.* ACS Publications; 2009;43:453–459.

39. Banciu HL, Sorokin DY, Tourova TP, Galinski EA, Muntyan MS, Kuenen JG, Muyzer G. Influence of salts and pH on growth and activity of a novel facultatively alkaliphilic, extremely salt-tolerant, obligately chemolithoautotrophic sufur-oxidizing Gammaproteobacterium *Thioalkalibacter halophilus* gen. nov., sp. nov. from South-Western Siberian soda lakes. *Extremophiles*. Springer; 2008;12:391–404.

40. Chiu H-H, Rogozin DY, Huang S-P, Degermendzhy AG, Shieh WY, Tang S-L. Aliidiomarina shirensis sp. nov., a halophilic bacterium isolated from Shira Lake in Khakasia, southern Siberia, and a proposal to transfer Idiomarina maris to the genus Aliidiomarina. *Int. J. Syst. Evol. Microbiol.* Soc General Microbiol; 2014;64:1334–1339.

6

Supporting Information

Table S1. Relative abundance of microorganisms in the biomass from the sulfide oxidizing bioreactors of the Thiopaq full scale plant in Eerbeek (A) and in North America (B), as well as from the laboratory bioreactor after 20 days (C) and 61 days (D). Others are represented by all the families with less than 0.5 % relative abundance. 1 and 2 represent duplicates.

Family	Relative abundance [%]							
	A		B		C		D	
	1	2	1	2	1	2	1	2
Ectothiorhodospiraceae	50.8	50.3	28.0	27.8	5.4	0.5	20.5	21.6
Piscirickettsiaceae	24.8	26.1	0.0	0.0	3.3	0.1	0.0	0.0
Bacillaceae	8.3	12.7	12.7	13.0	28.0	23.4	0.4	0.2
Halomonadaceae	7.7	8.9	49.8	52.7	52.6	57.3	11.1	10.8
Marinicellaceae	4.5	0.2	0.0	1.8	0.0	0.0	0.0	0.0
Campylobacteraceae	2.6	0.0	0.0	0.0	0.0	0.0	0.0	0.0
Idiomarinaceae	0.6	0.1	0.0	0.0	0.3	0.3	0.1	0.0
Clostridiaceae	0.1	0.0	2.4	2.8	0.5	0.6	0.1	0.3
Erysipelotrichaceae	0.1	0.0	0.5	0.8	8.0	7.3	0.0	0.1
Chrysiogenaceae	0.0	0.0	6.3	0.2	0.0	0.0	0.1	0.0
Halothiobacillaceae	0.0	0.0	0.0	0.0	1.3	4.7	67.3	67.0
Others (< 0.5%)	0.6	1.7	0.2	0.8	0.7	5.8	0.2	0.1

Table S2. Relative abundance of microorganisms in the inoculum and final biomass after experiments with methanethiol, ethanethiol, and propanethiol. Others are represented by all the families with less than 0.5 % relative abundance. A and B represent duplicates.

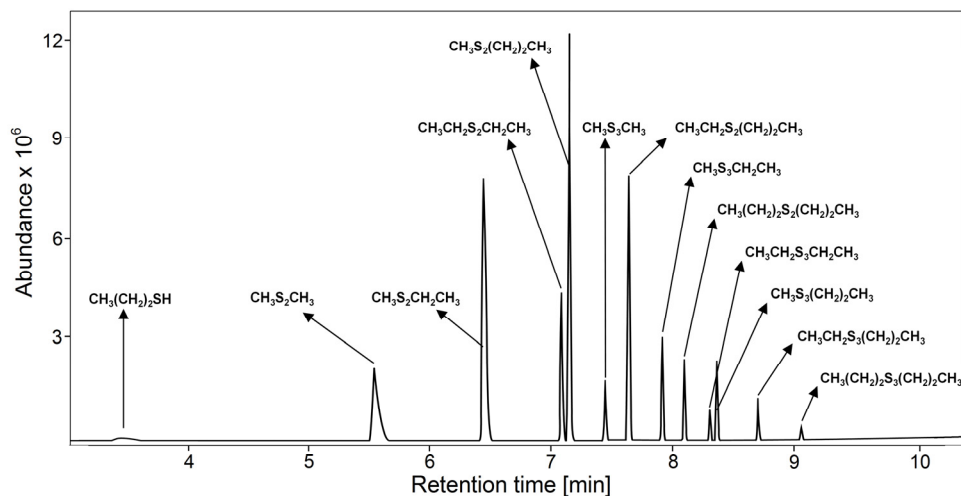| Family	Relative abundance [%]							
	Inoculum		Methanethiol		Ethanethiol		Propanethiol	
	A	B	A	B	A	B	A	B
Halothiobacillaceae	15.8	15.1	30.8	37.6	28.5	21.9	5.1	4.2
Ectothiorhodospiraceae	6.3	6.2	6.9	6.0	3.0	3.9	6.9	7.9
Idiomarinaceae	8.1	6.8	1.4	2.2	30.6	23.9	15.1	12.1
Halomonadaceae	8.7	9.8	2.9	3.5	8.1	6.7	7.0	5.7
Clostridiaceae	0.2	0.6	4.7	1.7	0.4	8.7	10.1	12.0
Others	60.8	61.5	53.3	48.9	29.4	35.0	55.8	58.0

Figure S1. Chromatogram of the bioreactor headspace during experiments where methanethiol, ethanethiol, and propanethiol were simultaneously supplied to the laboratory system for gas desulfurization.

Chapter 7

Summary and general discussion

7.1. Introduction

The need for desulfurization of sour gas streams, such as biogas, landfill gas, refinery gases and natural gas became urgent after the US EPA set a maximal allowable sulfur content for fuels [1,2] in order to reduce emissions of sulfur dioxide to the atmosphere. A variety of physicochemical and biological processes have been applied to desulfurize sour gas streams but for some hydrocarbon streams biological processes can be economically more attractive as these are operated under ambient temperature and pressure conditions leading to lower investment and operating cost [3,4]. However, biological processes are typically used to remove hydrogen sulfide (H_2S), whilst other volatile sulfur compounds such as thiols are only partially removed (**Chapter 3 - 5**). Broadening the application range of these processes will have a positive impact on air pollution and will allow for further cost reductions. Therefore, the aim of this thesis is to describe the effect of thiols on the biological removal of H_2S from sour gas streams. The main research tasks are defined in **Chapter 1**.

In this thesis, gas biodesulfurization is performed under haloalkaliphilic conditions to assure high absorption rates of sulfurous pollutants and provide appropriate bioreactor conditions for sulfur oxidizing bacteria (SOB). Under the prevailing conditions no clear evidence was found that haloalkaliphilic SOB can degrade thiols. Moreover, we found that organosulfur compounds inhibit SOB and thus need to be removed down to concentrations at which no inhibition occurs. In the current chapter an overview is provided of ways to mitigate any inhibitory effects caused by the presence of thiols. A modified process to remove H_2S and thiols is presented. The last section includes recommendations for further research.

7.2. Mitigation strategies to prevent the inhibitory effects of thiols on biodesulfurization systems

In this thesis several ways to mitigate the adverse effects of thiols in biodesulfurization systems are proposed:

1) Increase of the biomass concentration and maintaining a low redox potential. In **Chapter 3 and 5** it was demonstrated that thiols act as competitive

inhibitors on the biological oxidation of sulfides. Therefore, the inhibitory effects caused by thiols can be mitigated by increasing the biomass concentration, i.e. the enzyme concentration and by increasing the sulfide concentration in the bioreactor. This can be achieved by operating the system at a somewhat lower redox potential [5]. We recommend to control the redox potential below -390 mV (Ag|AgCl reference electrode). In **Chapter 4 and 5** two complementary mathematical models to describe the biodesulfurization process have been proposed. The first model (**Chapter 4**) describes an integrated reactor system for the combined removal of H_2S and MT and the subsequent biological oxidation of the absorbed sulfide. The second model (**Chapter 5**) describes sulfide oxidation pathways in SOB and the inhibitory effects of thiols and diorgano polysulfanes. By introducing rate equations which are corrected for the type of inhibition (**Chapter 5**) to the model structure described in **Chapter 4**, it is possible to calculate the maximum allowable H_2S to methanethiol supply ratio at which maximum sulfur production occurs (Fig. 1).
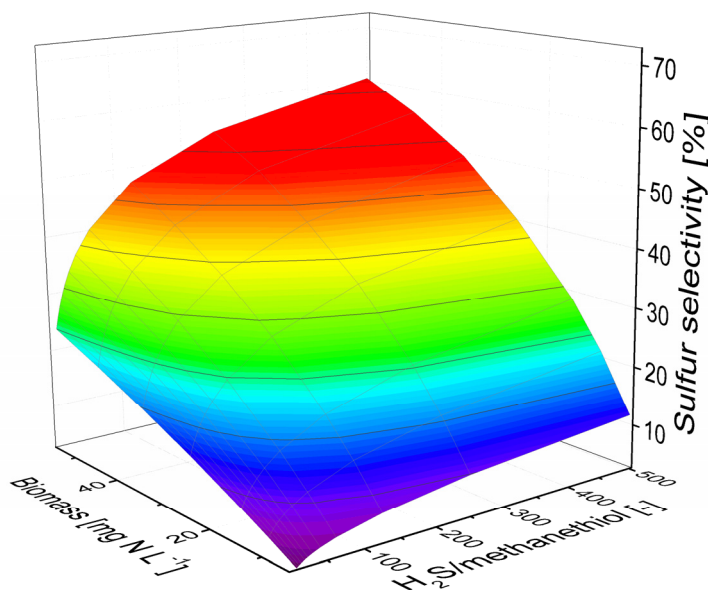

Figure 1. Calculated molar selectivity for sulfur formation at different biomass concentrations and H_2S/methanethiol supply ratios. The graph represents the output of model combination from Chapter 4 and 5. The presented output space has been experimentally validated.

In Figure 1, it can be seen that the selectivity for sulfur formation mainly depends on the biomass concentration and on the inhibition rate. Therefore, by applying high biomass concentrations and low redox conditions, the bioprocess is less vulnerable to MT. It should be noted that the remaining oxidation product of sulfide oxidation is thiosulfate, which is formed from the abiotic reaction between dissolved sulfide and oxygen (**Chapter 1**, eq. 17 - 22) due to biomass inhibition by MT.

2) Control of the salinity of the bioreactor medium. In **Chapter 4** it was found that the suppression of the biomass activity by MT can be decreased by lowering salinity (from 1.5 to 0.5 M Na$^+$). Apparently more metabolic energy is available which can be used by the microorganisms to withstand MT. Especially under sulfur-forming conditions limited amounts of energy are released from the oxidation of sulfide, while high maintenance requirements exist to control the osmotic pressure over the cell membrane. Hence, a small change in the energy balance, e.g. by increasing the salinity, can be detrimental for the SOB activity.

3) Enhancement of the chemical oxidation of thiols to diorgano polysulfanes. In the presence of sulfur or oxygen, thiols can be chemically oxidized to their corresponding and less toxic diorgano polysulfanes (**Chapter 1**, Eq. 14 - 16). These hydrophobic compounds adsorb onto biosulfur particles in a reversible manner. We found that the absorption affinity increases with increasing sulfur-chain length (**Chapter 3**). The total thiol oxidation yield can be increased by increasing the contact time between thiols and biosulfur in the gas absorber. This offers an elegant way for removing these compounds from the bioreactor suspension along with the formed biosulfur particles.

4) Stripping of thiols from the reactor suspension. The inhibitory effects of thiols on the sulfide-oxidizing biomass can be mitigated by lowering their concentration in the bioreactor medium via gas stripping (**Chapter 6**). Selectivity for biosulfur production was increased up to 40% by stripping thiols from the bioreactor suspension.

7

7.3. Description of a modified process for combined H₂S and thiols removal

Based on the findings described in this thesis it can be concluded that, in principle, the combined removal of H_2S and thiols from sour gas streams is feasible by a combination of biochemical and physicochemical reactions. However, to prevent any inhibition of SOB by thiols, their concentration shall be lowered to below their toxicity threshold levels, which can be achieved by air stripping or stimulating a chemical reaction with biosulfur particles. Based on these principles a modification of a conventionally applied three-step biodesulfurization process (**Chapter 1**, Fig. 6) has been proposed (Fig. 2). In the modified process, H_2S is removed from the gas stream by washing the sour gas with a mildly alkaline solution in an absorption column (A). It shall be noted that the partial removal of thiols in the absorber (A) should be low in order to avoid any toxicity in the bioreactor section (C). This can be achieved by adjusting the wash water flow over the absorber column and the pH as H_2S ($pK_a \approx 7$) is a stronger acid than e.g. CH_3SH ($pK_a \approx 10$) [6,7]. Thiols will be partly removed in a bioreactor section (C) by air stripping. However, if the concentration of dissolved thiols would become too high and start to impact on the process performance they can be removed in a stripping vessel (B) (**Chapter 6**). Here, thiols can be stripped with a small volume of recycled clean gas. It should be noted that stripping of H_2S can be neglected because of high pH conditions at which H_2S is mainly in its dissociated form. Produced biosulfur taken from bioreactor (C) is separated from the liquid in a gravity settler (D) or in another removal step such as a decanter centrifuge. In case the sour gas contains high levels of thiols, a split absorber design could be applied to remove the majority of the H_2S in the first absorber (A) whilst thiols are removed in the second absorber (E) by reaction with an alkaline medium and biosulfur. A similar concept has been proposed by Kijlstra et al. [8]. The absorbed thiols from the second absorber are chemically transformed to diorgano polysulfanes by a reaction with biosulfur (**Chapter 6**). Biosulfur particles covered with adsorbed diorgano polysulfanes can be disposed or sent to an anaerobic bioreactor (F) where these organosulfur compounds, together with sulfur, are converted to sulfide and recycled to the sulfide oxidizing bioreactor (C). The spent gas from the bioreactor C and F is discharged to atmosphere after passing a compost filter (G) to remove traces of odorous sulfur compounds.
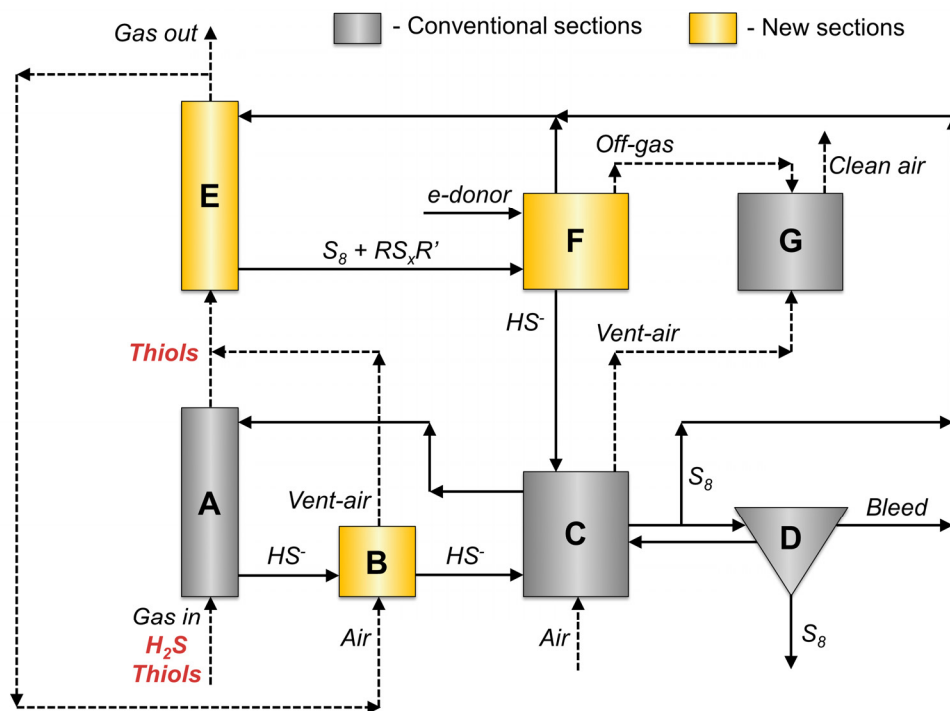
7

Figure 2. Scheme for combined H₂S and thiols removal process.

In the anaerobic reactor (F) three different processes may need to be taken into account: (1) coagulation of biosulfur by diorgano polysulfanes (**Chapter 6**); (2) biological conversion of biosulfur and diorgano polysulfanes to sulfide; (3) chemical formation of polysulfide anions from the reaction between produced sulfide and biosulfur. Under anaerobic conditions, the formed polysulfide anions can be biologically converted to sulfide [9–11] or oxidized to biosulfur in aerobic reactor [12,13]. Anaerobic degradation of dimethyl disulfide (DMDS) does not require an electron donor [14,15], but in its presence the degradation is faster and higher concentrations of substrate can be treated [16]. The effect of coagulated sulfur on the process performance requires further investigations. It may pose operational issues such as clogging but on the other hand, diorgano polysulfanes are immo-bilized onto biosulfur particles which can result in increasing biodegradation rates.

7.4. Recommendations for future research

In this thesis, topics from various disciplines, ranging from analytical chemistry and microbiology to bioprocess engineering, were studied to broaden the application window of an existing gas biodesulfurization process for the removal of H_2S and thiols from sour gas stream. During this PhD project a number of knowledge gaps were identified which require further studies in order to build a robust process for total gas desulfurization. In the next sections directions for future research are proposed.

7.4.1. Combined removal of H_2S and thiols from gas streams

In **section 7.3**, a new system for the combined removal of H_2S and thiols process has been described (Fig. 2). The proposed system can be readily tested under laboratory conditions. Integration of an anaerobic reactor in the process line-up (Fig. 2; F) would allow for a complete treatment of the gas streams with minimal waste production. Investigations of this anaerobic process should focus on the characterization of biosulfur particles covered with a layer of diorgano polysulfanes. Also the biological reduction of biosulfur covered with a layer of diorgano polysulfanes should be studied whilst the optimal conditions for reduction should be assessed.

In **Chapter 6** it was shown that a standard way to control the selectivity of biological sulfide oxidation is insufficient when other compounds than sulfide are present that influence the redox potential. Further investigations should focus on the development of a new controlling system. This system should be based on the direct measurement of dissolved sulfide. A new sulfide sensor was proposed [17] that can be implemented in such controlling system. However, further research should be performed to find out whether the proposed solution will work under the prevailing process conditions.

Furthermore, another area for research concerns the coagulation of biosulfur particles (**Chapter 6**) and its effect on the process performance.

Based on the data presented in **Chapters 3, 4 and 6**, it can be seen that when thiols are present in the feed gas stream, the main organosulfur compounds present in the bioreactor are diorgano polysulfanes. These form a complex mixture ranging

7

from disulfide up to octasulfide, where pentasulfide is the most dominant compound [18]. Further research on the effect of these organosulfur compounds on sulfur oxidizing bacteria is necessary. Unfortunately, due to the instability of diorgano polysulfanes consisting of more than three sulfur atoms, they are not commercially available, which means that these compounds should be synthesized in the laboratory (**Chapter 2)**. Another possibility is to perform tests with stable diorgano polysulfanes, e.g. with dimethyl sulfide, disulfide and trisulfide where after an extrapolation for higher polysulfanes may be possible.

7.4.2. Sulfide oxidation pathway

More research is needed to understand the underlying metabolic principles to properly describe the biological sulfide oxidation pathways. For this purpose analysis of product formation within the living single cell using Raman spectroscopy could be helpful [19] and more advanced genomic and metabolomic tools can be applied. However, a new experimental setup for these tests has to be designed to keep dissolved oxygen constant even at micro-molar concentrations. Dissolved oxygen should be measured with the highest accuracy using a sensor that can detect micro-molar concentrations. The setup should also be equipped with a UV-sensor as proposed [17] to measure consumption rate of sulfide.

In **Chapters 3 and 5** it is shown that the biological production of sulfate is much more susceptible to inhibitors than the biological sulfur production. Especially, sulfate production is easily affected by hydrophobic inhibitors, like diorgano polysulfanes, while sulfide production is easily affected by more hydrophilic inhibitors, like thiols (**Chapter 5**). An interesting proposition is to investigate the effect of hydrophobic compounds on maximization of sulfur production by suppressing sulfate production, i.e. validation weather hydrophobic compounds can act as selective inhibitors. From our laboratory experiments (**Chapter 6**) it follows that the selectivity for sulfur production increases in the presence of hydrocarbons.

7

7.4.3. Investigation of thermodynamic properties

The thermodynamic properties of organosulfur compounds are required as input parameters for many models that rely on describing phase behavior

e.g. for designing absorption columns. Unfortunately, data in literature are incomplete. Therefore, further research should focus on determining basic data such as Henry coefficients for thiols under the prevailing process conditions (salinity, pH, temperature). It is advised to apply the static synthetic method using high pressure autoclaves [20], which is less susceptible to analytical errors compared to the static headspace method. Furthermore, sorption isotherm of biosulfur for diorgano polysulfanes can be determined to assess the adsorption capacity.

7.4.4. Application of biosulfur

Another interesting field of research is the broadening of the application of biosulfur as a raw material. As stated in **Chapter 1**, biosulfur can be used as a fertilizer or as a substrate in sulfuric acid production. Unfortunately, a common practice is to dispose the recovered biosulfur in a landfill. To contribute to a sustainable circular economy, new application strategies for biosulfur should be developed.

References

1. Song C. An overview of new approaches to deep desulfurization for ultra-clean gasoline, diesel fuel and jet fuel. *Catal. Today*. Elsevier; 2003;86:211–263.
2. Federal Emission Standards [Internet]. Available from: http://www3.epa.gov/otaq/standards/allstandards.htm.
3. Janssen AJH, Lens PNL, Stams AJM, Plugge CM, Sorokin DY, Muyzer G, Dijkman H, Van Zessen E, Luimes P, Buisman CJN. Application of bacteria involved in the biological sulfur cycle for paper mill effluent purification. *Sci. Total Environ.* Elsevier; 2009;407:1333–1343.
4. Van den Bosch PLF, van Beusekom OC, Buisman CJN, Janssen AJH. Sulfide oxidation at halo-alkaline conditions in a fed-batch bioreactor. *Biotechnol. Bioeng.* Wiley Online Library; 2007;97:1053–1063.
5. Janssen AJH, Meijer S, Bontsema J, Lettinga G. Application of the redox potential for controling a sulfide oxidizing bioreactor. *Biotechnol. Bioeng.* Wiley Online Library; 1998;60:147–155.
6. Weast RC. CRC handbook of chemistry and physics. CRC Press, Boca Raton; 1986.
7. Crampton M. The Chemistry of the Thiol Group: Part 1. Patai, S., editor. Acidity and Hydrogen Bonding. New York, NY: John Wiley & Sons; 1974. p. 379–415.
8. Kijlstra WS, Lammers J.N.J.J.L., Wernersson CI. Process for the removal of H_2S and mercaptans from a gas stream. Patent 7588627.

7

9. Sorokin DY, Kuenen JG. Haloalkaliphilic sulfur-oxidizing bacteria in soda lakes. *FEMS Microbiol. Rev.* Wiley Online Library; 2005;29:685–702.

10. Sorokin DY, Foti M, Tindall B, Muyzer G. *Desulfurispirillum alkaliphilum* gen. nov. sp. nov., a novel obligately anaerobic sulfur-and dissimilatory nitrate-reducing bacterium from a full-scale sulfide-removing bioreactor. *Extremophiles*. Springer; 2007;11:363–370.

11. Sorokin D, van den Bosch PLF, Abbas B, Janssen AJH, Muyzer G. Microbiological analysis of the population of extremely haloalkaliphilic sulfur-oxidizing bacteria dominating in lab-scale sulfide-removing bioreactors. *Appl. Microbiol. Biotechnol.* Springer; 2008;80:965–975.

12. Blumentals I, Itoh M, Olson G, Kelly R. Role of polysulfides in reduction of elemental sulfur by the hyperthermophilic archaebacterium Pyrococcus furiosus. *Appl. Environ. Microbiol.* Am Soc Microbiol; 1990;56:1255–1262.

13. Sorokin DY, Kublanov IV, Gavrilov SN, Rojo D, Roman P, Golyshin PN, Slepak VZ, Smedile F, Ferrer M, Messina E, others. Elemental sulfur and acetate can support life of a novel strictly anaerobic haloarchaeon. *The ISME journal*. Nature Publishing Group; 2015.

14. De Bok FA, van Leerdam RC, Lomans BP, Smidt H, Lens PN, Janssen AJH, Stams AJ. Degradation of methanethiol by methylotrophic methanogenic archaea in a lab-scale upflow anaerobic sludge blanket reactor. *Appl. Environ. Microbiol.* Am Soc Microbiol; 2006;72:7540–7547.

15. Van Leerdam RC, de Bok FA, Bonilla-Salinas M, van Doesburg W, Lomans BP, Lens PN, Stams AJ, Janssen AJH. Methanethiol degradation in anaerobic bioreactors at elevated pH ($\geqslant$ 8): Reactor performance and microbial community analysis. *Bioresour. Technol.* Elsevier; 2008;99:8967–8973.

16. Leerdam van R. Anaerobic degradation of methanethiol in a process for liquefied petroleum gas (LPG) biodesulfurization. 2007.

17. Roman P, Yntema D, Bijmans MFM, Janssen AJH. Sensor system for spectrophotometric measurement of components and method therefore. NL Patent 2015580, Filed October 7, 2015.

18. Steudel R. The chemistry of organic polysulfanes RS (n)-R (n> 2). *Chem. Rev.* 2002;102:3905.

19. Berg JS, Schwedt A, Kreutzmann A-C, Kuypers MM, Milucka J. Polysulfides as Intermediates in the Oxidation of Sulfide to Sulfate by Beggiatoa spp. *Appl. Environ. Microbiol.* Am Soc Microbiol; 2014;80:629–636.

20. Kiepe J, Horstmann S, Fischer K, Gmehling J. Experimental determination and prediction of gas solubility data for CO_2 + H_2O mixtures containing NaCl or KCl at temperatures between 313 and 393 K and pressures up to 10 MPa. *Ind. Eng. Chem. Res.* ACS Publications; 2002;41:4393–4398.

7

Acknowledgments

Multidisciplinary research that finish after four years with a PhD thesis requires lots of determination, systematic work and patience. Its completion would be impossible without the help and support of other people whom I would like to thank.

I would like to express my sincere thanks and appreciations to my promotor Prof. Dr Albert Janssen for the fruitful discussions, valuable advices and time spent for corrections of my work. Thank you for your guidance, eye for detail and precision.

I sincere gratitude to my daily supervisor Dr Martijn Bijmans for guidance and the support during my PhD. The freedom and trust you gave me were very encouraging.

I especially want to thank Dr Dimitry Sorokin for enormous contribution to my work by reviewing manuscripts, patient explanations and many discussions. Your knowledge is invaluable for me and I am privileged that I could work with you.

Another person that I would like to thank is Prof. Dr Karel Keesman, who introduced me to Matlab and showed how mathematics is a powerful tool. Thanks to you, I developed a lot in these fields.

I would like to thank Dr Erik van Zessen for your supervision. Thank you for valuable comments and sharing your wisdom.

Person that I especially would like to thank is João Sousa. João thank you for good advises, the support and for countless discussions. It was a great time working with you at Wetsus.

Many thanks to the other research members of the Sulfur Theme: Caroline Plugge, Jan Klok, Gijs Van Heeringen, Jan Henk van Dijk, Fons Stams and Gerard Muyzer for interest in my results and very fruitful discussions during our meetings that kept the direction of my work on a good track.

Then I would like to thank Doekle Yntema for his help during development the sulfide sensor and for Maarten Biesheuvel for introducing me into the modelling. Your help resulted in my interest in further development in electronics and modelling which had a positive impact on my thesis.

I also would like to thank René Veltman, Joanna Lipińska, Elias Broman and Mark Dopson for their cooperation and input to the scientific papers that we are coauthors.

Wetsus is an amazing place to work and conduct research. Therefore, I would like to thank Cees Buisman and Johannes Boonstra for giving me the opportunity to perform my work at such an inspiring place.

In my research I had to build complex experimental setup and use multiple analytical technics and procedures. This would not be possible without Wetsus analytical staff: Mieke Kersaan-Haan, Ton van der Zande, Jelmer Dijkstra and Marianne Heegstra; and technical staff: Harm van der Kooi, Wim Borgonje, Ernst Panstra, Harrie Bos. Thank you so much for your time, effort and discussions.

I also would like to thank those people who contributed to my PhD period not only in a scientific way. Thanks to my office mates: Anna, Oane, Daniel and Roel for a nice time that we spent in the old building and for interesting discussions.

Special thanks to my good friends Rungnapha and Vytautas for invaluable support that you gave me during my PhD and a great time after working hours. I cannot imagine this part of my life without you.

Last but not least, I would like to give my deepest appreciation to my closest family: Emilia, Andrzej, Krystyna and Małgorzata for their support that have enabled me to successfully complete my PhD work.

About the Author

Paweł Roman was born on March 11, 1987 in Gdańsk, Poland. In 2006 he started to study *Applied Chemistry* at the Gdańsk University of Technology (GUT). Paweł obtained his Master of Science degree in 2011 by completing a thesis on airborne research: *Chemistry and transport of pollutants in cumulus cloud water*. This work was performed under the supervision of GUT and University of the West of Scotland.

From November 2011, Paweł started a PhD project guided by the Sub-department of Environmental Technology at Wageningen University and performed at Wetsus, European centre of excellence for sustainable water technology located in Leeuwarden, the Netherlands. The results obtained during his PhD are presented in this dissertation.

Author's publications and patents

Roman P., Lipińska J., Bijmans M.F.M, Sorokin D.Y., Keesman K.J., Janssen A.J.H. Inhibition of a biological sulfide oxidation under haloalkaline conditions by thiols and diorgano polysulfanes. Has been submitted for publication.

Roman P., Klok J.B.M., Sousa J.A.B., Broman E., Dopson M., Zessen E., Bijmans M.F.M., Sorokin D.Y., Janssen A.J.H. Removal of H_2S and thiols from sour gas streams under haloalkaline conditions. Has been submitted for publication.

Ni G., Christel S., Roman P. Wong Z.L., Bijmans M.F.M, Dopson M. Electricity generation from inorganic sulfur compound containing mining wastewater by acidophilic microorganisms. Has been submitted for publication.

Sorokin D.Y., Kublanov I.V., Gavrilov S.N., Rojo D., Roman P., Golyshin P.N., Slepak V.Z., Smedile F., Ferrer M., Messina E., others. Elemental sulfur and acetate can support life of a novel strictly anaerobic haloarchaeon. *The ISME journal.* 2016, 10.1: 240-252.

Roman P., Yntema D., Bijmans M.F.M., Janssen A.J.H. 2015. Sensor system for spectrophotometric measurement of components and method therefore. NL2015580. Filed October 7, 2015.

Roman P., Veltman R., Bijmans M.F.M, Keesman K., Janssen A.J.H. Effect of methanethiol concentration on sulfur production in biological desulfurization systems under haloalkaline conditions. *Environ. Sci. Technol.* 2015, 49:9212-9221.

Roman P., Bijmans M.F.M, Janssen A.J.H. Influence of methanethiol on biological sulfide oxidation in gas treatment system. *Environ. Tech.* 2015, 1-42.

Roman P., Bijmans M.F.M, Janssen A.J.H. Quantification of individual polysulfides in lab-scale and full-scale desulfurisation bioreactors. Environ. Chem. 2014, 11 (6), 702-708.

Roman P., Polkowska Ż., Namieśnik J. Sampling Procedures in Studies of Cloud Water Composition: A Review. *Crit. Rev. Env. Sci. Tec.* 2013, 43(14), 1517-1555.

Baranowska, K., Roman, P., Socha, J. 2,2,6,6-Tetramethylpiperidinium triiso-propoxysilanethiolate. *Acta Crystallographica Section E: Structure Reports Online*. 2009, 65(11), 2825-2825.

Netherlands Research School for the
Socio-Economic and Natural Sciences of the Environment

D I P L O M A

For specialised PhD training

The Netherlands Research School for the
Socio-Economic and Natural Sciences of the Environment
(SENSE) declares that

Paweł Roman

born on 11 March 1987 in Gdańsk, Poland

has successfully fulfilled all requirements of the
Educational Programme of SENSE.

Wageningen, 12 May 2016

the Chairman of the SENSE board

Prof. dr. Huub Rijnaarts

the SENSE Director of Education

Dr. Ad van Dommelen

The SENSE Research School has been accredited by the Royal Netherlands Academy of Arts and Sciences (KNAW)

K O N I N K L I J K E   N E D E R L A N D S E
A K A D E M I E   V A N   W E T E N S C H A P P E N

The SENSE Research School declares that **Mr Paweł Roman** has successfully fulfilled all requirements of the Educational PhD Programme of SENSE with a work load of 55.0 EC, including the following activities:

SENSE PhD Courses

o   Environmental Research in Context (2012)
o   Advanced Course on Environmental Biotechnology (2012)
o   Research in Context Activity: 'Co-organising Wetsus Sulfur Theme Meeting', Leeuwarden (2015)

Other PhD and Advanced MSc Courses

o   Working safely in Laboratories, Wetsus (2012)
o   OLI Stream Analyser, Wageningen University (2013)
o   Techniques for Writing and Presenting a Scientific Paper, Wageningen University (2013)
o   Presentation skills, Wageningen University (2013)
o   English for IELTS level B2 on the CEFR, Wageningen University (2014)
o   Matlab: introduction, modelling and data analysis, Wetsus (2014)
o   Advanced English writing course, DC Taleninstituut (2014)
o   Communication for Excellence, How Company (2015)
o   Leadership for Engineers, Delft University of Technology (2016)
o   Semi-intensive Dutch course, University of Groningen (2016)
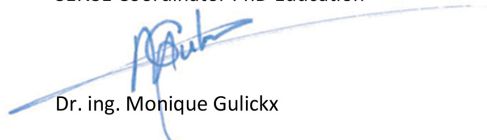o   Electronic interfaces: Bridging the physical and digital worlds, Berkeley University (2016)

Management and Didactic Skills Training

o   Supervising two MSc students with thesis entitled 'Estimation of toxicity parameters for sulfur-oxidizing bacteria under haloalkaliphilic conditions' (2012) and 'Inhibition of methanethiol on biological sulfide oxidation' (2014)
o   Supervising four internship students (2013-2015)

Oral Presentations

o   *Biological sulfur recovery from gas streams.* Wetsus Congress, 27 November 2014, Leeuwarden, The Netherlands
o   *Combined H$_2$S and thiols removal from sour gas streams.* Environmental Technology for Impact Conference, 30 April 2015, Wageningen, The Netherlands
o   *Sulfur recovery from thiol- and H$_2$S-containing gas streams.* Wetsus Congress, 29 September 2015, Leeuwarden, The Netherlands

SENSE Coordinator PhD Education

Dr. ing. Monique Gulickx